T.C.
İSTANBUL UNIVERSITY
INSTITUTE OF GRADUATE STUDIES IN
SCIENCE AND ENGINEERING

Ph.D. THESIS

ON THE NUMERICAL SOLUTION OF ADVECTION DIFFUSION REACTION EQUATIONS WITH SINGULAR SOURCE TERMS

İrfan TÜRK

Department of Mathematics

Mathematics Programme

Ph. D. transferred from Fatih University which has been closed

SUPERVISOR
Assoc. Prof. Dr. Maksat ASHRALIYEV

CO-SUPERVISOR
Asst. Prof. Dr. Okan GERÇEK

June, 2016

İSTANBUL

APPROVAL PAGE

This is to certify that I have read this thesis written by İrfan TÜRK and that in my opinion it is fully adequate, in scope and quality, as a thesis for the degree of Doctor of Philosophy in Mathematics.

Assoc. Prof. Maksat ASHYRALIYEV
Thesis Supervisor

Assist. Prof. Okan GERÇEK
Co-Supervisor

I certify that this thesis satisfies all the requirements as a thesis for the degree of Doctor of Philosophy in Mathematics.

Prof. Feyzi BAŞAR
Head of Department

Examining Committee Members

Assoc. Prof. Maksat ASHYRALIYEV

Assist. Prof. Okan GERÇEK

Prof. Halil Rıdvan ÖZ

Prof. Allaberen ASHYRALYEV

Prof. Nurullah ARSLAN

Prof. Feyzi BAŞAR

Assist. Prof. Necmettin AĞGEZ

It is approved that this thesis has been written in compliance with the formatting rules laid down by the Graduate School of Sciences and Engineering.

Prof. Nurullah ARSLAN
Director

June 2016

ON THE NUMERICAL SOLUTION OF ADVECTION-DIFFUSION-REACTION EQUATIONS WITH SINGULAR SOURCE TERMS

İrfan TÜRK

Ph.D. Thesis – Mathematics
June 2016

Thesis Supervisor: Assoc. Prof. Maksat ASHYRALIYEV

Co-Supervisor: Assist. Prof. Okan GERÇEK

ABSTRACT

Mathematical models of real life phenomena often are formulated by Partial Differential Equations. Partial Differential Equations with singular source terms arise in many different applications of science and engineering. Singular means that within the spatial domain the source is defined by a Dirac delta function.

In this thesis, we focus on specific type of Partial Differential Equations, Advection Diffusion Reaction Equations with singular source terms. An analytical solution of such equations can be found very rarely. Therefore, numerical methods play a significant role. Numerical methods for these equations require a special treatment. Due to the lack of smoothness or presence of discontinuities in the solutions of such equations, standard numerical methods may fail to converge.

Weighted essentially non-oscillatory (WENO) methods on non-uniform meshes are applied as numerical methods in this study. Construction of WENO methods and a new scheme for Advection Diffusion problems is presented.

Keywords: Advection-Diffusion-Reaction Equations, Singular source terms, Numerical methods, WENO

ADVEKSİYON-DİFÜZYON-REAKSİYON DENKLEMLERİNİN TEKİL KAYNAK TERİMİYLE BERABER SAYISAL ÇÖZÜMLERİ

İrfan TÜRK

Doktora Tezi – Matematik
Haziran 2016

Tez Danışmanı: Doç. Dr. Maksat ASHYRALIYEV

Eş Danışman: Yard. Doç. Dr. Okan GERÇEK

ÖZ

Gerçek hayattaki olayların matematiksel modellemeleri genellikle kısmi diferansiyel denklemler tarafından formülize edilir. Tekil kaynak terimleri içeren kısmi diferansiyel denklemler, fen ve mühendislik bilimlerinde birçok alanında karşımıza çıkar. Buradaki tekil ifadesi, uzaysal değer kümesinde kaynak, Dirac delta fonksiyonu tarafından tanımlanır anlamını taşımaktadır.

Bu tezde, özel bir kısmi diferansiyel denklem çeşidi olan, tekil kaynak terimleri içeren Adveksiyon-Difüzyon-Reaksiyon denklemleri üzerinde yoğunlaştık. Bu tip denklemlerin analitik çözümleri genellikle çok nadir bulunur. Bu gibi durumlarda, sayısal metotlar çok önemli bir rol oynar. Bu gibi denklemlerin sayısal çözüm metotları özel bir yaklaşım ister. Bu tip denklemlerin çözümlerinde, pürüzsüzlüklerden yoksun olma veya süreksizliklerden dolayı standart sayısal metotlar, yakınsamayı gerçekleştiremeyebilirler.

Bu çalışmada, düzensiz aralıklı ağlarda ağırlıklı esasen salınımsız (WENO) metodu sayısal metot olarak uygulanmıştır. WENO metotlarının kurulumu ve Adveksiyon-Difüzyon problemler için yeni bir şema sunulmuştur.

Anahtar Kelimeler: Adveksiyon-Difüzyon-Reaksion Denklemleri, Tekil kaynak terimleri, Sayısal metotlar, WENO

To my spouse Maksude, and my children Büşra and İhsan

ACKNOWLEDGEMENT

This thesis would not have been possible without the support of some people. It is a pleasure for me to convey my sincere gratitude to all of these names I would like to mention personally.

With the biggest contribution to this thesis, I would like to express my special appreciation and gratefully thanks to my main supervisor Maksat ASHYRALIYEV for the continuous support of my Ph.D study, for his patience, motivation, advice, inspiration, and immense knowledge. His mentorship was supreme from the very beginning of my research work to the final stages of writing this dissertation. Sir, you have been a tremendous mentor for me and I am deeply indebted to you for all your help.

I also would like to thank my co-advisor, Okan GERÇEK, for his assistance, knowledge, encouragement, and continuous support.

I wish to express my deepest gratitude to one of my thesis observation committee members, Allaberen ASHYRALYEV, for his mentorship, advice, and positive criticizings which motivate me to try harder. I wish to express my deepest gratitude to another of my thesis observation committee members, Halil Rıdvan ÖZ, for his mentorship, advice, and feedbacks for the dissertation study. I would also like to thank to head of the mathematics department and one of my committee members, Feyzi BAŞAR, for his encouragements, support and help. I would also like to thank my committee members, Nurullah ARSLAN, and Necmettin AĞGEZ.

Finally, I would like to express appreciation to my wife Maksude who spent sleepless nights with children and was always my support in the moments when there was no one to answer my queries.

TABLE OF CONTENTS

LIST OF TABLES

TABLE

LIST OF FIGURES

FIGURE

LIST OF SYMBOLS AND ABBREVIATIONS

SYMBOL/ABBREVIATION

ODE	Ordinary Differential Equation
PDE	Partial Differential Equation
DDE	Delay Differential Equation
ADE	Algebraic Differential Equation
ADRE	Advection Diffusion Reaction Equation
FDM	Finite Difference Method
FEM	Finite Element Method
FVM	Finite Volume Method
ENO	Essentially Non-Oscillatory method
WENO	Weighted Essentially Non-Oscillatory method
WENO3	Third order Weighted Essentially Non-Oscillatory method
WENO5	Fifth order Weighted Essentially Non-Oscillatory method

CHAPTER 1

INTRODUCTION

To explore the nature, it's mathematical connections need to be examined. At that point, modelling arises. Mathematical models of real life phenomena, often are formulated by Ordinary Differential Equations (ODEs) (Ross, 1989), Delay Differential Equations (DDEs) (Smith, 2011), Algebraic Differential Equations (ADEs) (Kunkel and Mehrmann, 2006), Partial Differential Equations (PDEs) (Salso, 2008), etc. Models with PDEs are used in many areas of science and engineering, such as Economics, Environment, Biology, Medicine, Drug design, Neural Networks, Fluid Dynamics, image processing, signal processing, etc. In order to find the analytical solution of PDE, techniques such as Laplace Transform Method, Fourier Series Method, Power Series Method, etc. are used. Unfortunately, most of the time, analytical solution cannot be found and therefore one has to apply numerical methods to obtain an approximation of the solution of PDE.

1.1 ADVECTION-DIFFUSION-REACTION EQUATION

In this thesis, we focus on specific type of PDEs, Advection-Diffusion-Reaction Equations (ADREs). Mathematical models with ADREs are widely used in applied sciences and engineering, such as modeling of chemical and biological processes (Hundsdorfer and Verwer, 2003); (Owolabi and Patidar, 2014); (Elias and Clairambault, 2014); (Zhang, 2012), forecasting and development of new gas reservoirs (Zakirov and Vasilyev, 1984); (Basniev et al., 1986); (Bedrikovetskii et al., 1993).

Most general form of one-dimensional ADRE is:

$$\frac{\partial}{\partial t}u(x,t)+\frac{\partial}{\partial x}\Big(a(x,t)u(x,t)\Big)=\frac{\partial}{\partial x}\left(d(x,t)\frac{\partial}{\partial x}u(x,t)\right)+f\big(x,t,u(x,t)\big),\quad (1.1.1)$$

where a, d, f are given functions and u is unknown function. Here, the term $\frac{\partial}{\partial x}\Big(a(x,t)u(x,t)\Big)$ models the advection, $\frac{\partial}{\partial x}\left(d(x,t)\frac{\partial}{\partial x}u(x,t)\right)$ models the diffusion and $f\big(x,t,u(x,t)\big)$ models the reaction. The advection term models the transport of something from one region to another by a flow. An example for the advection is the transport of pollutant or silt in a river by a flow. In meteorology and physical oceanography, advection is the transport of some property of atmosphere or ocean, such as heat, humidity or salinity. Diffusion term models mixing or mass transport without requiring bulk motion. Reaction term can come across in chemical and biological processes such as combining two different molecules to get different molecules, or reception of a cell having a cut in it.

1.2 DELTA FUNCTION

In various models of real life phenomena, reactions occur at a single point within the spatial domain. In such cases, reaction term in model equations can be defined by a Dirac delta function expression. For example, a static singular source term in (1.1.1) can have the following form:

$$f\big(x,t,u(x,t)\big)\equiv g\big(x,t,u(x,t)\big)\delta(x-\xi),\qquad (1.2.1)$$

where g is a smooth function with regard to all arguments, ξ lies in the spatial domain where equation (1.1.1) is defined, and $\delta(x-\xi)$ is the Dirac delta function described as a unit impulse at a position $x=\xi$ (Olver, 2013). Because an impulse happens at a single point, $\delta(x-\xi)=0$ for $x\neq\xi$. Besides this, because the delta function is an impulse, the total amount of force is aimed to be equal to 1. Thus, Dirac delta function is not a classical function but rather a distribution (Olver, 2013). It is defined as following:

$$\delta(x-\xi)=\begin{cases}0, & x\neq\xi\\ \infty, & x=\xi\end{cases},\qquad \int_{-\infty}^{\infty}\delta(x-\xi)dx=1.\qquad (1.2.2)$$

Note that for any function $f(x)$,

$$\int_{-\infty}^{\infty} f(x)\delta(x-\xi)dx = f(\xi) \tag{1.2.3}$$

holds. Alternatively, Dirac delta function can be considered as derivative of the unit step function, called Heaviside function, i.e.

$$\delta(x-\xi) \;=\; \frac{d}{dx}H(x-\xi). \tag{1.2.4}$$

1.3 NUMERICAL METHODS

An analytical solution of ADRE (1.1.1) can be found very rarely. Quite often, the use of analytical methods to solve (1.1.1) becomes extremely difficult or even impossible, especially when singular source terms are present in equation. For this reason numerical methods play a significant role.

There are various numerical methods for PDEs among which the most popular are Finite Difference methods (FDM), Finite Volume methods (FVM), Finite Element methods (FEM), Spectral methods, Boundary Element methods, Level set methods, etc. When reaction is defined as a singular source term, a special treatment is required when numerical methods are applied. It is mainly due to the fact that solution of ADREs with singular source terms have lack of smoothness. For instance, Finite Difference methods based on Taylor's formula, may fail to converge. Numerical methods, based on integral form of (1.1.1), such as FVM, seem to be more appropriate when reaction is singular (Ashyraliyev et al., 2008).

In the literature, related to the study of numerical solutions of Advection-Diffusion-Reaction equations with singular source terms the following studies are done by different authors.

"Numerical solutions of Diffusion Reaction equations with singular source terms" have been studied under the same paper name by M. Ashyraliyev, J.G. Bloom, and J.G. Verwer with a finite volume approach in 2006 (Ashyraliyev et al., 2008). In this work, due to the usage of singular source term, defined as Dirac delta function, order reduction occurred from two to one on a uniform grid with finite volume approach. To overcome this deficiency, the discretization is tested on special locally refined grids. It is established that with grid refinement, second order convergence can be restored.

Numerical solutions of Advection equations with singular source terms have been studied in the paper titled "A convergence finite volume scheme for hyperbolic conservation laws with source terms" by J. Santos, and P. de Oliveira (Santos and de Oliveira, 1999). In this study, the source term is also defined by Dirac delta function to use the fact that Dirac delta function is the derivative of Heaviside function. Finite Volume method is used in this paper. It is shown that the results obtained from the method converge to the weak solution of the problems.

Numerical solution of the Advection Reaction Diffusion equation at different scales has been studied by A.D. Rubio, A. Zalts, C.D. El Hasi (Rubio et al., 2008). A one-dimensional bimolecular model of a solute transport equation in porous media was investigated and solved by using forward in time, centered in space Finite Difference method. Numerical simulations are shown for both slow and fast reactions.

Numerical solution of the Reaction Advection Diffusion equation on the sphere has been studied by Janusz A. Pudykiewicz (Pudykiewicz, 2006). In this paper, an algorithm is derived by using Finite Volume approach for a Reaction Advection Diffusion equation on the sphere.

AMF-RungeKutta formulas and error estimates for the time integration of Advection Diffusion Reaction PDEs has been studied by S. Gonzalez-Pinto et al. (Gonzalez-Pinto et al., 2015). Semi discrete linear Advection Diffusion Reaction equations in multi dimensions are investigated and convergence estimates of some of the numerical methods are examined in the study.

A SIS Reaction Diffusion Advection model in a low-risk and high-risk domain has been studied by Jing Ge et al. (Ge et al., 2015). In this paper, spreading domain plays an important role for a disease in the epidemic SIS model. The claims are proved with some simulations and examples with the effect of advection.

A Reaction Diffusion Advection model of harmful algae growth with toxin degradation has been studied by Feng-Bin Wang et al. lately (Wang et al., 2015b). In this paper, the dynamics of algae and algal toxins are examined in a water flow. It is concluded that the basic reproduction number plays an important role for algae for surviving or extinction.

1.4 WEIGHTED ESSENTIALLY NON-OSCILLATORY METHOD

Essentially non-oscillatory (ENO) and Weighted essentially non-oscillatory (WENO) schemes are the standard methods to approximate solutions of hyperbolic partial differential equations (Huang et al., 2014). ENO methods, were first introduced by Harten et al. in 1987 (Harten et al., 1987); (Harten and Osher, 1987). In ENO methods, some high order reconstructions are computed by using several candidate stencils. Among these stencils, only the one that has the smoothest stencil is used. For problems in hyperbolic conservation laws, the difficult part is the treatment of the discontinuities when we construct numerical schemes. In ENO schemes, any order of accuracy can be designed in smooth regions without spurious oscillations near discontinuities (Liu and Osher, 2008); (Shu, 2009).

WENO methods achieve a higher order accuracy than ENO methods in smooth regions while maintaining the same property with ENO at discontinuities (Wang et al., 2008). The first WENO scheme was introduced by Liu et al. in 1994 (Liu et al., 1994) with the third order accurate finite volume WENO scheme. WENO schemes use convex combination of the stencils with weights rather than using the smoothest stencil as in ENO method. For the problems having strong discontinuities, WENO methods offer stable, non-oscillatory solutions (Shu, 2011). The main theme of the WENO methods is the fact that the method is based on the approximation by using polynomial interpolation. There is no direct relation between the method and any PDE. Therefore, it can be used for different topics as well such as image processing. A detailed information about WENO schemes can be found in the lecture notes (Barth and Deconinck, 1999). In the literature, related to the study of WENO methods, upcoming studies are done by different authors.

Essentially non-oscillatory (ENO) methods, were first introduced by Harten et al. in 1987 (Harten et al., 1987). This classical paper has made a marvelous impact on researchers. It has been cited more than 2280 times as of May 6, 2014. In this paper, uniformly high order accurate schemes of numerical approximation of weak solutions of hyperbolic systems of conservation laws were studied. The main idea is based on choosing interpolation polynomials from selected stencils. Among these stencils, the smoothest stencil is selected for ENO reconstruction.

WENO method was introduced by Xu-Dong Liu, Stanley Oshery, and Tony Chan in 1994 (Liu et al., 1994). It has been a new version of ENO method. Instead of choosing one stencil, the smoothest one, a convex combination of all selected stencils has been used in this new version. In this paper, the results show that WENO is more successful than ENO method in terms of accuracy.

Efficient implementation of weighted ENO schemes was studied by Guang-Shan Jiang, and Chi-Wang Shu in 1996 (Jiang and Shu, 1996). The WENO method was further analyzed and improved. A fifth order WENO scheme was introduced in this paper.

Central WENO schemes for hyperbolic systems of conservation laws was studied by Doron Levy, Gabriella Puppo, and Guivanni Russo in 1999 (Levy et al., 1999). Centered version of WENO schemes were first presented in this paper. Third and fourth order schemes were constructed and tested in this study.

Finite Volume WENO schemes for three-dimensional conservation laws has been studied by V.A. Titarev and E.F. Toro in 2004 (Titarev and Toro, 2004). In this paper, the Finite Volume WENO schemes are extended to three-dimensional case. A set of numerical simulations are presented.

High order Weighted essentially non-oscillatory schemes for convection dominated problems has been studied by Chi-Wang Shu in 2009 (Shu, 2009). The paper basically explains all the processes of WENO scheme and is a good manual for the method. It has the history of the method, and summarizes almost all the papers related to WENO up to published day.

A recent paper titled “A re-averaged WENO reconstruction and a third order CWENO scheme for hyperbolic conservation laws” has been studied by Chieh-Sen Huang, Todd Arbogast, and Chen-Hui Hung in 2014 (Huang et al., 2014). In this paper, a re-averaging technique is developed. It is shown that the constructed CWENO3 scheme is a third order accurate in smooth regions while giving good results for non-smooth problems.

The papers mentioned so far, mainly focus on the uniform grid cases. There are several papers for non-uniform grids as below.

The paper titled “Grid adaptation with WENO schemes for non-uniform grids to solve convection-dominated partial differential equations” has been studied by J. Smit, M. van Sint Annaland, and J.A.M. Kuipers in 2005 (Smit et al., 2005). In this paper, it is shown that the number of grid cells to solve the convection dominated PDE can be greatly reduced by using grid adaptation technique. A numerical algorithm is demonstrated. A set of formulas for grid adaptation is presented.

The paper titled “Observations on the fifth order WENO method with non-uniform meshes” has been studied by Rong Wang, Hui Feng, and Raymond J. Spiteri in 2008 (Wang et al., 2008). In this paper, a fifth order Finite Volume explicit formulas are presented and tested. Performance on uniform grid and non-uniform grid cases are compared. In this paper, it is shown that the non-uniform grid case is much better in terms of computational efficiency and memory usage.

The paper titled “Adaptive mesh refinement based on high order finite difference WENO scheme for multi-scale simulations” has been studied by Chaopeng Shen, Jing-Mei Qui, and Adrew Christlieb in 2011 (Shen et al., 2011). A Finite Difference AMR-WENO method for hyperbolic conservation laws is proposed in this paper. The proposed method is compared to the third order method and shown to give better results.

There are also a few papers about implicit WENO schemes that have been studied so far. We also summarize them as below.

The paper titled “Implicit WENO shock capturing scheme for unsteady flows. Application to one-dimensional Euler equations” has been studied by A. Cadiou and C. Tenaud in 2004 (Cadiou and Tenaud, 2004). Unsteady numerical simulation for one dimensional shock waves is studied by using total variation diminishing (TVD) schemes. Implicit resolution of Euler equation is performed and tested in this study.

The paper titled “ A fifth order flux implicit WENO method” has been studied by Sigal Gottlieb, Julia S. Mullen, and Steven J. Ruuth in 2006 (Gottlieb et al., 2006). In this paper, implicit schemes of first order flux-implicit Euler, as a corrector, first order implicit Euler, second order implicit Crank-Nicolson, a third order implicit Adams-Moulton, a third order Backward Differentiation Formula (BDF), implicit third order Adams-Moulton are compared with different schemes. Some numerical outcomes are presented in this paper.

Implicit WENO scheme and high order viscous formulas for compressible flows has been presented by Yiqing Shen, Baoyuan Wang, and Gecheng Zha in 2007 (Shen et al., 2007). In this paper, a high order Finite Difference scheme is developed for Navier-Stokes equations.

High order accurate semi-implicit WENO schemes for hyperbolic balance laws has been studied by Nelida Crnjaric-Zic, and Bojan Crnkovic in 2011 (Crnjaric-Zic and Crnkovic, 2011). In this paper, WENO spatial discretization is combined with SSP singly diagonally implicit (SDIRK) methods. Semi-implicit Finite Volume WENO schemes are constructed and tested.

Parallel adaptive mesh refinement method based on WENO Finite Difference scheme for the simulation of multi-dimensional detonation has been studied by Cheng Wang et al. in 2015 (Wang et al., 2015a). In this paper, an adaptive mesh refinement with Weighted essentially non-oscillatory (WENO) Finite Difference method is proposed (AMR&WENO). The method is tested and produced convergent results for 1-dimensional smooth problems.

1.5 OUTLINE OF THESIS

The thesis is organized in the following way. In Chapter 2, a mathematical model from gaz hydrodynamics, a coupled system of Diffusion and Advection equations with singular source terms, is examined. The analytical solution of this problem is obtained by using Laplace Transform method. In Chapter 3, a numerical study is presented for the Diffusion problem having singular source terms. In Chapter 4, the application of Finite Difference and Finite Volume methods for one-dimensional Advection Diffusion problem with source term is illustrated. The difference between the methods is discussed when the source term is singular. An example of one-dimensional heat equation with singular source term is used for numerical illustration. In Chapter 5, the third order of accuracy and the fifth order of accuracy WENO methods on non-uniform meshes are constructed. The order of accuracy of each method in case of smooth functions is established. In Chapter 6, constructed WENO schemes are used for Advection equation with singular source term and Advection Diffusion equation with singular source term. Numerical examples for both cases are provided. In Chapter 7, we extend the methodology to the non-linear equations. We conclude the thesis in Chapter 8 with final remarks.

CHAPTER 2

AN EXAMPLE FROM GAS HYDRODYNAMICS

In this chapter, we consider a mathematical model for spatio-temporal distribution of temperature and pressure in one dimensional gas pipe which has finite number of singular source points (see Figure 2.1).

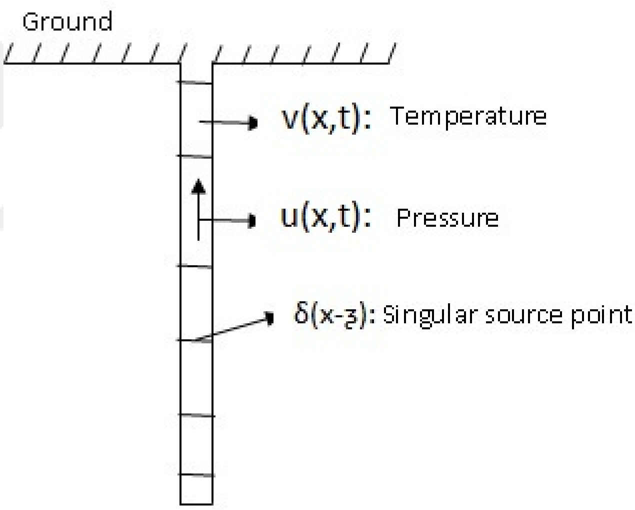

Figure 2.1 One-dimensional tube.

Denoting the temperature and pressure by $v(x,t)$ and $u(x,t)$, respectively, this dynamical system can be described by initial-boundary value problem

$$\begin{cases} u_t = Du_{xx} + \sum_{i=1}^{m} c_i \delta(x - \xi_i), & t > 0, \quad 0 < x < 1, \\ u(x,0) = \varphi(x), & 0 \le x \le 1, \\ u(0,t) = u_L, \ u(1,t) = u_R, & t \ge 0, \end{cases} \tag{2.0.1}$$

where $0 < \xi_1 < \xi_2 < ... < \xi_m < 1$, coupled with the initial-boundary value problem

$$\begin{cases} v_t + av_x = bu_x - \sum_{i=1}^{m} k_i \delta(x - \xi_i), \quad t > 0, \ \ 0 < x < 1, \\ v(x,0) = \psi(x), \quad 0 \le x \le 1, \\ v(0,t) = v_0(t), \qquad t \ge 0. \end{cases} \tag{2.0.2}$$

Here D, a, b, c_i, k_i are all given positive constants; $\varphi(x)$, $\psi(x)$, and $v_0(t)$ are given smooth functions. Note that the model (2.0.1)-(2.0.2) is an example of Advection Diffusion problem with singular source terms. We find the solution of (2.0.1)-(2.0.2) by using known analytical methods.

The analytical solution of (2.0.1) can be written as:

$$u(x,t) = U(x,t) + w(x), \quad 0 \le x \le 1, \ t \ge 0, \tag{2.0.3}$$

where $w(x)$ is the solution of the boundary problem:

$$\begin{cases} -Dw_{xx} = \sum_{i=1}^{m} c_i \delta(x - \xi_i), \quad 0 < x < 1, \\ w(0) = u_L, \ w(1) = u_R \end{cases} \tag{2.0.4}$$

and $U(x,t)$ is the solution of the initial-boundary value problem:

$$\begin{cases} U_t = D\, U_{xx}, \quad t > 0, \ \ 0 < x < 1, \\ U(x,0) = \varphi(x) - w(x), \quad 0 \le x \le 1, \\ U(0,t) = 0, \ U(1,t) = 0, \quad t \ge 0. \end{cases} \tag{2.0.5}$$

It is easy to show that the problem (2.0.4) has the following solution

$$w(x) = u_L - (u_R - u_L)\, x + \frac{1}{D} \sum_{i=1}^{m} c_i g_i(x), \tag{2.0.6}$$

where

$$g_i(x) = \begin{cases} x(1 - \xi_i), \quad \text{if} \ \ 0 \le x \le \xi_i, \\ \xi_i(1 - x), \quad \text{if} \ \ \xi_i < x \le 1. \end{cases}$$

It is well-known that the problem (2.0.5) has the following solution

$$U(x,t) = \sum_{j=1}^{\infty} r_j \exp\left(-j^2\pi^2 Dt\right) \sin(j\pi x), \tag{2.0.7}$$

where

$$r_j = 2\int_0^1 \left(\varphi(x) - w(x)\right) \sin(j\pi x) dx.$$

So, combining (2.0.3), (2.0.6) and (2.0.7), we obtain the analytical solution of (2.0.1)

$$u(x,t) = u_L - (u_R - u_L)\, x + \frac{1}{D}\sum_{i=1}^{m} c_i g_i(x) + \sum_{j=1}^{\infty} r_j \exp\left(-j^2\pi^2 Dt\right) \sin(j\pi x). \tag{2.0.8}$$

Remark 2.0.1. Note that the steady state solution of (2.0.1)

$$u^*(x) = u_L - (u_R - u_L)\, x + \frac{1}{D}\sum_{i=1}^{m} c_i g_i(x)$$

is a continuous function.

By differentiating (2.0.8) with respect to x, we have

$$\begin{aligned} u_x = u_L - u_R &+ \frac{1}{D}\sum_{i=1}^{m} c_i\Big(1 - \xi_i - H(x-\xi_i)\Big) \\ &+ \sum_{j=1}^{\infty} r_j \exp\left(-j^2\pi^2 Dt\right) \pi j \cos(j\pi x) \end{aligned} \tag{2.0.9}$$

Now, plugging (2.0.9) into the right-hand side of equation in (2.0.2) gives

$$\begin{aligned} v_t + av_x = b &\left(u_L - u_R + \frac{1}{D}\sum_{i=1}^{m} c_i\Big(1 - \xi_i - H(x-\xi_i)\Big)\right) \\ &+ b\sum_{j=1}^{\infty} r_j \exp\left(-j^2\pi^2 Dt\right) \pi j \cos(j\pi x) - \sum_{i=1}^{m} k_i \delta(x-\xi_i). \end{aligned}$$

By taking the Laplace Transform with respect to t, from the last equation we obtain

$$\begin{aligned} sV(x,s) - \psi(x) + a\frac{d}{dx}V(x,s) = \frac{b}{s} &\left(u_L - u_R + \frac{1}{D}\sum_{i=1}^{m} c_i\Big(1 - \xi_i - H(x-\xi_i)\Big)\right) \\ &+ b\sum_{j=1}^{\infty} \frac{r_j \pi j \cos(j\pi x)}{s + j^2\pi^2 D} - \frac{1}{s}\sum_{i=1}^{m} k_i \delta(x-\xi_i), \end{aligned}$$

where $V(x,s) = L\{v(x,t)\}$. Then, we have

$$\frac{d}{dx}\left(\exp\left(\frac{sx}{a}\right)V(x,s)\right) = \frac{1}{a}\exp\left(\frac{sx}{a}\right)\left[\frac{b}{s}\left(u_L - u_R + \frac{1}{D}\sum_{i=1}^{m} c_i\Big(1-\xi_i - H(x-\xi_i)\Big)\right)\right.$$
$$\left. + b\sum_{j=1}^{\infty}\frac{r_j\pi j\cos(j\pi x)}{s+j^2\pi^2 D} - \frac{1}{s}\sum_{i=1}^{m} k_i\delta(x-\xi_i) + \psi(x)\right].$$

Integrating both sides of this equation from 0 to x, we get

$$\exp\left(\frac{sx}{a}\right)V(x,s) - V_0(s) = \frac{b}{as}(u_L - u_R)\int_0^x \exp\left(\frac{s\zeta}{a}\right)d\zeta$$
$$+\frac{b}{aDs}\sum_{i=1}^{m} c_i(1-\xi_i)\int_0^x \exp\left(\frac{s\zeta}{a}\right)d\zeta$$
$$-\frac{b}{aDs}\sum_{i=1}^{m} c_i\int_0^x \exp\left(\frac{s\zeta}{a}\right)H(\zeta-\xi_i)d\zeta$$
$$+\frac{b}{a}\sum_{j=1}^{\infty}\frac{j\pi r_j}{s+j^2\pi^2 D}\int_0^x \exp\left(\frac{s\zeta}{a}\right)\cos(j\pi\zeta)d\zeta$$
$$-\frac{1}{as}\sum_{i=1}^{m} k_i\int_0^x \exp\left(\frac{s\zeta}{a}\right)\delta(\zeta-\xi_i)d\zeta + \frac{1}{a}\int_0^x \exp\left(\frac{s\zeta}{a}\right)\psi(\zeta)d\zeta,$$

where $V_0(s) = L\{v_0(t)\}$. Since

$$\int_0^x \exp\left(\frac{s\zeta}{a}\right)d\zeta = \frac{a}{s}\left(\exp\left(\frac{sx}{a}\right) - 1\right),$$

$$\int_0^x \exp\left(\frac{s\zeta}{a}\right)H(\zeta-\xi_i)d\zeta = \frac{a}{s}H(x-\xi_i)\left(\exp\left(\frac{sx}{a}\right) - \exp\left(\frac{s\xi_i}{a}\right)\right),$$

$$\int_0^x \exp\left(\frac{s\zeta}{a}\right)\delta(\zeta-\xi_i)d\zeta = \exp\left(\frac{s\xi_i}{a}\right)H(x-\xi_i),$$

$$\int_0^x \exp\left(\frac{s\zeta}{a}\right)\cos(j\pi\zeta)d\zeta = \frac{as}{s^2+a^2j^2\pi^2}\exp\left(\frac{sx}{a}\right)\cos(j\pi x)$$
$$-\frac{as}{s^2+a^2j^2\pi^2} + \frac{a^2 j\pi}{s^2+a^2j^2\pi^2}\exp\left(\frac{sx}{a}\right)\sin(j\pi x),$$

we have

$$V(x,s)=\frac{b}{s^2}(u_L-u_R)\left(1-\exp\left(-\frac{sx}{a}\right)\right)+\frac{b}{Ds^2}\sum_{i=1}^{m}c_i(1-\xi_i)\left(1-\exp\left(-\frac{sx}{a}\right)\right)$$
$$-\frac{b}{Ds^2}\sum_{i=1}^{m}c_iH(x-\xi_i)\left(1-\exp\left(-\frac{s(x-\xi_i)}{a}\right)\right)$$
$$+\frac{b}{a}\sum_{j=1}^{\infty}\frac{j\pi r_j}{s+j^2\pi^2D}\frac{as}{s^2+a^2j^2\pi^2}\cos(j\pi x)$$
$$+\frac{b}{a}\sum_{j=1}^{\infty}\frac{j\pi r_j}{s+j^2\pi^2D}\left(-\frac{as}{s^2+a^2j^2\pi^2}\exp\left(-\frac{sx}{a}\right)+\frac{a^2j\pi}{s^2+a^2j^2\pi^2}\sin(j\pi x)\right)$$
$$-\frac{1}{as}\sum_{i=1}^{m}k_i\exp\left(-\frac{s(x-\xi_i)}{a}\right)H(x-\xi_i)$$
$$+\frac{1}{a}\int_0^x\exp\left(-\frac{s(x-\zeta)}{a}\right)\psi(\zeta)d\zeta+V_0(s)\exp\left(-\frac{sx}{a}\right).$$

By using

$$L^{-1}\left(\frac{j\pi s}{(s+j^2\pi^2D)(s^2+a^2j^2\pi^2)}\right)=\pi j\frac{\pi jD\cos(\pi ajt)+a\sin(\pi ajt)}{\pi j(a^2+\pi^2D^2j^2)}$$
$$-\pi j\frac{D\exp(-Dj^2\pi^2t)}{a^2+\pi^2D^2j^2},$$

$$L^{-1}\left(\frac{j\pi s}{(s+j^2\pi^2D)(s^2+(aj\pi)^2)}\exp\left(-\frac{sx}{a}\right)\right)$$
$$=\pi jH\left(t-\frac{x}{a}\right)\frac{\pi jD\cos(\pi j(at-x))+a\sin(\pi j(at-x))}{\pi j(a^2+\pi^2D^2j^2)}$$
$$-\pi jH\left(t-\frac{x}{a}\right)\frac{D\exp\left(-Dj^2\pi^2\left(t-\frac{x}{a}\right)\right)}{a^2+\pi^2D^2j^2},$$

$$L^{-1}\left(\frac{aj^2\pi^2}{(s+j^2\pi^2D)(s^2+(aj\pi)^2)}\right)$$
$$=\frac{a\exp(-Dj^2\pi^2t)+\pi jD\sin(\pi ajt)-a\cos(\pi ajt)}{a^2+\pi^2D^2j^2},$$

we obtain the analytical solution of (2.0.2)

$$v(x,t) = b(u_L - u_R)\left(t-(t-\frac{x}{a})H(t-\frac{x}{a})\right)$$

$$+\frac{b}{D}\sum_{i=1}^{m} c_i(1-\xi_i)\left(t-(t-\frac{x}{a})H(t-\frac{x}{a})\right)$$

$$-\frac{b}{D}\sum_{i=1}^{m} c_i H(x-\xi_i)\left(t-(t-\frac{x-\xi_i}{a})H(t-\frac{x-\xi_i}{a})\right)$$

$$+b\sum_{j=1}^{\infty} r_j\left[\pi j\left(\frac{\pi jD\cos(\pi ajt)+a\sin(\pi ajt)}{\pi j(a^2+\pi^2D^2j^2)}-\frac{D\exp(-Dj^2\pi^2t)}{a^2+\pi^2D^2j^2}\right)\cos(j\pi x)\right.$$

$$-\pi jH(t-\frac{x}{a})\frac{\pi jD\cos(\pi j(at-x))+a\sin(\pi j(at-x))}{\pi j(a^2+\pi^2D^2j^2)}$$

$$+\pi jH(t-\frac{x}{a})\frac{D\exp(-Dj^2\pi^2(t-\frac{x}{a}))}{a^2+\pi^2D^2j^2}$$

$$\left.+\frac{a\exp(-Dj^2\pi^2t)+\pi jD\sin(\pi ajt)-a\cos(\pi ajt)}{a^2+\pi^2D^2j^2}\sin(j\pi x)\right]$$

$$-\frac{1}{a}\sum_{i=1}^{m} k_i H(t-\frac{x-\xi_i}{a})H(x-\xi_i)$$

$$+\frac{1}{a}\int_0^x \delta(t-\frac{x-\zeta}{a})\psi(\zeta)d\zeta + H(t-\frac{x}{a})v_0(t-\frac{x}{a})$$

or

$$v(x,t) = \frac{b}{a}\Big(x-(x-at)H(x-at)\Big)\left(u_L-u_R+\frac{1}{D}\sum_{i=1}^{m} c_i(1-\xi_i)\right)$$

$$-\frac{b}{aD}\sum_{i=1}^{m} c_i H(x-\xi_i)\Big(x-\xi_i-(x-at-\xi_i)H(x-at-\xi_i)\Big)$$

$$+b\sum_{j=1}^{\infty} r_j\left[\frac{\pi jD\cos(\pi j(at-x))+a\sin(\pi j(at-x))}{a^2+\pi^2D^2j^2}H(x-at)\right.$$

$$\left.+\frac{\exp(-Dj^2\pi^2t)}{a^2+\pi^2D^2j^2}\Big(a\sin(j\pi x)-\pi jD\cos(j\pi x)+\pi jD\exp\big(Dj^2\pi^2x\big)H(at-x)\Big)\right]$$

$$-\frac{1}{a}\sum_{i=1}^{m} k_i H(at-x+\xi_i)H(x-\xi_i)+H(x-at)\psi(x-at)+H(at-x)v_0(t-\frac{x}{a}).$$

Remark 2.0.2. The steady state solution of (2.0.2) when $v_0(t) = v_0 \equiv$ const is given by

$$v^*(x) = \frac{bx}{a}\left(u_L - u_R + \frac{1}{D}\sum_{i=1}^{m} c_i(1-\xi_i)\right) - \frac{b}{aD}\sum_{i=1}^{m} c_i(x-\xi_i)H(x-\xi_i)$$

$$-\frac{1}{a}\sum_{i=1}^{m} k_i H(x-\xi_i) + v_0.$$

Note that this steady state solution has discontinuities at all points $x = \xi_i$. When $v_0(t) \not\equiv$ const, (2.0.2) does not have a steady state solution.

CHAPTER 3

NUMERICAL SOLUTION OF DIFFUSION PROBLEMS WITH SINGULAR SOURCE TERMS

In this chapter, we discuss the numerical solution of initial-boundary value problem with singular source terms

$$\begin{cases} u_t = D\ u_{xx} + k_1\delta(x-a_1) + k_2\delta(x-a_2), \quad 0 < x < 1, \quad t > 0, \quad 0 < a_1 < a_2 < 1, \\ u(0,t) = u_L, \quad u(1,t) = u_R, \quad t \geq 0, \\ u(x,0) = \phi(x), \quad 0 \leq x \leq 1, \end{cases} \tag{3.0.1}$$

where $\delta(x)$ is a Dirac delta function. For ease of presentation, we assume that there are only two source terms. The presented material is extendable to the case with more than two source terms. Additionally, this study can be readily extended to the case with time-dependent source terms.

3.1 THE ANALYTICAL SOLUTION

Suppose that the solution of problem (3.0.1) can be written as:

$$u(x,t) = v(x,t) + w(x), \quad 0 \leq x \leq 1, \quad t \geq 0, \tag{3.1.1}$$

where $w(x)$ is the solution of boundary value problem

$$\begin{cases} -D\ w_{xx} = k_1\delta(x-a_1) + k_2\delta(x-a_2), \quad 0 < x < 1, \quad 0 < a_1 < a_2 < 1, \\ w(0) = u_L, \quad w(1) = u_R \end{cases} \tag{3.1.2}$$

and $v(x,t)$ is the solution of diffusion problem

$$\begin{cases} v_t = D\ v_{xx}, \quad 0 < x < 1, \quad t > 0, \\ v(0,t) = 0, \quad v(1,t) = 0, \quad t \geq 0, \\ v(x,0) = \phi(x) - w(x), \quad 0 \leq x \leq 1. \end{cases} \tag{3.1.3}$$

It is easy to show that problem (3.1.2) has the following formal solution

$$w(x) = \begin{cases} c_1 x + c_2, & 0 \leq x < a_1 \\ -\dfrac{k_1}{D}(x-a_1) + c_1 x + c_2, & a_1 \leq x < a_2 \\ -\dfrac{k_1}{D}(x-a_1) - \dfrac{k_2}{D}(x-a_2) + c_1 x + c_2, & a_2 \leq x \leq 1, \end{cases} \tag{3.1.4}$$

where $c_2 = u_L$ and $c_1 = u_R - u_L + \dfrac{k_1}{D}(1-a_1) + \dfrac{k_2}{D}(1-a_2)$.

It is well-known that the problem (3.1.3) has the following solution

$$v(x,t) = \sum_{k=1}^{\infty} b_k \ \exp\left(-k^2\pi^2 D t\right) \sin\left(k\pi x\right), \tag{3.1.5}$$

where

$$b_k = 2\int_0^1 \left(\phi(x)) - w(x)\right) \sin\left(k\pi x\right) dx.$$

Combining (3.1.1), (3.1.4) and (3.1.5), we obtain the solution of problem (3.0.1).

3.2 THE FINITE VOLUME APPROACH

Let $h = 1/M$ where M is the number of uniform grid cells $\Omega_i = [(i-1)h, ih]$ for $i = 1, 2, \ldots, M$ covering $[0,1]$. Let $x_i = (i - 1/2)h$ denote the cell center of Ω_i. The finite volume method for (3.0.1) amounts to first integrating (3.0.1) over Ω_i and dividing by the cell volume, which gives

$$\frac{1}{h}\int_{\Omega_i} u_t(x,t)dx = \frac{D}{h}\int_{\Omega_i} u_{xx}(x,t)dx + \frac{k_1}{h}\int_{\Omega_i} \delta(x-a_1)dx + \frac{k_2}{h}\int_{\Omega_i} \delta(x-a_2)dx \tag{3.2.1}$$

for $i = 1, 2, \ldots M$. Applying the fundamental theorem of calculus, we have

$$\begin{aligned} \frac{\partial}{\partial t}\left(\frac{1}{h}\int_{\Omega_i} u(x,t)dx\right) &= \frac{D}{h}\Big(u_x(x_{i+1/2},t) - u_x(x_{i-1/2},t)\Big) \\ &+ \frac{k_1}{h}\int_{\Omega_i} \delta(x-a_1)dx + \frac{k_2}{h}\int_{\Omega_i} \delta(x-a_2)dx, \quad i = 1, 2, \ldots M. \end{aligned} \tag{3.2.2}$$

Let us assume that $a_1 \in \Omega_{j_1}$ and $a_2 \in \Omega_{j_2}$. Then (3.2.2) becomes

$$\frac{\partial}{\partial t}\left(\frac{1}{h}\int\limits_{\Omega_i} u(x,t)dx\right) = \frac{D}{h}\Big(u_x(x_{i+1/2},t) - u_x(x_{i-1/2},t)\Big) + k_1\frac{\delta_{ij_1}}{h} + k_2\frac{\delta_{ij_2}}{h}, \quad i = 1,2,\dots M, \tag{3.2.3}$$

where δ_{ij} is the Kronecker delta symbol. Next, let us denote

$$\bar{u}_i(t) = \frac{1}{h}\int\limits_{\Omega_i} u(x,t)dx, \quad \bar{\phi}_i = \frac{1}{h}\int\limits_{\Omega_i}\phi(x)dx, \quad i = 1,2,...,M$$

and

$$\bar{U}(t) = \begin{pmatrix} \bar{u}_1(t) \\ \bar{u}_2(t) \\ \cdot \\ \cdot \\ \cdot \\ \bar{u}_M(t) \end{pmatrix}, \qquad \bar{\Phi} = \begin{pmatrix} \bar{\phi}_1 \\ \bar{\phi}_2 \\ \cdot \\ \cdot \\ \cdot \\ \bar{\phi}_M \end{pmatrix}.$$

Then, approximating $u_x(x_{i+1/2},t)$ and $u_x(x_{i-1/2},t)$ in (3.2.3) by $\big(\bar{u}_{i+1}(t) - \bar{u}_i(t)\big)/h$ and $\big(\bar{u}_i(t) - \bar{u}_{i-1}(t)\big)/h$, respectively, results in the system of linear ordinary differential equations:

$$\begin{cases} \bar{U}'(t) = A\,\bar{U}(t) + b, \quad t > 0, \\ \bar{U}(0) = \bar{\Phi}, \end{cases} \tag{3.2.4}$$

where

$$A = \frac{D}{h^2}\begin{pmatrix} -3 & 1 & & & \\ 1 & -2 & 1 & & \\ & \ddots & \ddots & \ddots & \\ & & 1 & -2 & 1 \\ & & & 1 & -3 \end{pmatrix}, \quad b = \frac{1}{h}\begin{pmatrix} 0 \\ \cdot \\ k_1 \\ \cdot \\ k_2 \\ \cdot \\ 0 \end{pmatrix}.$$

Here vector b has zero entries except at entries j_1 and j_2. Note that the values -3 at the corner entries of matrix A are due to the fact that we have chosen a cell-centered grid and have Dirichlet boundary values (Hundsdorfer and Verwer, 2003).

Now what remains is to turn the continuous time solution $\bar{U}(t)$ in a fully discrete solution by numerical time integration. We use the second order of accuracy Crank-Nicolson scheme for this.

3.3 NUMERICAL EXAMPLE

We consider the initial-boundary value problem

$$\begin{cases} u_t = u_{xx} + \delta(x - \frac{1}{3}) + \delta(x - \frac{2}{3}), \quad 0 < x < 1, \quad 0 < t < 5, \\ u(0,t) = u(1,t) = 0, \quad 0 \geq t \geq 5, \\ u(x,0) = \sin 2\pi x + z(x), \quad 0 \leq x \leq 1, \end{cases} \tag{3.3.1}$$

where

$$z(x) = \begin{cases} x, & 0 \leq x < \frac{1}{3} \\ \frac{1}{3}, & \frac{1}{3} \leq x < \frac{2}{3} \\ 1 - x, & \frac{2}{3} \leq x \leq 1 \end{cases}$$

The exact solution of the problem (3.3.1) is

$$u(x,t) = \exp\left(-4\pi^2 t\right) \sin 2\pi x + z(x), \quad 0 \leq x \leq 1, \quad 0 \leq t \leq 5. \tag{3.3.2}$$

We compute the error between the exact solution and the numerical solution by:

$$Error = \max_{\substack{1 \leq k \leq N \\ 1 \leq i \leq M}} \left| \bar{u}_i(t_k) - \bar{u}_i^k \right|,$$

where $\bar{u}_i^k$ represents the solution of the numerical scheme at $t = t_k$.

The numerical solutions are computed for different values of M, while the time step in all cases is kept fixed $\tau = 10^{-3}$. Table 3.1 shows the errors between the exact solution of the problem (3.3.1) and the numerical solutions. Note that with standard Finite Volume method we obtain the first order convergence instead of expected second order. This order reduction is due to the fact that the solution of problem (3.3.1) is not continuously differentiable and has a lack of smoothness (Ashyraliyev et al., 2008).

Table 3.1 The errors between the exact solution of problem (3.3.1) and the numerical solutions for different values of $h = 1/M$.

	$M = 20$	$M = 40$	$M = 80$	$M = 160$
Error	0.0083	0.0042	0.0021	0.0010

CHAPTER 4

FINITE DIFFERENCE METHOD VERSUS FINITE VOLUME METHOD

In this chapter, we will compare FDM (LeVeque, 2007) and FVM (LeVeque, 2002) in case of having singular source term in a simple 1-d Advection-Diffusion equation

$$u_t + au_x = du_{xx} + f(x,t), \quad 0 < x < l, \quad 0 < t < T, \tag{4.0.1}$$

where a and d are positive constants. We discuss the pitfalls in numerical integration of (4.0.1) by using FDM and FVM when the source term is singular, i.e. expression of $f(x,t)$ involves Dirac delta function.

4.1 FINITE DIFFERENCE METHOD

FDM is widely used to approximate solutions of partial differential equations. In the method, the derivatives are replaced by difference operators. For example, Crank-Nicolson difference scheme for equation (4.0.1) has the following form:

$$\begin{aligned} &\frac{u_i^{n+1} - u_i^n}{\tau} + \frac{a}{2}\left(\frac{u_{i+1}^{n+1} - u_{i-1}^{n+1}}{2h} + \frac{u_{i+1}^n - u_{i-1}^n}{2h}\right) \\ &= \frac{d}{2}\left(\frac{u_{i+1}^{n+1} - 2u_i^{n+1} + u_{i-1}^{n+1}}{h^2} + \frac{u_{i+1}^n - 2u_i^n + u_{i-1}^n}{h^2}\right) + \frac{f(x_i,t_n) + f(x_i,t_{n+1})}{2}, \end{aligned} \tag{4.1.1}$$

where u_i^n represents the numerical approximation of the solution $u(x,t)$ at $t = t_n$, $x = x_i$. It is the second order method both in space and time.

We note that scheme (4.1.1) or any other Finite Difference scheme cannot be used directly if the source term in (4.0.1) is singular, i.e. an expression of $f(x,t)$

involves Dirac delta function. In order to overcome this obstacle, normally equation (4.0.1) is regularized. For example, assume that $f(x,t) = g(t)\delta(x-\xi)$, where $g(t)$ is smooth function. Then $f(x,t)$ in (4.0.1) and therefore in (4.1.1) is replaced by function $f_\varepsilon(x,t) = g(t)\delta_\varepsilon(x-\xi)$, where $\delta_\varepsilon(x-\xi)$ is a regularization of Dirac delta function (Tornberg and Engquist, 2003), (Jung and Don, 2009). For instance, a piecewise linear function

$$\delta_\varepsilon(x-\xi) = \begin{cases} \dfrac{x-\xi+\varepsilon}{\varepsilon^2}, & \text{if } \ \xi-\varepsilon \le x \le \xi, \\ \dfrac{-x+\xi+\varepsilon}{\varepsilon^2}, & \text{if } \ \xi < x \le \xi+\varepsilon, \\ 0, & \text{if } \ x > \xi+\varepsilon \quad \text{or} \quad x < \xi-\varepsilon \end{cases} \tag{4.1.2}$$

is the simplest way to regularize $\delta(x-\xi)$ (see Figure 4.1). Other smoother regularizations are also possible (Tornberg and Engquist, 2004).

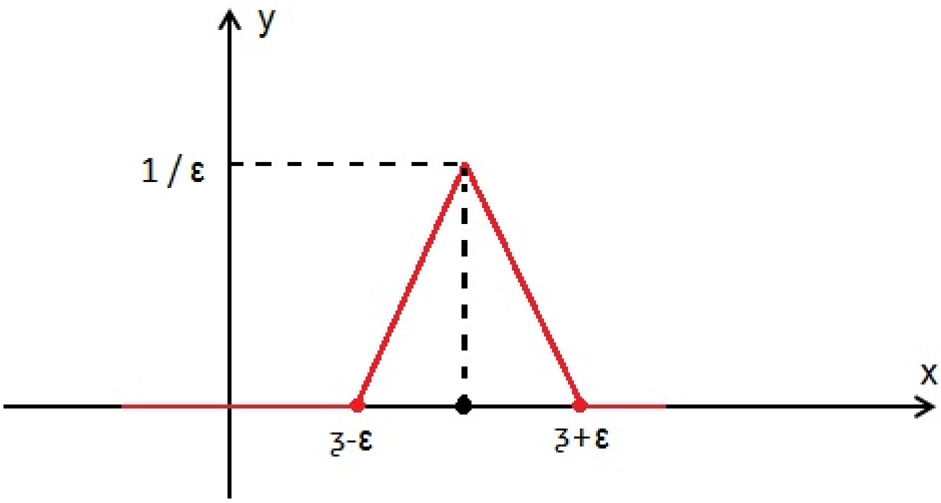

Figure 4.1 Regularization of Dirac delta function defined by (4.1.2).

When equation (4.0.1) is regularized, the first question which should be addressed is: does the solution $u_\varepsilon(x,t)$ of the regularized equation converge to the solution $u(x,t)$ of equation (4.0.1) as $\varepsilon \to 0$? If so, ε has to be chosen small enough. Moreover, for practical reasons one has to choose mesh size h in (4.1.1) smaller than 2ε. Therefore, for small value of ε really fine mesh is required for implementation of (4.1.1). For numerical illustration, we consider the following example.

Example 4.1.1. Consider initial boundary value problem:

$$\begin{cases} u_t = u_{xx} + \delta(x - \frac{1}{3}), & 0 < t < 1, \quad 0 < x < 1, \\ u(x,0) = \sin(2\pi x) + z(x), & 0 \le x \le 1, \\ u(0,t) = u(1,t) = 0, & 0 \le t \le 1, \end{cases} \tag{4.1.3}$$

where

$$z(x) = \begin{cases} \frac{2x}{3}, & 0 \le x < \frac{1}{3}, \\ \frac{1-x}{3}, & \frac{1}{3} \le x < 1. \end{cases}$$

The exact solution of the problem (4.1.3) has the form

$$u(x,t) = \exp(-4\pi^2 t) \sin(2\pi x) + z(x).$$

We first replace $\delta(x-\frac{1}{3})$ in the problem (4.1.3) with $\delta_\varepsilon(x-\frac{1}{3})$ given by (4.1.2). Next, we discretize the regularized problem bu using (4.1.1)

$$\begin{cases} \frac{u_i^{n+1} - u_i^n}{\tau} = \frac{u_{i+1}^{n+1} - 2u_i^{n+1} + u_{i-1}^{n+1}}{2h^2} + \frac{u_{i+1}^n - 2u_i^n + u_{i-1}^n}{2h^2} + \delta_\varepsilon(x_i - \frac{1}{3}), \\ i = 1, 2, \ldots, M-1, \quad n = 0, 1, \ldots, N-1, \quad hM = 1, \quad \tau N = 1, \\ u_i^0 = \sin(2\pi x_i) + z(x_i), \quad x_i = ih, \quad i = 0, 1, \ldots, M, \\ u_0^n = u_M^n = 0, \quad t_n = n\tau, \quad n = 0, 1, \ldots, N \end{cases} \tag{4.1.4}$$

We solve (4.1.4) with $N = 10^4$, $\varepsilon = 0.1$ and $\varepsilon = 0.01$ for different values of M. Table 4.1 shows the errors between the exact solution of the problem (4.1.3) and the numerical solutions computed by (4.1.4), defined by

$$\|E\|_\infty = \max_{\substack{1 \le i \le M-1 \\ 1 \le n \le N}} |u(x_i, t_n) - u_i^n| .$$

As we can see from the Table 4.1, there is no convergence for moderate values of ε. Normally, one has to tune up the value of ε in order to find sufficiently good numerical approximation of solution of the problem (4.1.3).

Table 4.1 The errors between the exact solution of the problem (4.1.3) and the numerical solutions computed by (4.1.4) with $N = 10^4$, $\varepsilon = 0.1$ and $\varepsilon = 0.01$ for different values of M.

$\epsilon = 0.1$		$\epsilon = 0.01$	
M	$\|E\|_\infty$	M	$\|E\|_\infty$
250	$1.60e-02$	250	$3.90e-03$
500	$1.63e-02$	500	$1.79e-03$
1000	$1.65e-02$	1000	$2.10e-03$
2000	$1.66e-02$	2000	$2.26e-03$

4.2 FINITE VOLUME METHOD

FVM is another common numerical method successfully used for approximating the solutions of PDEs. FVM is widely used to solve models in fluid dynamics, heat and mass transfer, Computational Biology, etc.

We illustrate here FVM for 1-dimensional Advection-Diffusion equation (4.0.1). We define the grid, cells, cell volumes and cell centers as

$$0 = x_{\frac{1}{2}} < x_{\frac{3}{2}} < x_{\frac{5}{2}} ...... < x_{M-\frac{1}{2}} < x_{M+\frac{1}{2}} = l,$$

$$\Omega_i = \left[x_{i-\frac{1}{2}}, x_{i+\frac{1}{2}}\right], \qquad |\Omega_i| = h_i = x_{i+\frac{1}{2}} - x_{i-\frac{1}{2}},$$

$$x_i = \frac{x_{i-\frac{1}{2}} + x_{i+\frac{1}{2}}}{2}, \quad i = 1, 2, ..., M,$$

respectively. Let

$$\bar{u}_i(t) = \frac{1}{h_i} \int\limits_{\Omega_i} u(x,t)dx, \quad i = 1, 2, ..., M$$

be the cell average values of function $u(x,t)$. The finite volume approach for (4.0.1) amounts to first integrating (4.0.1) over cell Ω_i and dividing by the cell volume,

$$\frac{1}{h_i} \int\limits_{\Omega_i} u_t(x,t)dx + \frac{a}{h_i} \int\limits_{\Omega_i} u_x(x,t)dx \;=\; \frac{d}{h_i} \int\limits_{\Omega_i} u_{xx}(x,t)dx + \frac{1}{h_i} \int\limits_{\Omega_i} f(x,t)dx.$$

Assuming that the mesh is uniform, we have

$$\frac{d}{dt}\bar{u}_i(t) = -\frac{a}{h}\Big(u(x_{i+\frac{1}{2}},t) - u(x_{i-\frac{1}{2}},t)\Big) + \frac{d}{h}\Big(u_x(x_{i+\frac{1}{2}},t) - u_x(x_{i-\frac{1}{2}},t)\Big) + \bar{f}_i(t), \tag{4.2.1}$$

where

$$\bar{f}_i(t) = \frac{1}{h}\int\limits_{\Omega_i} f(x,t)dx.$$

Approximating $u(x_{i+\frac{1}{2}},t)$ and $u_x(x_{i+\frac{1}{2}},t)$ in (4.2.1) by $\dfrac{\bar{u}_i(t)+\bar{u}_{i+1}(t)}{2}$ and $\dfrac{\bar{u}_{i+1}(t)-\bar{u}_i(t)}{h}$, respectively, for $i = 1, 2, ..., M$ we have

$$\frac{d}{dt}\bar{u}_i(t) = -\frac{a}{2h}\left(\bar{u}_{i+1}(t) - \bar{u}_{i-1}(t)\right) + \frac{d}{h^2}\left(\bar{u}_{i+1}(t) - 2\bar{u}_i(t) + \bar{u}_{i-1}(t)\right) + \bar{f}_i(t). \quad (4.2.2)$$

The system of ODEs (4.2.2) can be now solved by any time integrator method.

Now, assume again that the source term in (4.0.1) is singular. For example, assume that $f(x,t) = g(t)\delta(x-\xi)$, where $g(t)$ is smooth function and $\xi \in \Omega_j$. Then (4.2.2) becomes

$$\frac{d}{dt}\bar{u}_i(t) = -\frac{a}{2h}\left(\bar{u}_{i+1}(t) - \bar{u}_{i-1}(t)\right) + \frac{d}{h^2}\left(\bar{u}_{i+1}(t) - 2\bar{u}_i(t) + \bar{u}_{i-1}(t)\right) + \frac{\delta_{ij}}{h}g(t), \quad (4.2.3)$$

where

$$\delta_{ij} = \begin{cases} 0, & \text{if } i \neq j, \\ 1, & \text{if } i = j \end{cases} \quad (4.2.4)$$

is the Kronecker delta symbol.

We emphasize that the application of FVM for Advection-Diffusion equation (4.0.1) with singular source term does not require the regularization technique.

As for numerical illustration, we consider again the problem (4.1.3). Applying first FVM for spatial discretization, followed by trapezoidal method for resulting system of ODE's, we get the following scheme

$$\begin{cases} \dfrac{\bar{u}_i^{n+1} - \bar{u}_i^n}{\tau} = \dfrac{\bar{u}_{i+1}^{n+1} - 2\bar{u}_i^{n+1} + \bar{u}_{i-1}^{n+1}}{2h^2} + \dfrac{\bar{u}_{i+1}^{n} - 2\bar{u}_i^{n} + \bar{u}_{i-1}^{n}}{2h^2} + \dfrac{\delta_{ij}}{h}, \\ i = 2, 3, \ldots, M-1, \quad n = 0, 1, \ldots, N-1, \quad hM = 1, \quad \tau N = 1, \\ \dfrac{\bar{u}_1^{n+1} - \bar{u}_1^n}{\tau} = \dfrac{\bar{u}_2^{n+1} - 3\bar{u}_1^{n+1}}{2h^2} + \dfrac{\bar{u}_2^{n} - 3\bar{u}_1^{n}}{2h^2} + \dfrac{\delta_{1j}}{h}, \\ \dfrac{\bar{u}_M^{n+1} - \bar{u}_M^n}{\tau} = \dfrac{\bar{u}_{M-1}^{n+1} - 3\bar{u}_M^{n+1}}{2h^2} + \dfrac{\bar{u}_{M-1}^{n} - 3\bar{u}_M^{n}}{2h^2} + \dfrac{\delta_{Mj}}{h}, \\ \bar{u}_i^o = \dfrac{\cos(\pi(2x_i - h)) - \cos(\pi(2x_i + h))}{2\pi h} + \bar{z}_i, \quad i = 1, 2, \ldots, M. \end{cases} \quad (4.2.5)$$

Here

$$\bar{z}_i = \begin{cases} \dfrac{2x_i}{3}, & \text{if} \quad i = 1, \dots, j-1, \\ \dfrac{1-x_i}{3}, & \text{if} \quad i = j+1, \dots, M, \\ \dfrac{1}{h}\left[\dfrac{1}{9} - \dfrac{1}{3}\left(x_i - \dfrac{h}{2}\right)^2 - \dfrac{1}{6}\left(1 - x_i - \dfrac{h}{2}\right)^2\right], & \text{if} \quad i = j, \end{cases}$$

where j is the index of the cell which contains the point $x = \frac{1}{3}$.

We solve (4.2.5) with $N = 10^4$ for different values of M. Table 4.2 shows the errors between the exact solution of the problem (4.1.3) and the numerical solutions computed by (4.2.5), defined by

$$\|E\|_\infty = \max_{\substack{1 \le i \le M \\ 1 \le n \le N}} \left| u(x_i, t_n) - \bar{u}_i^n \right|.$$

Table 4.2 The errors between the exact solution of the problem (4.1.3) and the numerical solutions computed by (4.2.5) with $N = 10^4$ for different values of M.

M	$\|E\|_\infty$
250	$4.853974e-04$
500	$2.866981e-04$
1000	$1.549177e-04$
2000	$8.039052e-05$

As we can see from the Table 4.2, there is a first order convergence in space. We note that the order reduction from two to one occurs here due to lack of smoothness in the solution of problem (4.1.3). However, FVM applied to problem (4.1.3) still gives a better numerical approximation of solution than FDM does. It shows the advantage of using FVM for numerical solutions of PDE's having singular source terms.

CHAPTER 5

CONSTRUCTION OF WENO APPROXIMATIONS ON NON-UNIFORM MESHES

WENO approximations can be applied both in the Finite Difference and the Finite Volume Methods. In this work, we consider only the WENO approaches suitable for Finite Volume Methods. The core of the WENO method is based on the polynomial interpolation. First, interpolations by using lower order polynomials are constructed on different stencils. Then, convex combination of these approximations is used to get the higher order approximation. In this chapter, we present the construction of third and fifth order WENO methods (WENO3 and WENO5, respectively) on non-uniform meshes.

We define the grid, cells, cell volumes and cell centers as

$$0 = x_{\frac{1}{2}} < x_{\frac{3}{2}} < x_{\frac{5}{2}} < \ldots < x_{M-\frac{1}{2}} < x_{M+\frac{1}{2}} = l,$$

$$\Omega_i = \left[x_{i-\frac{1}{2}}, x_{i+\frac{1}{2}}\right], \qquad |\Omega_i| = h_i = x_{i+\frac{1}{2}} - x_{i-\frac{1}{2}},$$

$$x_i = \frac{x_{i-\frac{1}{2}} + x_{i+\frac{1}{2}}}{2}, \qquad i = 1, 2, \ldots, M,$$

respectively (see Figure 5.1).

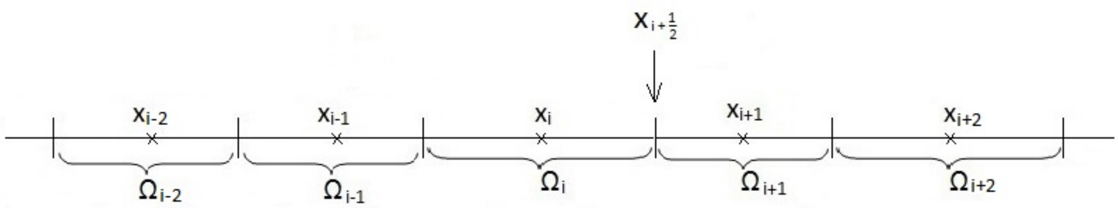

Figure 5.1 Cells and cell centers.

Assume that cell average values of some function $u(x)$, defined as

$$\bar{u}_i = \frac{1}{h_i} \int\limits_{\Omega_i} u(x)dx, \quad i = 1, 2, \ldots, M,$$

are given. The aim of the WENO methods is to find the approximation formulas for $u(x)$ at the cell boundary $x = x_{i+\frac{1}{2}}$ (see Figure 5.1). The order of approximation formula defines the order of the WENO method.

5.1 CONSTRUCTION OF WENO3 METHOD

WENO3 method is based on approximation by using linear polynomials. Firstly, we consider the stencil $S_0 = \{\Omega_{i-1}, \Omega_i\}$ (see Figure 5.1). It is obvious that there is a unique linear polynomial whose cell average values on stencil S_0 agree with corresponding cell average values of function $u(x)$ on S_0. We search this polynomial in the following form:

$$p_0^{(i)}(x) = a_0^{(i)}(x - x_i) + b_0^{(i)}. \tag{5.1.1}$$

Then,

$$\begin{cases} \dfrac{1}{h_{i-1}} \displaystyle\int\limits_{\Omega_{i-1}} p_0^{(i)}(x)dx = \bar{u}_{i-1}, \\ \\ \dfrac{1}{h_i} \displaystyle\int\limits_{\Omega_i} p_0^{(i)}(x)dx = \bar{u}_i. \end{cases} \tag{5.1.2}$$

Plugging (5.1.1) into (5.1.2) and evaluating integrals, we obtain:

$$\begin{cases} -\dfrac{h_{i-1} + h_i}{2} a_0^{(i)} + b_0^{(i)} = \bar{u}_{i-1}, \\ \\ b_0^{(i)} = \bar{u}_i. \end{cases}$$

Solving this system, we get

$$a_0^{(i)} = \frac{2}{h_{i-1} + h_i}(\bar{u}_i - \bar{u}_{i-1}), \quad b_0^{(i)} = \bar{u}_i. \tag{5.1.3}$$

Then, the approximation $u^{(0)}_{i+\frac{1}{2}}$ for function $u(x)$ at $x = x_{i+\frac{1}{2}}$ using the polynomial $p_0^{(i)}(x)$ has the form:

$$u^{(0)}_{i+\frac{1}{2}} = p_0^{(i)}(x_{i+\frac{1}{2}}) = \frac{h_i}{2} a_0^{(i)} + b_0^{(i)}$$

or

$$u^{(0)}_{i+\frac{1}{2}} = -\frac{h_i}{h_{i-1}+h_i}\bar{u}_{i-1} + \frac{h_{i-1}+2h_i}{h_{i-1}+h_i}\bar{u}_i. \tag{5.1.4}$$

Remark 5.1.1. In case of uniform grid, i.e. when $h_i = h_{i-1} = h$, from (5.1.4) we have

$$u^{(0)}_{i+\frac{1}{2}} = -\frac{\bar{u}_{i-1}}{2} + \frac{3\bar{u}_i}{2}$$

as in (Barth and Deconinck, 1999).

Theorem 5.1.2. If $u(x)$ is sufficiently smooth on stencil S_0 then for approximation (5.1.4) we have

$$u^{(0)}_{i+\frac{1}{2}} = u(x_{i+\frac{1}{2}}) + O\Big(h_i(h_{i-1}+h_i)\Big). \tag{5.1.5}$$

Proof Using the Taylor's formula, we have

$$\begin{aligned} u^{(0)}_{i+\frac{1}{2}} &= -\frac{h_i}{h_{i-1}+h_i}\bar{u}_{i-1} + \frac{h_{i-1}+2h_i}{h_{i-1}+h_i}\bar{u}_i \\ &= -\frac{h_i}{h_{i-1}(h_{i-1}+h_i)}\int\limits_{\Omega_{i-1}} u(x)dx + \frac{h_{i-1}+2h_i}{h_i(h_{i-1}+h_i)}\int\limits_{\Omega_i} u(x)dx \end{aligned}$$

$$= \frac{-h_i}{h_{i-1}(h_{i-1}+h_i)}\int\limits_{\Omega_{i-1}}\left(u(x_{i+\frac{1}{2}}) + (x-x_{i+\frac{1}{2}})u'(x_{i+\frac{1}{2}}) + \frac{(x-x_{i+\frac{1}{2}})^2}{2}u''(x_{i+\frac{1}{2}}) + \dots\right)dx$$

$$+ \frac{h_{i-1}+2h_i}{h_i(h_{i-1}+h_i)}\int\limits_{\Omega_i}\left(u(x_{i+\frac{1}{2}}) + (x-x_{i+\frac{1}{2}})u'(x_{i+\frac{1}{2}}) + \frac{(x-x_{i+\frac{1}{2}})^2}{2}u''(x_{i+\frac{1}{2}}) + \dots\right)dx$$

$$= u(x_{i+\frac{1}{2}}) - \frac{h_i\,(h_{i-1}+h_i)}{6}u''(x_{i+\frac{1}{2}}) + h.o.t.$$

Corollary 5.1.3. Formula (5.1.5) implies that (5.1.4) is the second order approximation for u(x) at $x = x_{i+\frac{1}{2}}$.

Remark 5.1.4. In case of uniform grid, i.e. when $h_i = h_{i-1} = h$, we have

$$u^{(0)}_{i+\frac{1}{2}} = u(x_{i+\frac{1}{2}}) + O\left(h^2\right)$$

as in (Barth and Deconinck, 1999).

Now, we consider the stencil $S_1 = \{\Omega_i, \Omega_{i+1}\}$ (see Figure 5.1). Obviously, there is a unique linear polynomial whose cell average values on stencil S_1 agree with corresponding cell average values of function $u(x)$ on S_1. We search this polynomial in the following form:

$$p_1^{(i)}(x) = a_1^{(i)}(x - x_i) + b_1^{(i)}. \tag{5.1.6}$$

Then,

$$\begin{cases} \dfrac{1}{h_i}\displaystyle\int\limits_{\Omega_i} p_1^{(i)}(x)dx = \bar{u}_i, \\ \\ \dfrac{1}{h_{i+1}}\displaystyle\int\limits_{\Omega_{i+1}} p_1^{(i)}(x)dx = \bar{u}_{i+1}. \end{cases} \tag{5.1.7}$$

Plugging (5.1.6) into (5.1.7) and evaluating integrals, we obtain:

$$\begin{cases} b_1^{(i)} = \bar{u}_i, \\ \dfrac{h_i + h_{i+1}}{2} a_1^{(i)} + b_1^{(i)} = \bar{u}_{i+1}. \end{cases}$$

Solving this system, we get

$$a_1^{(i)} = \frac{2}{h_i + h_{i+1}}(\bar{u}_{i+1} - \bar{u}_i), \quad b_1^{(i)} = \bar{u}_i. \tag{5.1.8}$$

Then, the approximation $u^{(1)}_{i+\frac{1}{2}}$ for function $u(x)$ at $x = x_{i+\frac{1}{2}}$ using the polynomial $p_1^{(i)}(x)$ has the form:

$$u^{(1)}_{i+\frac{1}{2}} = p_1^{(i)}(x_{i+\frac{1}{2}}) = \frac{h_i}{2} a_1^{(i)} + b_1^{(i)}$$

or

$$u^{(1)}_{i+\frac{1}{2}} = \frac{h_{i+1}}{h_i + h_{i+1}}\bar{u}_i + \frac{h_i}{h_i + h_{i+1}}\bar{u}_{i+1}. \tag{5.1.9}$$

Remark 5.1.5. In case of uniform grid, i.e. when $h_i = h_{i+1} = h$, we have

$$u^{(1)}_{i+\frac{1}{2}} = \frac{\bar{u}_i}{2} + \frac{\bar{u}_{i+1}}{2}$$

as in (Barth and Deconinck, 1999).

Theorem 5.1.6. If $u(x)$ is sufficiently smooth on stencil S_1 then for approximation (5.1.9) we have

$$u^{(1)}_{i+\frac{1}{2}} = u(x_{i+\frac{1}{2}}) + O\Big(h_i h_{i+1}\Big). \tag{5.1.10}$$

Proof Using the Taylor's formula, we have

$$u^{(1)}_{i+\frac{1}{2}} = \frac{h_{i+1}}{h_i+h_{i+1}}\bar{u}_i + \frac{h_i}{h_i+h_{i+1}}\bar{u}_{i+1}$$

$$= \frac{h_{i+1}}{h_i(h_i+h_{i+1})}\int\limits_{\Omega_i} u(x)dx \ + \ \frac{h_i}{h_{i+1}(h_i+h_{i+1})}\int\limits_{\Omega_{i+1}} u(x)dx$$

$$= \frac{h_{i+1}}{h_i(h_i+h_{i+1})}\int\limits_{\Omega_i}\left(u(x_{i+\frac{1}{2}}) + (x-x_{i+\frac{1}{2}})u'(x_{i+\frac{1}{2}}) + \frac{(x-x_{i+\frac{1}{2}})^2}{2}u''(x_{i+\frac{1}{2}}) + \dots\right)dx$$

$$+ \frac{h_i}{h_{i+1}(h_i+h_{i+1})}\int\limits_{\Omega_{i+1}}\left(u(x_{i+\frac{1}{2}}) + (x-x_{i+\frac{1}{2}})u'(x_{i+\frac{1}{2}}) + \frac{(x-x_{i+\frac{1}{2}})^2}{2}u''(x_{i+\frac{1}{2}}) + \dots\right)dx$$

$$= u(x_{i+\frac{1}{2}}) \ + \ \frac{h_i h_{i+1}}{6}u''(x_{i+\frac{1}{2}}) \ + \ h.o.t.$$

Corollary 5.1.7. Formula (5.1.10) implies that (5.1.9) is the second order approximation for function u(x) at $x = x_{i+\frac{1}{2}}$.

Remark 5.1.8. In case of uniform grid, i.e. when $h_i = h_{i+1} = h$, we have

$$u^{(1)}_{i+\frac{1}{2}} = u(x_{i+\frac{1}{2}}) + O\left(h^2\right)$$

as in (Barth and Deconinck, 1999).

Finally, we consider extended stencil $S = S_0 \cup S_1 = \{\Omega_{i-1}, \Omega_i, \Omega_{i+1}\}$. There is a unique quadratic polynomial whose cell average values on stencil S agree with corresponding cell average values of function $u(x)$ on S. We search this polynomial in the following form:

$$P^{(i)}(x) = a^{(i)}(x-x_i)^2 + b^{(i)}(x-x_i) + c^{(i)}. \tag{5.1.11}$$

Then,

$$\begin{cases} \dfrac{1}{h_{i-1}}\displaystyle\int\limits_{\Omega_{i-1}} P^{(i)}(x)dx = \bar{u}_{i-1}, \\ \dfrac{1}{h_i}\displaystyle\int\limits_{\Omega_i} P^{(i)}(x)dx = \bar{u}_i, \\ \dfrac{1}{h_{i+1}}\displaystyle\int\limits_{\Omega_{i+1}} P^{(i)}(x)dx = \bar{u}_{i+1}. \end{cases} \tag{5.1.12}$$

Plugging (5.1.11) into (5.1.12) and evaluating integrals, we obtain:

$$\begin{cases} \left(\dfrac{h_{i-1}^2}{3} + \dfrac{h_{i-1}h_i}{2} + \dfrac{h_i^2}{4}\right) a^{(i)} - \dfrac{h_{i-1}+h_i}{2} b^{(i)} + c^{(i)} = \bar{u}_{i-1}, \\ \dfrac{h_i^2}{12} a^{(i)} + c^{(i)} = \bar{u}_i, \\ \left(\dfrac{h_i^2}{4} + \dfrac{h_i h_{i+1}}{2} + \dfrac{h_{i+1}^2}{3}\right) a^{(i)} + \dfrac{h_i + h_{i+1}}{2} b^{(i)} + c^{(i)} = \bar{u}_{i+1}. \end{cases}$$

Solving this system, we get

$$\begin{aligned} a^{(i)} = \;& \frac{3}{(h_{i-1}+h_i)(h_{i-1}+h_i+h_{i+1})}\bar{u}_{i-1} \\ & - \frac{3(h_{i-1}+2h_i+h_{i+1})}{(h_{i-1}+h_i)(h_i+h_{i+1})(h_{i-1}+h_i+h_{i+1})}\bar{u}_i \\ & + \frac{3}{(h_i+h_{i+1})(h_{i-1}+h_i+h_{i+1})}\bar{u}_{i+1}, \\ b^{(i)} = \;& -\frac{h_i+2h_{i+1}}{(h_{i-1}+h_i)(h_{i-1}+h_i+h_{i+1})}\bar{u}_{i-1} \\ & + \frac{(h_{i+1}-h_{i-1})(2h_{i-1}+3h_i+2h_{i+1})}{(h_{i-1}+h_i)(h_i+h_{i+1})(h_{i-1}+h_i+h_{i+1})}\bar{u}_i \\ & + \frac{2h_{i-1}+h_i}{(h_i+h_{i+1})(h_{i-1}+h_i+h_{i+1})}\bar{u}_{i+1}, \\ c^{(i)} = \;& -\frac{h_i^2}{4(h_{i-1}+h_i)(h_{i-1}+h_i+h_{i+1})}\bar{u}_{i-1} \\ & + \left(1 + \frac{h_i^2(h_{i-1}+2h_i+h_{i+1})}{4(h_{i-1}+h_i)(h_i+h_{i+1})(h_{i-1}+h_i+h_{i+1})}\right)\bar{u}_i \\ & - \frac{h_i^2}{4(h_i+h_{i+1})(h_{i-1}+h_i+h_{i+1})}\bar{u}_{i+1}. \end{aligned}$$

Then, the approximation $u_{i+\frac{1}{2}}$ for function $u(x)$ at $x = x_{i+\frac{1}{2}}$ using the polynomial $P^{(i)}(x)$ has the form:

$$u_{i+\frac{1}{2}} = P^{(i)}(x_{i+\frac{1}{2}}) = \frac{h_i^2}{4}a^{(i)} + \frac{h_i}{2}b^{(i)} + c^{(i)}$$

or

$$u_{i+\frac{1}{2}} = -\frac{h_i h_{i+1}}{(h_{i-1}+h_i)(h_{i-1}+h_i+h_{i+1})}\bar{u}_{i-1}$$

$$+\left(1+\frac{h_i h_{i+1}}{(h_{i-1}+h_i)(h_{i-1}+h_i+h_{i+1})}-\frac{h_i(h_{i-1}+h_i)}{(h_i+h_{i+1})(h_{i-1}+h_i+h_{i+1})}\right)\bar{u}_i$$

$$+\frac{h_i(h_{i-1}+h_i)}{(h_i+h_{i+1})(h_{i-1}+h_i+h_{i+1})}\bar{u}_{i+1}. \tag{5.1.13}$$

Remark 5.1.9. In case of uniform grid, i.e. when $h_{i-1} = h_i = h_{i+1} = h$, we have

$$u_{i+\frac{1}{2}} = -\frac{\bar{u}_{i-1}}{6}+\frac{5\bar{u}_i}{6}+\frac{\bar{u}_{i+1}}{3}$$

as in (Barth and Deconinck, 1999).

Theorem 5.1.10. If $u(x)$ is sufficiently smooth on stencil S then for approximation (5.1.13) we have

$$u_{i+\frac{1}{2}} = u(x_{i+\frac{1}{2}}) + O\Big(h_i h_{i+1}(h_{i-1}+h_i)\Big). \tag{5.1.14}$$

Proof Using the Taylor's formula

$$u(x) = u(x_{i+\frac{1}{2}})+(x-x_{i+\frac{1}{2}})u'(x_{i+\frac{1}{2}})+\frac{(x-x_{i+\frac{1}{2}})^2}{2}u''(x_{i+\frac{1}{2}})+\frac{(x-x_{i+\frac{1}{2}})^3}{6}u'''(x_{i+\frac{1}{2}})+\dots$$

we have

$$\bar{u}_{i-1} = \frac{1}{h_{i-1}}\int\limits_{\Omega_{i-1}} u(x)dx = u(x_{i+\frac{1}{2}}) - \frac{h_{i-1}+2h_i}{2}u'(x_{i+\frac{1}{2}})$$

$$+\frac{3h_i^2+3h_ih_{i-1}+h_{i-1}^2}{6}u''(x_{i+\frac{1}{2}}) - \frac{4h_i^3+6h_i^2h_{i-1}+4h_ih_{i-1}^2+h_{i-1}^3}{24}u'''(x_{i+\frac{1}{2}}) + h.o.t.,$$

$$\bar{u}_i = \frac{1}{h_i}\int\limits_{\Omega_i} u(x)dx = u(x_{i+\frac{1}{2}}) - \frac{h_i}{2}u'(x_{i+\frac{1}{2}}) + \frac{h_i^2}{6}u''(x_{i+\frac{1}{2}}) - \frac{h_i^3}{24}u'''(x_{i+\frac{1}{2}}) + h.o.t.,$$

$$\bar{u}_{i+1} = \frac{1}{h_{i+1}}\int\limits_{\Omega_{i+1}} u(x)dx = u(x_{i+\frac{1}{2}}) + \frac{h_{i+1}}{2}u'(x_{i+\frac{1}{2}}) + \frac{h_{i+1}^2}{6}u''(x_{i+\frac{1}{2}})$$

$$+\tfrac{h_{i+1}^3}{24}u'''(x_{i+\frac{1}{2}}) + h.o.t.$$

Putting all these in (5.1.13) and making simplifications, we obtain

$$u_{i+\frac{1}{2}} = u(x_{i+\frac{1}{2}}) + \frac{h_ih_{i+1}(h_{i-1}+h_i)}{24}u'''(x_{i+\frac{1}{2}}) + h.o.t.$$

Corollary 5.1.11. Formula (5.1.14) implies that (5.1.13) is the third order approximation for function $u(x)$ at $x = x_{i+\frac{1}{2}}$.

Remark 5.1.12. In case of uniform grid, i.e. when $h_{i-1} = h_i = h_{i+1} = h$, we have

$$u_{i+\frac{1}{2}} \;=\; u(x_{i+\frac{1}{2}}) + O\left(h^3\right)$$

as in (Barth and Deconinck, 1999).

The following result states that third order approximation $u_{i+\frac{1}{2}}$ given by (5.1.13) can be written as a linear combination of second order approximations $u^{(0)}_{i+\frac{1}{2}}$ and $u^{(1)}_{i+\frac{1}{2}}$ given by (5.1.4) and (5.1.9), respectively.

Theorem 5.1.13. There exist unique $\gamma_0^{(i)}$ and $\gamma_1^{(i)}$ values such that

$$u_{i+\frac{1}{2}} = \gamma_0^{(i)} u^{(0)}_{i+\frac{1}{2}} + \gamma_1^{(i)} u^{(1)}_{i+\frac{1}{2}} \tag{5.1.15}$$

holds.

Proof Using (5.1.4), (5.1.9) and (5.1.13), equality (5.1.15) can be rewritten as

$$-\frac{h_i h_{i+1}}{(h_{i-1}+h_i)(h_{i-1}+h_i+h_{i+1})}\bar{u}_{i-1}$$

$$\left(1+\frac{h_i h_{i+1}}{(h_{i-1}+h_i)(h_{i-1}+h_i+h_{i+1})}-\frac{h_i(h_{i-1}+h_i)}{(h_i+h_{i+1})(h_{i-1}+h_i+h_{i+1})}\right)\bar{u}_i$$

$$+\frac{h_i(h_{i-1}+h_i)}{(h_i+h_{i+1})(h_{i-1}+h_i+h_{i+1})}\bar{u}_{i+1}$$

$$= \gamma_0^{(i)}\left(-\frac{h_i}{h_{i-1}+h_i}\bar{u}_{i-1}+\frac{h_{i-1}+2h_i}{h_{i-1}+h_i}\bar{u}_i\right)+\gamma_1^{(i)}\left(\frac{h_{i+1}}{h_i+h_{i+1}}\bar{u}_i+\frac{h_i}{h_i+h_{i+1}}\bar{u}_{i+1}\right)$$

It is easy to verify that last equality and therefore (5.1.15) holds if and only if

$$\gamma_0^{(i)} = \frac{h_{i+1}}{h_{i-1}+h_i+h_{i+1}}, \quad \gamma_1^{(i)} = \frac{h_{i-1}+h_i}{h_{i-1}+h_i+h_{i+1}} \tag{5.1.16}$$

In WENO literature, $\gamma_0^{(i)}$ and $\gamma_1^{(i)}$ are called **linear weights**. Note that in case of uniform grid, i.e. when $h_{i-1} = h_i = h_{i+1} = h$, from (5.1.16) we have $\gamma_0^{(i)} = \dfrac{1}{3}$ and $\gamma_1^{(i)} = \dfrac{2}{3}$. So, in case of uniform grid the linear weights are independent of index i.

To summarize, if $u(x)$ is sufficiently smooth on the extended stencil S then the linear combination $\gamma_0^{(i)} u_{i+\frac{1}{2}}^{(0)} + \gamma_1^{(i)} u_{i+\frac{1}{2}}^{(1)}$, where linear weights $\gamma_0^{(i)}$ and $\gamma_1^{(i)}$ are defined by (5.1.16), results in a third order approximation for $u(x)$ at $x = x_{i+\frac{1}{2}}$. Moreover, if $u(x)$ is sufficiently smooth on stencil S, then

$$\gamma_0^{(i)} u_{i+\frac{1}{2}}^{(0)} + \gamma_1^{(i)} u_{i+\frac{1}{2}}^{(1)} = u(x_{i+\frac{1}{2}}) + O\Big(h_i h_{i+1}(h_{i-1} + h_i)\Big) \tag{5.1.17}$$

holds.

Now, suppose that $u(x)$ is smooth everywhere on the extended stencil S except one point of cell Ω_{i-1}, where $u(x)$ or derivative of $u(x)$ is discontinuous. Then (5.1.17) obviously does not hold, i.e. (5.1.15) is not the third order approximation for $u(x)$ at $x = x_{i+\frac{1}{2}}$. However, since $u(x)$ is smooth in Ω_i and Ω_{i+1}, (5.1.15) gives the second order approximation if one chooses $\gamma_0^{(i)} = 0$ and $\gamma_1^{(i)} = 1$.

Similarly, assume that $u(x)$ is smooth everywhere on the extended stencil S except one point of cell Ω_{i+1}, where $u(x)$ or derivative of $u(x)$ is discontinuous. Then (5.1.17) does not hold and therefore (5.1.15) is not the third order approximation for $u(x)$ at $x = x_{i+\frac{1}{2}}$. However, since $u(x)$ is smooth in Ω_{i-1} and Ω_i, (5.1.15) gives the second order approximation if one chooses $\gamma_0^{(i)} = 1$ and $\gamma_1^{(i)} = 0$.

We note that when $u(x)$ is smooth everywhere on the extended stencil S except one point of cell Ω_i, approximation (5.1.15) is not consistent. It is due to the fact that $u(x)$ is not smooth on both stencils S_0 and S_1, and therefore both approximation formulas (5.1.4) and (5.1.9) are inconsistent. Unfortunately, this kind of local inconsistency cannot be eliminated and therefore one has to anticipate the order reduction when WENO approximations are used for solving problems with non-smooth solutions.

Linear weights $\gamma_0^{(i)}$ and $\gamma_1^{(i)}$ defined by (5.1.16) are independent of $u(x)$. Therefore, these weights cannot be used when $u(x)$ is non-smooth. The purpose of the WENO3 method is to find the approximation of $u(x_{i+\frac{1}{2}})$ by using a convex combination of approximations $u_{i+\frac{1}{2}}^{(0)}$ and $u_{i+\frac{1}{2}}^{(1)}$ defined by (5.1.4) and (5.1.9), respectively. In other words, (5.1.15) is replaced with:

$$u_{i+\frac{1}{2}} = \omega_0^{(i)} u_{i+\frac{1}{2}}^{(0)} + \omega_1^{(i)} u_{i+\frac{1}{2}}^{(1)} \tag{5.1.18}$$

where $\omega_0^{(i)} \geq 0$ and $\omega_1^{(i)} \geq 0$ are called **nonlinear weights** and $\omega_0^{(i)} + \omega_1^{(i)} = 1$.

Lemma 5.1.14. Assume that $u(x)$ is sufficiently smooth on the extended stencil S. If

$$\omega_0^{(i)} = \gamma_0^{(i)} + O\Big(h_{i-1} + h_i + h_{i+1}\Big), \qquad \omega_1^{(i)} = \gamma_1^{(i)} + O\Big(h_{i-1} + h_i + h_{i+1}\Big), \quad (5.1.19)$$

then (5.1.18) is the third order approximation for $u(x)$ at $x = x_{i+\frac{1}{2}}$.

Proof Using (5.1.5), (5.1.10), (5.1.17) and (5.1.19), for (5.1.18) we have

$$u_{i+\frac{1}{2}} \;=\; \omega_0^{(i)} u_{i+\frac{1}{2}}^{(0)} \;+\; \omega_1^{(i)} u_{i+\frac{1}{2}}^{(1)}$$

$$= \Big(\omega_0^{(i)} - \gamma_0^{(i)}\Big)\, u_{i+\frac{1}{2}}^{(0)} \;+\; \Big(\omega_1^{(i)} - \gamma_1^{(i)}\Big)\, u_{i+\frac{1}{2}}^{(1)} \;+\; \gamma_0^{(i)} u_{i+\frac{1}{2}}^{(0)} \;+\; \gamma_1^{(i)} u_{i+\frac{1}{2}}^{(1)}$$

$$= \Big(\omega_0^{(i)} - \gamma_0^{(i)}\Big)\Big(u_{i+\frac{1}{2}}^{(0)} - u(x_{i+\frac{1}{2}})\Big) \;+\; \Big(\omega_1^{(i)} - \gamma_1^{(i)}\Big)\Big(u_{i+\frac{1}{2}}^{(1)} - u(x_{i+\frac{1}{2}})\Big)$$

$$+\; \gamma_0^{(i)} u_{i+\frac{1}{2}}^{(0)} \;+\; \gamma_1^{(i)} u_{i+\frac{1}{2}}^{(1)} \;=\; u(x_{i+\frac{1}{2}}) + \Big(\omega_0^{(i)} - \gamma_0^{(i)}\Big)\cdot O\Big(h_i(h_{i-1} + h_i)\Big)$$

$$+\; \Big(\omega_1^{(i)} - \gamma_1^{(i)}\Big)\cdot O\Big(h_i h_{i+1}\Big) \;+\; O\Big(h_i h_{i+1}(h_{i-1} + h_i)\Big)$$

$$= \; u(x_{i+\frac{1}{2}}) \;+\; O\Big(h_i\,(h_{i-1} + h_i + h_{i+1})^2\Big)$$

In order to define the nonlinear weights $\omega_0^{(i)}$ and $\omega_1^{(i)}$ in (5.1.18), we first introduce so-called smoothness indicators $\beta_0^{(i)}$ and $\beta_1^{(i)}$ to measure the smoothness of $u(x)$ in stencils S_0 and S_1, respectively. Interpolating polynomials (5.1.1) and (5.1.6) are used to define the smoothness indicators in the following way:

$$\beta_0^{(i)} = h_i \int\limits_{\Omega_i} \left(\frac{d}{dx} p_0^{(i)}(x)\right)^2 dx = h_i \int\limits_{\Omega_i} \left(a_0^{(i)}\right)^2 dx = \left(h_i a_0^{(i)}\right)^2 = \frac{4h_i^2(\bar{u}_i - \bar{u}_{i-1})^2}{(h_{i-1} + h_i)^2},$$

$$\beta_1^{(i)} = h_i \int\limits_{\Omega_i} \left(\frac{d}{dx} p_1^{(i)}(x)\right)^2 dx = h_i \int\limits_{\Omega_i} \left(a_1^{(i)}\right)^2 dx = \left(h_i a_1^{(i)}\right)^2 = \frac{4h_i^2(\bar{u}_{i+1} - \bar{u}_i)^2}{(h_i + h_{i+1})^2}. \quad (5.1.20)$$

Now, normalized nonlinear weights in (5.1.18) are defined as following:

$$\omega_0^{(i)} = \frac{\tilde{\omega}_0^{(i)}}{\tilde{\omega}_0^{(i)} + \tilde{\omega}_1^{(i)}}, \qquad \omega_1^{(i)} = \frac{\tilde{\omega}_1^{(i)}}{\tilde{\omega}_0^{(i)} + \tilde{\omega}_1^{(i)}}, \quad (5.1.21)$$

where

$$\tilde{\omega}_0^{(i)} = \frac{\gamma_0^{(i)}}{\left(\epsilon + \beta_0^{(i)}\right)^2}, \qquad \tilde{\omega}_1^{(i)} = \frac{\gamma_1^{(i)}}{\left(\epsilon + \beta_1^{(i)}\right)^2}. \quad (5.1.22)$$

Here, $\epsilon = 10^{-6}$ is taken to prevent the denominators becoming zero.

Lemma 5.1.15. Assume that $u(x)$ is sufficiently smooth on the extended stencil S. If there is non-zero constant D such that

$$\beta_0^{(i)} = D\Big(1 + O\left(h_{i-1} + h_i\right)\Big), \qquad \beta_1^{(i)} = D\Big(1 + O\left(h_i + h_{i+1}\right)\Big) \tag{5.1.23}$$

then the nonlinear weights $\omega_0^{(i)}$ and $\omega_1^{(i)}$, defined by (5.1.21)-(5.1.22), satisfy (5.1.19) and therefore (5.1.18) results in the third order approximation for $u(x)$ at $x = x_{i+\frac{1}{2}}$.

Proof Putting (5.1.23) in (5.1.22) and using the Taylor expansion, we first obtain

$$\tilde{\omega}_0^{(i)} = \frac{\gamma_0^{(i)}}{(\epsilon + D)^2} + O\big(h_{i-1} + h_i\big), \qquad \tilde{\omega}_1^{(i)} = \frac{\gamma_1^{(i)}}{(\epsilon + D)^2} + O\big(h_i + h_{i+1}\big).$$

Then, putting these in (5.1.21) and using again the Taylor expansion gives (5.1.19).

Theorem 5.1.16. Assume that $u(x)$ is sufficiently smooth on the extended stencil S. Then the smoothness indicators $\beta_0^{(i)}$ and $\beta_1^{(i)}$, defined by (5.1.20), satisfy (5.1.23) and therefore (5.1.18) results in the third order approximation for $u(x)$ at $x = x_{i+\frac{1}{2}}$ when the nonlinear weights $\omega_0^{(i)}$ and $\omega_1^{(i)}$ are defined by (5.1.21)-(5.1.22).

Proof By using Taylor's formula in (5.1.20), we can easily verify that (5.1.23) holds with $D = \Big(h_i u'(x_i)\Big)^2$.

Summary

- If $u(x)$ is smooth everywhere on the extended stencil S then (5.1.18) gives the third order approximation for $u(x)$ at $x = x_{i+\frac{1}{2}}$.

- Suppose that $u(x)$ is smooth everywhere on the extended stencil S except one point of cell Ω_{i-1}, where $u(x)$ is discontinuous. Then, it is easy to verify that $\beta_0^{(i)} = O(1)$ and $\beta_1^{(i)} = O(h_i^2)$. Therefore, in this case we have $\tilde{\omega}_0^{(i)} << \tilde{\omega}_1^{(i)}$, which results in $\omega_0^{(i)} \approx 0$ and $\omega_1^{(i)} \approx 1$. Thus, (5.1.18) gives the second order approximation for $u(x)$ at $x = x_{i+\frac{1}{2}}$ as it was expected to be.

- Suppose that $u(x)$ is smooth everywhere on the extended stencil S except one point of cell Ω_{i+1}, where $u(x)$ is discontinuous. Then, it is easy to verify that $\beta_0^{(i)} = O(h_i^2)$ and $\beta_1^{(i)} = O(1)$. Therefore, in this case we have $\tilde{\omega}_0^{(i)} >> \tilde{\omega}_1^{(i)}$, which results in $\omega_0^{(i)} \approx 1$ and $\omega_1^{(i)} \approx 0$. Thus, (5.1.18) gives again the second order approximation for $u(x)$ at $x = x_{i+\frac{1}{2}}$.

5.2 CONSTRUCTION OF WENO5 METHOD

WENO5 method is based on approximation by using quadratic polynomials. Firstly, we consider the stencil $S_0 = \{\Omega_{i-2}, \Omega_{i-1}, \Omega_i\}$ (see Figure 5.1). It is obvious that there is a unique quadratic polynomial whose cell average values on the stencil S_0 agree with corresponding cell average values of function $u(x)$ on S_0. We search this polynomial in the following form:

$$p_0^{(i)}(x) = a_0^{(i)}(x - x_i)^2 + b_0^{(i)}(x - x_i) + c_0^{(i)}. \tag{5.2.1}$$

Then,

$$\begin{cases} \dfrac{1}{h_{i-2}} \displaystyle\int\limits_{\Omega_{i-2}} p_0^{(i)}(x)dx &= \bar{u}_{i-2}, \\ \dfrac{1}{h_{i-1}} \displaystyle\int\limits_{\Omega_{i-1}} p_0^{(i)}(x)dx &= \bar{u}_{i-1}, \\ \dfrac{1}{h_i} \displaystyle\int\limits_{\Omega_i} p_0^{(i)}(x)dx &= \bar{u}_i. \end{cases} \tag{5.2.2}$$

Plugging (5.2.1) into (5.2.2) and evaluating integrals, we get:

$$\begin{cases} \left(\dfrac{h_{i-2}^2}{3} + h_{i-2}\left(h_{i-1} + \dfrac{h_i}{2}\right) + \left(h_{i-1} + \dfrac{h_i}{2}\right)^2\right) a_0^{(i)} - \dfrac{h_{i-2} + 2h_{i-1} + h_i}{2} b_0^{(i)} + c_0^{(i)} \\ = \bar{u}_{i-2}, \\ \left(\dfrac{h_{i-1}^2}{3} + \dfrac{h_{i-1}h_i}{2} + \dfrac{h_i^2}{4}\right) a_0^{(i)} - \dfrac{h_{i-1} + h_i}{2} b_0^{(i)} + c_0^{(i)} = \bar{u}_{i-1}, \\ \dfrac{h_i^2}{12} a_0^{(i)} + c_0^{(i)} = \bar{u}_i. \end{cases}$$

Solving this system, we obtain the coefficients of polynomial (5.2.1)

$$\begin{aligned} a_0^{(i)} = & \frac{3}{(h_{i-2} + h_{i-1})(h_{i-2} + h_{i-1} + h_i)} \bar{u}_{i-2} \\ & - \frac{3(h_{i-2} + 2h_{i-1} + h_i)}{(h_{i-2} + h_{i-1})(h_{i-1} + h_i)(h_{i-2} + h_{i-1} + h_i)} \bar{u}_{i-1} \\ & + \frac{3}{(h_{i-1} + h_i)(h_{i-2} + h_{i-1} + h_i)} \bar{u}_i, \end{aligned} \tag{5.2.3}$$

$$b_0^{(i)} = \frac{2h_{i-1}+h_i}{(h_{i-2}+h_{i-1})(h_{i-2}+h_{i-1}+h_i)}\bar{u}_{i-2}$$

$$-\left(\frac{2h_{i-1}+h_i}{(h_{i-2}+h_{i-1})(h_{i-2}+h_{i-1}+h_i)}+\frac{2h_{i-2}+4h_{i-1}+3h_i}{(h_{i-1}+h_i)(h_{i-2}+h_{i-1}+h_i)}\right)\bar{u}_{i-1}$$

$$+\frac{2h_{i-2}+4h_{i-1}+3h_i}{(h_{i-1}+h_i)(h_{i-2}+h_{i-1}+h_i)}\bar{u}_i, \tag{5.2.4}$$

$$c_0^{(i)} = -\frac{h_i^2}{4(h_{i-2}+h_{i-1})(h_{i-2}+h_{i-1}+h_i)}\bar{u}_{i-2}$$

$$+\frac{h_i^2(h_{i-2}+2h_{i-1}+h_i)}{4(h_{i-2}+h_{i-1})(h_{i-1}+h_i)(h_{i-2}+h_{i-1}+h_i)}\bar{u}_{i-1} \tag{5.2.5}$$

$$+\left(1-\frac{h_i^2}{4(h_{i-1}+h_i)(h_{i-2}+h_{i-1}+h_i)}\right)\bar{u}_i.$$

Then, the approximation $u^{(0)}_{i+\frac{1}{2}}$ for function $u(x)$ at $x = x_{i+\frac{1}{2}}$ using the polynomial $p_0^{(i)}(x)$ has the form:

$$u^{(0)}_{i+\frac{1}{2}} = p_0^{(i)}(x_{i+\frac{1}{2}}) = \frac{h_i^2}{4}a_0^{(i)} + \frac{h_i}{2}b_0^{(i)} + c_0^{(i)}$$

or

$$u^{(0)}_{i+\frac{1}{2}} = \frac{h_i(h_{i-1}+h_i)}{(h_{i-2}+h_{i-1})(h_{i-2}+h_{i-1}+h_i)}\bar{u}_{i-2}$$

$$-\left(\frac{h_i(h_{i-1}+h_i)}{(h_{i-2}+h_{i-1})(h_{i-2}+h_{i-1}+h_i)}+\frac{h_i(h_{i-2}+2h_{i-1}+2h_i)}{(h_{i-1}+h_i)(h_{i-2}+h_{i-1}+h_i)}\right)\bar{u}_{i-1}$$

$$+\left(1+\frac{h_i(h_{i-2}+2h_{i-1}+2h_i)}{(h_{i-1}+h_i)(h_{i-2}+h_{i-1}+h_i)}\right)\bar{u}_i. \tag{5.2.6}$$

Remark 5.2.1. In case of uniform grid, i.e. when $h_{i-2} = h_{i-1} = h_i = h$, from (5.2.6) we have

$$u^{(0)}_{i+\frac{1}{2}} = \frac{\bar{u}_{i-2}}{3} - \frac{7\bar{u}_{i-1}}{6} + \frac{11\bar{u}_i}{6}$$

as in (Barth and Deconinck, 1999).

Theorem 5.2.2. If $u(x)$ is sufficiently smooth on stencil S_0, then for approximation (5.2.6) we have

$$u^{(0)}_{i+\frac{1}{2}} = u(x_{i+\frac{1}{2}}) + O\Big(h_i(h_{i-1}+h_i)(h_{i-2}+h_{i-1}+h_i)\Big). \tag{5.2.7}$$

The proof of this theorem is based on Taylor's formula similar to the proof of the Theorem 5.1.10.

Corollary 5.2.3. Formula (5.2.7) implies that (5.2.6) is the third order approximation for u(x) at $x = x_{i+\frac{1}{2}}$.

Remark 5.2.4. In case of uniform grid, i.e. when $h_{i-2} = h_{i-1} = h_i = h$, from (5.2.7) we have

$$u^{(0)}_{i+\frac{1}{2}} \;=\; u(x_{i+\frac{1}{2}}) + O\left(h^3\right)$$

as in (Barth and Deconinck, 1999).

Now, we consider the stencil $S_1 = \{\Omega_{i-1}, \Omega_i, \Omega_{i+1}\}$ (see Figure 5.1). Obviously, there is a unique quadratic polynomial whose cell average values on the stencil S_1 agree with corresponding cell average values of function $u(x)$ on S_1. We search this polynomial in the following form:

$$p_1^{(i)}(x) = a_1^{(i)}(x - x_i)^2 + b_1^{(i)}(x - x_i) + c_1^{(i)}. \tag{5.2.8}$$

Then,

$$\begin{cases} \dfrac{1}{h_{i-1}} \displaystyle\int\limits_{\Omega_{i-1}} p_1^{(i)}(x)dx \;=\; \bar{u}_{i-1}, \\ \dfrac{1}{h_i} \displaystyle\int\limits_{\Omega_i} p_1^{(i)}(x)dx \;=\; \bar{u}_i, \\ \dfrac{1}{h_{i+1}} \displaystyle\int\limits_{\Omega_{i+1}} p_1^{(i)}(x)dx \;=\; \bar{u}_{i+1}. \end{cases} \tag{5.2.9}$$

Plugging (5.2.8) into (5.2.9) and evaluating integrals, we obtain

$$\begin{cases} \left(\dfrac{h_{i-1}^2}{3} + \dfrac{h_{i-1}h_i}{2} + \dfrac{h_i^2}{4}\right) a_1^{(i)} - \dfrac{h_{i-1} + h_i}{2} b_1^{(i)} + c_1^{(i)} \;=\; \bar{u}_{i-1}, \\ \dfrac{h_i^2}{12} a_1^{(i)} + c_1^{(i)} \;=\; \bar{u}_i, \\ \left(\dfrac{h_i^2}{4} + \dfrac{h_i h_{i+1}}{2} + \dfrac{h_{i+1}^2}{3}\right) a_1^{(i)} + \dfrac{h_i + h_{i+1}}{2} b_1^{(i)} + c_1^{(i)} \;=\; \bar{u}_{i+1}. \end{cases}$$

Solving this system, we obtain the coefficients of polynomial (5.2.8)

$$
\begin{aligned}
a_1^{(i)} &= \frac{3}{(h_{i-1}+h_i)(h_{i-1}+h_i+h_{i+1})}\bar{u}_{i-1} \\
&\quad - \frac{3(h_{i-1}+2h_i+h_{i+1})}{(h_{i-1}+h_i)(h_i+h_{i+1})(h_{i-1}+h_i+h_{i+1})}\bar{u}_i \\
&\quad + \frac{3}{(h_i+h_{i+1})(h_{i-1}+h_i+h_{i+1})}\bar{u}_{i+1}, \\
b_1^{(i)} &= -\frac{h_i+2h_{i+1}}{(h_{i-1}+h_i)(h_{i-1}+h_i+h_{i+1})}\bar{u}_{i-1} \\
&\quad + \frac{(h_{i+1}-h_{i-1})(2h_{i-1}+3h_i+2h_{i+1})}{(h_{i-1}+h_i)(h_i+h_{i+1})(h_{i-1}+h_i+h_{i+1})}\bar{u}_i \\
&\quad + \frac{2h_{i-1}+h_i}{(h_i+h_{i+1})(h_{i-1}+h_i+h_{i+1})}\bar{u}_{i+1}, \\
c_1^{(i)} &= -\frac{h_i^2}{4(h_{i-1}+h_i)(h_{i-1}+h_i+h_{i+1})}\bar{u}_{i-1} \\
&\quad + \left(1+\frac{h_i^2(h_{i-1}+2h_i+h_{i+1})}{4(h_{i-1}+h_i)(h_i+h_{i+1})(h_{i-1}+h_i+h_{i+1})}\right)\bar{u}_i \\
&\quad - \frac{h_i^2}{4(h_i+h_{i+1})(h_{i-1}+h_i+h_{i+1})}\bar{u}_{i+1}.
\end{aligned}
\tag{5.2.10}
$$

Then, the approximation $u^{(1)}_{i+\frac{1}{2}}$ for function $u(x)$ at $x = x_{i+\frac{1}{2}}$ using the polynomial $p_1^{(i)}(x)$ has the form:

$$
u^{(1)}_{i+\frac{1}{2}} = p_1^{(i)}(x_{i+\frac{1}{2}}) = \frac{h_i^2}{4}a_1^{(i)} + \frac{h_i}{2}b_1^{(i)} + c_1^{(i)}
$$

or

$$
\begin{aligned}
u^{(1)}_{i+\frac{1}{2}} &= -\frac{h_i h_{i+1}}{(h_{i-1}+h_i)(h_{i-1}+h_i+h_{i+1})}\bar{u}_{i-1} \\
&\quad + \left(1+\frac{h_i h_{i+1}}{(h_{i-1}+h_i)(h_{i-1}+h_i+h_{i+1})} - \frac{h_i(h_{i-1}+h_i)}{(h_i+h_{i+1})(h_{i-1}+h_i+h_{i+1})}\right)\bar{u}_i \\
&\quad + \frac{h_i(h_{i-1}+h_i)}{(h_i+h_{i+1})(h_{i-1}+h_i+h_{i+1})}\bar{u}_{i+1}.
\end{aligned}
\tag{5.2.11}
$$

Remark 5.2.5. In case of uniform grid, i.e. when $h_{i-1} = h_i = h_{i+1} = h$, from (5.2.11) we have

$$
u^{(1)}_{i+\frac{1}{2}} = -\frac{\bar{u}_{i-1}}{6} + \frac{5\bar{u}_i}{6} + \frac{\bar{u}_{i+1}}{3}
$$

as in (Barth and Deconinck, 1999).

Theorem 5.2.6. If $u(x)$ is sufficiently smooth on stencil S_1, then for approximation (5.2.11) we have

$$u^{(1)}_{i+\frac{1}{2}} \;=\; u(x_{i+\frac{1}{2}}) \;+\; O\Big(h_i h_{i+1}(h_{i-1}+h_i)\Big). \tag{5.2.12}$$

The proof of this theorem is based on Taylor's formula similar to the proof of the Theorem 5.1.10.

Corollary 5.2.7. Formula (5.2.12) implies that (5.2.11) is the third order approximation for u(x) at $x = x_{i+\frac{1}{2}}$.

Remark 5.2.8. In case of uniform grid, i.e. when $h_{i-1} = h_i = h_{i+1} = h$, from (5.2.12) we have

$$u^{(1)}_{i+\frac{1}{2}} \;=\; u(x_{i+\frac{1}{2}}) + O\left(h^3\right)$$

as in (Barth and Deconinck, 1999).

Next, we consider the stencil $S_2 = \{\Omega_i, \Omega_{i+1}, \Omega_{i+2}\}$. Obviously, there is a unique quadratic polynomial whose cell average values on the stencil S_2 agree with corresponding cell average values of function $u(x)$ on S_2. We search this polynomial in the following form:

$$p_2^{(i)}(x) = a_2^{(i)}(x-x_i)^2 + b_2^{(i)}(x-x_i) + c_2^{(i)}. \tag{5.2.13}$$

Then,

$$\begin{cases} \dfrac{1}{h_i}\displaystyle\int\limits_{\Omega_i} p_2^{(i)}(x)dx \;=\; \bar{u}_i, \\[2ex] \dfrac{1}{h_{i+1}}\displaystyle\int\limits_{\Omega_{i+1}} p_2^{(i)}(x)dx \;=\; \bar{u}_{i+1}, \\[2ex] \dfrac{1}{h_{i+2}}\displaystyle\int\limits_{\Omega_{i+2}} p_2^{(i)}(x)dx \;=\; \bar{u}_{i+2}. \end{cases} \tag{5.2.14}$$

Plugging (5.2.13) into (5.2.14) and evaluating integrals, we obtain

$$\begin{cases} \dfrac{h_i^2}{12}a_2^{(i)} + c_2^{(i)} \;=\; \bar{u}_i, \\ \left(\dfrac{h_i^2}{4} + \dfrac{h_i h_{i+1}}{2} + \dfrac{h_{i+1}^2}{3}\right) a_2^{(i)} + \dfrac{h_i + h_{i+1}}{2} b_2^{(i)} + c_2^{(i)} \;=\; \bar{u}_{i+1}, \\ \left(\left(\dfrac{h_i}{2} + h_{i+1}\right)^2 + h_{i+2}\left(\dfrac{h_i}{2} + h_{i+1}\right) + \dfrac{h_{i+2}^2}{3}\right) a_2^{(i)} + \dfrac{h_i + 2h_{i+1} + h_{i+2}}{2} b_2^{(i)} + c_2^{(i)} \\ \;=\; \bar{u}_{i+2}. \end{cases}$$

Solving this system, we obtain the coefficients of polynomial (5.2.13)

$$\begin{aligned} a_2^{(i)} \;=\;& \frac{3}{(h_i + h_{i+1})(h_i + h_{i+1} + h_{i+2})}\bar{u}_i \\ & - \frac{3(h_i + 2h_{i+1} + h_{i+2})}{(h_i + h_{i+1})(h_{i+1} + h_{i+2})(h_i + h_{i+1} + h_{i+2})}\bar{u}_{i+1} \\ & + \frac{3}{(h_{i+1} + h_{i+2})(h_i + h_{i+1} + h_{i+2})}\bar{u}_{i+2}, \\ b_2^{(i)} \;=\;& -\frac{3h_i + 4h_{i+1} + 2h_{i+2}}{(h_i + h_{i+1})(h_i + h_{i+1} + h_{i+2})}\bar{u}_i \\ & + \left(\frac{3h_i + 4h_{i+1} + 2h_{i+2}}{(h_i + h_{i+1})(h_i + h_{i+1} + h_{i+2})} + \frac{h_i + 2h_{i+1}}{(h_{i+1} + h_{i+2})(h_i + h_{i+1} + h_{i+2})}\right)\bar{u}_{i+1} \\ & - \frac{h_i + 2h_{i+1}}{(h_{i+1} + h_{i+2})(h_i + h_{i+1} + h_{i+2})}\bar{u}_{i+2}, \\ c_2^{(i)} \;=\;& \left(1 - \frac{h_i^2}{4(h_i + h_{i+1})(h_i + h_{i+1} + h_{i+2})}\right)\bar{u}_i \\ & + \frac{h_i^2(h_i + 2h_{i+1} + h_{i+2})}{4(h_i + h_{i+1})(h_{i+1} + h_{i+2})(h_i + h_{i+1} + h_{i+2})}\bar{u}_{i+1} \\ & - \frac{h_i^2}{4(h_{i+1} + h_{i+2})(h_i + h_{i+1} + h_{i+2})}\bar{u}_{i+2}. \end{aligned} \tag{5.2.15}$$

Then, the approximation $u^{(2)}_{i+\frac{1}{2}}$ for function $u(x)$ at $x = x_{i+\frac{1}{2}}$ using the polynomial $p_2^{(i)}(x)$ has the form:

$$u^{(2)}_{i+\frac{1}{2}} \;=\; p_2^{(i)}(x_{i+\frac{1}{2}}) \;=\; \frac{h_i^2}{4}a_2^{(i)} + \frac{h_i}{2}b_2^{(i)} + c_2^{(i)}$$

or

$$u^{(2)}_{i+\frac{1}{2}} = \frac{h_{i+1}(h_{i+1}+h_{i+2})}{(h_i+h_{i+1})(h_i+h_{i+1}+h_{i+2})}\bar{u}_i$$
$$+\left(1+\frac{h_i h_{i+1}}{(h_{i+1}+h_{i+2})(h_i+h_{i+1}+h_{i+2})}-\frac{h_{i+1}(h_{i+1}+h_{i+2})}{(h_i+h_{i+1})(h_i+h_{i+1}+h_{i+2})}\right)\bar{u}_{i+1}$$
$$-\frac{h_i h_{i+1}}{(h_{i+1}+h_{i+2})(h_i+h_{i+1}+h_{i+2})}\bar{u}_{i+2}. \tag{5.2.16}$$

Remark 5.2.9. In case of uniform grid, i.e. when $h_i = h_{i+1} = h_{i+2} = h$, from (5.2.16) we have

$$u^{(2)}_{i+\frac{1}{2}} = \frac{\bar{u}_i}{3}+\frac{5\bar{u}_{i+1}}{6}-\frac{\bar{u}_{i+2}}{6}$$

as in (Barth and Deconinck, 1999).

Theorem 5.2.10. If $u(x)$ is sufficiently smooth on stencil S_2, then for approximation (5.2.16) we have

$$u^{(2)}_{i+\frac{1}{2}} = u(x_{i+\frac{1}{2}}) + O\Big(h_i h_{i+1}(h_{i+1}+h_{i+2})\Big). \tag{5.2.17}$$

The proof of this theorem is based on Taylor's formula similar to the proof of the Theorem 5.1.10.

Corollary 5.2.11. Formula (5.2.17) implies that (5.2.16) is the third order approximation for u(x) at $x = x_{i+\frac{1}{2}}$.

Remark 5.2.12. In case of uniform grid, i.e. when $h_i = h_{i+1} = h_{i+2} = h$, from (5.2.17) we have

$$u^{(2)}_{i+\frac{1}{2}} = u(x_{i+\frac{1}{2}}) + O\left(h^3\right)$$

as in (Barth and Deconinck, 1999).

Finally, we consider the extended stencil

$$S = S_0 \cup S_1 \cup S_2 = \{\Omega_{i-2}, \Omega_{i-1}, \Omega_i, \Omega_{i+1}, \Omega_{i+2}\}.$$

There is a unique fourth order polynomial whose cell average values on the extended stencil S agree with corresponding cell average values of function $u(x)$ on S. We search this polynomial in the following form:

$$P^{(i)}(x) = a^{(i)}(x-x_i)^4 + b^{(i)}(x-x_i)^3 + c^{(i)}(x-x_i)^2 + d^{(i)}(x-x_i) + e^{(i)}. \quad (5.2.18)$$

Then,

$$\begin{cases} \dfrac{1}{h_{i-2}} \displaystyle\int_{\Omega_{i-2}} P^{(i)}(x)dx = \bar{u}_{i-2}, \\ \dfrac{1}{h_{i-1}} \displaystyle\int_{\Omega_{i-1}} P^{(i)}(x)dx = \bar{u}_{i-1}, \\ \dfrac{1}{h_{i}} \displaystyle\int_{\Omega_{i}} P^{(i)}(x)dx = \bar{u}_{i}, \\ \dfrac{1}{h_{i+1}} \displaystyle\int_{\Omega_{i+1}} P^{(i)}(x)dx = \bar{u}_{i+1}, \\ \dfrac{1}{h_{i+2}} \displaystyle\int_{\Omega_{i+2}} P^{(i)}(x)dx = \bar{u}_{i+2}. \end{cases} \quad (5.2.19)$$

Plugging (5.2.18) into (5.2.19), evaluating integrals and solving the resulting system, we obtain the coefficients $a^{(i)}$, $b^{(i)}$, $c^{(i)}$, $d^{(i)}$, $e^{(i)}$ of the polynomial $P^{(i)}(x)$ (we do not give formulas here due to their large sizes).

Now, the approximation $u_{i+\frac{1}{2}}$ for function $u(x)$ at $x = x_{i+\frac{1}{2}}$ using the polynomial $P^{(i)}(x)$ has the form:

$$u_{i+\frac{1}{2}} = P^{(i)}(x_{i+\frac{1}{2}}) = \frac{h_i^4}{16}a^{(i)} + \frac{h_i^3}{8}b^{(i)} + \frac{h_i^2}{4}c^{(i)} + \frac{h_i}{2}d^{(i)} + e^{(i)}$$

or

$$u_{i+\frac{1}{2}} = \alpha_{i-2}\bar{u}_{i-2} + \alpha_{i-1}\bar{u}_{i-1} + \alpha_i\bar{u}_i + \alpha_{i+1}\bar{u}_{i+1} + \alpha_{i+2}\bar{u}_{i+2} \quad (5.2.20)$$

where coefficients α_{i-2}, α_{i-1}, α_i, α_{i+1}, α_{i+2} depend only on h values (we do not give formulas here due to their large sizes).

Remark 5.2.13. In case of uniform grid, i.e. when $h_{i-2} = h_{i-1} = h_i = h_{i+1} = h_{i+2}$, (5.2.20) results in

$$u_{i+\frac{1}{2}} = \frac{1}{30}\bar{u}_{i-2} - \frac{13}{60}\bar{u}_{i-1} + \frac{47}{60}\bar{u}_i + \frac{9}{20}\bar{u}_{i+1} - \frac{1}{20}\bar{u}_{i+2}$$

as in (Barth and Deconinck, 1999).

Theorem 5.2.14. If $u(x)$ is sufficiently smooth on stencil S, then for approximation (5.2.20) we have

$$u_{i+\frac{1}{2}} \;=\; u(x_{i+\frac{1}{2}}) \;+\; O\Big(h_i h_{i+1}(h_{i-1}+h_i)(h_{i+1}+h_{i+2})(h_{i-2}+h_{i-1}+h_i)\Big). \quad (5.2.21)$$

The proof of this theorem is based on Taylor's formula similar to the proof of the Theorem 5.1.10.

Corollary 5.2.15. Formula (5.2.21) implies that (5.2.20) is the fifth order approximation for u(x) at $x = x_{i+\frac{1}{2}}$.

Remark 5.2.16. In case of uniform grid, i.e. when $h_{i-2} = h_{i-1} = h_i = h_{i+1} = h_{i+2} = h$, from (5.2.21) we have

$$u_{i+\frac{1}{2}} \;=\; u(x_{i+\frac{1}{2}}) + O\left(h^5\right)$$

as in (Barth and Deconinck, 1999).

The following result states that the fifth order approximation $u_{i+\frac{1}{2}}$ given by (5.2.20) can be written as a linear combination of third order approximations $u^{(0)}_{i+\frac{1}{2}}$, $u^{(1)}_{i+\frac{1}{2}}$ and $u^{(2)}_{i+\frac{1}{2}}$ given by (5.2.6), (5.2.11) and (5.2.16), respectively.

Theorem 5.2.17. There exist unique $\gamma_0^{(i)}$, $\gamma_1^{(i)}$ and $\gamma_2^{(i)}$ values such that

$$u_{i+\frac{1}{2}} = \gamma_0^{(i)} u^{(0)}_{i+\frac{1}{2}} + \gamma_1^{(i)} u^{(1)}_{i+\frac{1}{2}} + \gamma_2^{(i)} u^{(2)}_{i+\frac{1}{2}} \quad (5.2.22)$$

holds.

Proof Using (5.2.6), (5.2.11) and (5.2.16), one can verify that (5.2.22) holds if and only if

$$\begin{aligned}
\gamma_0^{(i)} &= \frac{h_{i+1}(h_{i+1}+h_{i+2})}{(h_{i-2}+h_{i-1}+h_i+h_{i+1})(h_{i-2}+h_{i-1}+h_i+h_{i+1}+h_{i+2})}, \\
\gamma_1^{(i)} &= \frac{(h_{i-2}+h_{i-1}+h_i)(h_{i+1}+h_{i+2})(h_{i-2}+2h_{i-1}+2h_i+2h_{i+1}+h_{i+2})}{(h_{i-2}+h_{i-1}+h_i+h_{i+1})(h_{i-1}+h_i+h_{i+1}+h_{i+2})(h_{i-2}+h_{i-1}+h_i+h_{i+1}+h_{i+2})}, \\
\gamma_2^{(i)} &= \frac{(h_{i-1}+h_i)(h_{i-2}+h_{i-1}+h_i)}{(h_{i-1}+h_i+h_{i+1}+h_{i+2})(h_{i-2}+h_{i-1}+h_i+h_{i+1}+h_{i+2})}.
\end{aligned} \quad (5.2.23)$$

In WENO literature, $\gamma_0^{(i)}$, $\gamma_1^{(i)}$ and $\gamma_2^{(i)}$ are called **linear weights**. Note that in case of uniform grid, i.e. when $h_{i-2} = h_{i-1} = h_i = h_{i+1} = h_{i+2}$, from (5.2.23) we have $\gamma_0^{(i)} = \dfrac{1}{10}$, $\gamma_1^{(i)} = \dfrac{3}{5}$ and $\gamma_2^{(i)} = \dfrac{3}{10}$ as in (Barth and Deconinck, 1999).

To summarize, if $u(x)$ is sufficiently smooth on the extended stencil S, the linear combination $\gamma_0^{(i)} u_{i+\frac{1}{2}}^{(0)} + \gamma_1^{(i)} u_{i+\frac{1}{2}}^{(1)} + \gamma_2^{(i)} u_{i+\frac{1}{2}}^{(2)}$, where linear weights $\gamma_0^{(i)}$, $\gamma_1^{(i)}$ and $\gamma_2^{(i)}$ are given by (5.2.23), results in the fifth order approximation for $u(x)$ at $x = x_{i+\frac{1}{2}}$. Moreover, if $u(x)$ is sufficiently smooth on the extended stencil S, then

$$\begin{aligned} &\gamma_0^{(i)} u_{i+\frac{1}{2}}^{(0)} + \gamma_1^{(i)} u_{i+\frac{1}{2}}^{(1)} + \gamma_2^{(i)} u_{i+\frac{1}{2}}^{(2)} \\ = \;& u(x_{i+\frac{1}{2}}) \; + \; O\Big(h_i h_{i+1}(h_{i-1}+h_i)(h_{i+1}+h_{i+2})(h_{i-2}+h_{i-1}+h_i)\Big) \end{aligned} \tag{5.2.24}$$

holds.

Let us discuss now a few different scenarios when $u(x)$ is not smooth on the extended stencil S.

- Suppose that $u(x)$ is smooth everywhere on the extended stencil S except one point of cell Ω_{i-2}, where $u(x)$ or derivative of $u(x)$ is discontinuous. Then (5.2.24) obviously does not hold, i.e. (5.2.22) is not the fifth order approximation for $u(x)$ at $x = x_{i+\frac{1}{2}}$. However, since $u(x)$ is still smooth in stencils S_1 and S_2, (5.2.22) gives the third order approximation if one chooses $\gamma_0^{(i)} = 0$ and $\gamma_1^{(i)} + \gamma_2^{(i)} = 1$.

- Suppose that $u(x)$ is smooth everywhere on the extended stencil S except one point of cell Ω_{i-1}, where $u(x)$ or derivative of $u(x)$ is discontinuous. Then (5.2.24) obviously does not hold, i.e. (5.2.22) is not the fifth order approximation for $u(x)$ at $x = x_{i+\frac{1}{2}}$. However, since $u(x)$ is still smooth in stencil S_2, (5.2.22) gives the third order approximation if one chooses $\gamma_0^{(i)} = \gamma_1^{(i)} = 0$ and $\gamma_2^{(i)} = 1$.

- Assume that $u(x)$ is smooth everywhere on the extended stencil S except one point of cell Ω_{i+1}, where $u(x)$ or derivative of $u(x)$ is discontinuous. Then (5.2.24) obviously does not hold, i.e. (5.2.22) is not the fifth order approximation for $u(x)$ at $x = x_{i+\frac{1}{2}}$. However, since $u(x)$ is still smooth in stencil S_0, (5.2.22) gives the third order approximation if one chooses $\gamma_1^{(i)} = \gamma_2^{(i)} = 0$ and $\gamma_0^{(i)} = 1$.

- Assume that $u(x)$ is smooth everywhere on the extended stencil S except one point of cell Ω_{i+2}, where $u(x)$ or derivative of $u(x)$ is discontinuous. Then (5.2.24) does not hold and therefore (5.2.22) is not the fifth order approximation for $u(x)$ at $x = x_{i+\frac{1}{2}}$. However, since $u(x)$ is smooth in stencils S_0 and S_1, (5.2.22) gives the third order approximation if one chooses $\gamma_0^{(i)} + \gamma_1^{(i)} = 1$ and $\gamma_2^{(i)} = 0$.

- Finally, we note that when $u(x)$ is smooth everywhere on the extended stencil S except one point of cell Ω_i, approximation (5.2.22) is not consistent. It is due to the fact that $u(x)$ is not smooth on all stencils S_0, S_1 and S_2, and therefore all approximation formulas (5.2.6), (5.2.11) and (5.2.16) are inconsistent. Unfortunately, this kind of local inconsistency cannot be eliminated and therefore one has to anticipate the order reduction when WENO approximations are used for solving problems with non-smooth solutions.

Linear weights $\gamma_0^{(i)}$, $\gamma_1^{(i)}$ and $\gamma_2^{(i)}$ defined by (5.2.23) are independent of $u(x)$. Therefore, these weights cannot be used when $u(x)$ is non-smooth. The purpose of the WENO5 method is to find the approximation of $u(x_{i+\frac{1}{2}})$ by using a convex combination of approximations $u_{i+\frac{1}{2}}^{(0)}$, $u_{i+\frac{1}{2}}^{(1)}$ and $u_{i+\frac{1}{2}}^{(2)}$ defined by (5.2.6), (5.2.11) and (5.2.16), respectively. In other words, (5.2.22) is replaced with:

$$u_{i+\frac{1}{2}} = \omega_0^{(i)} u_{i+\frac{1}{2}}^{(0)} + \omega_1^{(i)} u_{i+\frac{1}{2}}^{(1)} + \omega_2^{(i)} u_{i+\frac{1}{2}}^{(2)} \tag{5.2.25}$$

where $\omega_0^{(i)} \geq 0$, $\omega_1^{(i)} \geq 0$, $\omega_2^{(i)} \geq 0$ are called **nonlinear weights** and
$\omega_0^{(i)} + \omega_1^{(i)} + \omega_2^{(i)} = 1.$

Lemma 5.2.18. Assume that $u(x)$ is sufficiently smooth on the extended stencil S. If

$$\begin{aligned}
\omega_0^{(i)} &= \gamma_0^{(i)} + O\Big((h_{i-1} + h_i + h_{i+1})(h_{i-2} + h_{i-1} + h_i + h_{i+1} + h_{i+2})\Big), \\
\omega_1^{(i)} &= \gamma_1^{(i)} + O\Big((h_{i-1} + h_i + h_{i+1})(h_{i-2} + h_{i-1} + h_i + h_{i+1} + h_{i+2})\Big), \qquad (5.2.26) \\
\omega_2^{(i)} &= \gamma_2^{(i)} + O\Big((h_{i-1} + h_i + h_{i+1})(h_{i-2} + h_{i-1} + h_i + h_{i+1} + h_{i+2})\Big),
\end{aligned}$$

then (5.2.25) is a fifth order approximation for $u(x)$ at $x = x_{i+\frac{1}{2}}$.

Proof Using (5.2.7), (5.2.12), (5.2.17) and (5.2.21), we have

$$
\begin{aligned}
u_{i+\frac{1}{2}} &= \omega_0^{(i)} u_{i+\frac{1}{2}}^{(0)} + \omega_1^{(i)} u_{i+\frac{1}{2}}^{(1)} + \omega_2^{(i)} u_{i+\frac{1}{2}}^{(2)} \\
&= \left(\omega_0^{(i)} - \gamma_0^{(i)}\right) u_{i+\frac{1}{2}}^{(0)} + \left(\omega_1^{(i)} - \gamma_1^{(i)}\right) u_{i+\frac{1}{2}}^{(1)} + \left(\omega_2^{(i)} - \gamma_2^{(i)}\right) u_{i+\frac{1}{2}}^{(2)} \\
&\quad + \gamma_0^{(i)} u_{i+\frac{1}{2}}^{(0)} + \gamma_1^{(i)} u_{i+\frac{1}{2}}^{(1)} + \gamma_2^{(i)} u_{i+\frac{1}{2}}^{(2)} \\
&= \left(\omega_0^{(i)} - \gamma_0^{(i)}\right)\left(u_{i+\frac{1}{2}}^{(0)} - u(x_{i+\frac{1}{2}})\right) + \left(\omega_1^{(i)} - \gamma_1^{(i)}\right)\left(u_{i+\frac{1}{2}}^{(1)} - u(x_{i+\frac{1}{2}})\right) \\
&\quad + \left(\omega_2^{(i)} - \gamma_2^{(i)}\right)\left(u_{i+\frac{1}{2}}^{(2)} - u(x_{i+\frac{1}{2}})\right) + \gamma_0^{(i)} u_{i+\frac{1}{2}}^{(0)} + \gamma_1^{(i)} u_{i+\frac{1}{2}}^{(1)} + \gamma_2^{(i)} u_{i+\frac{1}{2}}^{(2)} \\
&= u(x_{i+\frac{1}{2}}) + \left(\omega_0^{(i)} - \gamma_0^{(i)}\right) \cdot O\Big(h_i(h_{i-1}+h_i)(h_{i-2}+h_{i-1}+h_i)\Big) \\
&\quad + \left(\omega_1^{(i)} - \gamma_1^{(i)}\right) \cdot O\Big(h_i h_{i+1}(h_{i-1}+h_i)\Big) \\
&\quad + \left(\omega_2^{(i)} - \gamma_2^{(i)}\right) \cdot O\Big(h_i h_{i+1}(h_{i+1}+h_{i+2})\Big) \\
&\quad + O\Big(h_i h_{i+1}(h_{i-1}+h_i)(h_{i+1}+h_{i+2})(h_{i-2}+h_{i-1}+h_i)\Big).
\end{aligned}
$$

Now, using (5.2.26), we obtain

$$
u_{i+\frac{1}{2}} = u(x_{i+\frac{1}{2}}) + O\Big(h_i\,(h_{i-1}+h_i+h_{i+1})^2\,(h_{i-2}+h_{i-1}+h_i+h_{i+1}+h_{i+2})^2\Big).
$$

In order to define nonlinear weights $\omega_0^{(i)}$, $\omega_1^{(i)}$ and $\omega_2^{(i)}$, we first introduce smoothness indicators $\beta_0^{(i)}, \beta_1^{(i)}$, and $\beta_2^{(i)}$ to measure the smoothness of $u(x)$ in stencils S_0, S_1 and S_2, respectively. Interpolating polynomials (), () and () are used to define the smoothness indicators in the following way:

$$
\begin{aligned}
\beta_0^{(i)} &= h_i \int\limits_{\Omega_i} \left(\frac{d}{dx} p_0^{(i)}(x)\right)^2 dx + h_i^3 \int\limits_{\Omega_i} \left(\frac{d^2}{dx^2} p_0^{(i)}(x)\right)^2 dx = \frac{13}{3}\left(a_0^{(i)} h_i^2\right)^2 + \left(b_0^{(i)} h_i\right)^2, \\
\beta_1^{(i)} &= h_i \int\limits_{\Omega_i} \left(\frac{d}{dx} p_1^{(i)}(x)\right)^2 dx + h_i^3 \int\limits_{\Omega_i} \left(\frac{d^2}{dx^2} p_1^{(i)}(x)\right)^2 dx = \frac{13}{3}\left(a_1^{(i)} h_i^2\right)^2 + \left(b_1^{(i)} h_i\right)^2, \\
\beta_2^{(i)} &= h_i \int\limits_{\Omega_i} \left(\frac{d}{dx} p_2^{(i)}(x)\right)^2 dx + h_i^3 \int\limits_{\Omega_i} \left(\frac{d^2}{dx^2} p_2^{(i)}(x)\right)^2 dx = \frac{13}{3}\left(a_2^{(i)} h_i^2\right)^2 + \left(b_2^{(i)} h_i\right)^2,
\end{aligned}
\tag{5.2.27}
$$

where $a_r^{(i)}$, $b_r^{(i)}$, and $c_r^{(i)}$, $r = 0, 1, 2$, are coefficients that can be used from the previous found approximations in $u_{i+\frac{1}{2}}^{(0)}$, $u_{i+\frac{1}{2}}^{(1)}$ and $u_{i+\frac{1}{2}}^{(2)}$.

Now, normalized nonlinear weights in (5.2.25) are defined as following:

$$\omega_0^{(i)} = \frac{\tilde{\omega}_0^{(i)}}{\tilde{\omega}_0^{(i)} + \tilde{\omega}_1^{(i)} + \tilde{\omega}_2^{(i)}}, \quad \omega_1^{(i)} = \frac{\tilde{\omega}_1^{(i)}}{\tilde{\omega}_0^{(i)} + \tilde{\omega}_1^{(i)} + \tilde{\omega}_2^{(i)}}, \quad \omega_2^{(i)} = \frac{\tilde{\omega}_2^{(i)}}{\tilde{\omega}_0^{(i)} + \tilde{\omega}_1^{(i)} + \tilde{\omega}_2^{(i)}}, \tag{5.2.28}$$

where

$$\tilde{\omega}_0^{(i)} = \frac{\gamma_0^{(i)}}{\left(\epsilon + \beta_0^{(i)}\right)^2}, \quad \tilde{\omega}_1^{(i)} = \frac{\gamma_1^{(i)}}{\left(\epsilon + \beta_1^{(i)}\right)^2}, \quad \tilde{\omega}_2^{(i)} = \frac{\gamma_2^{(i)}}{\left(\epsilon + \beta_2^{(i)}\right)^2}. \tag{5.2.29}$$

Here, $\epsilon = 10^{-6}$ is taken to prevent the denominators to become zero.

Lemma 5.2.19. Assume that $u(x)$ is sufficiently smooth on the extended stencil S. If there is non-zero constant D such that

$$\begin{aligned}
\beta_0^{(i)} &= D\Big(1 + O\Big((h_{i-1} + h_i)(h_{i-2} + h_{i-1} + h_i)\Big)\Big), \\
\beta_1^{(i)} &= D\Big(1 + O\Big((h_{i-1} + h_i)(h_i + h_{i+1})\Big)\Big), \\
\beta_2^{(i)} &= D\Big(1 + O\Big((h_i + h_{i+1})(h_i + h_{i+1} + h_{i+2})\Big)\Big),
\end{aligned} \tag{5.2.30}$$

then (5.2.26) are satisfied and therefore (5.2.25) results in a fifth order approximation for $u(x)$ at $x = x_{i+\frac{1}{2}}$.

Proof Putting (5.2.30) in (5.2.29) and using Taylor expansion we first obtain

$$\begin{aligned}
\tilde{\omega}_0^{(i)} &= \frac{\gamma_0^{(i)}}{(\epsilon + D)^2} + O\Big((h_{i-1} + h_i)(h_{i-2} + h_{i-1} + h_i)\Big), \\
\tilde{\omega}_1^{(i)} &= \frac{\gamma_1^{(i)}}{(\epsilon + D)^2} + O\Big((h_{i-1} + h_i)(h_i + h_{i+1})\Big), \\
\tilde{\omega}_2^{(i)} &= \frac{\gamma_2^{(i)}}{(\epsilon + D)^2} + O\Big((h_i + h_{i+1})(h_i + h_{i+1} + h_{i+2})\Big).
\end{aligned}$$

Then putting these in (5.2.28) gives (5.2.26).

Theorem 5.2.20. Assume that $u(x)$ is sufficiently smooth on the extended stencil S. Then smoothness indicators defined by (5.2.27) satisfy (5.2.30) and therefore (5.2.25) results in a fifth order approximation for $u(x)$ at $x = x_{i+\frac{1}{2}}$ when nonlinear weights are defined by (5.2.28)-(5.2.29).

Proof By using Taylor's formula in (5.2.27), we can easily verify that (5.2.30) holds with $D = \Big(h_i u'(x_i)\Big)^2$.

Summary

- If $u(x)$ is smooth everywhere on the extended stencil S then (5.2.25) gives the fifth order approximation for $u(x)$ at $x = x_{i+\frac{1}{2}}$.

- Suppose that $u(x)$ is smooth everywhere on the extended stencil S except one point of cell Ω_{i-2}, where $u(x)$ or derivative of $u(x)$ is discontinuous. Then, it is easy to verify that $\beta_0^{(i)} = O(1)$, $\beta_1^{(i)} = O(h_i^2)$ and $\beta_2^{(i)} = O(h_i^2)$. Therefore, in this case we have $\tilde{\omega}_0^{(i)} << \tilde{\omega}_1^{(i)}$ and $\tilde{\omega}_0^{(i)} << \tilde{\omega}_2^{(i)}$, which results in $\omega_0^{(i)} \approx 0$ and $\omega_1^{(i)} + \omega_2^{(i)} \approx 1$. Thus, (5.2.25) gives the third order approximation for $u(x)$ at $x = x_{i+\frac{1}{2}}$ as it was expected to be.

- Suppose that $u(x)$ is smooth everywhere on the extended stencil S except one point of cell Ω_{i-1}, where $u(x)$ is discontinuous. Then, it is easy to verify that $\beta_0^{(i)} = O(1)$, $\beta_1^{(i)} = O(1)$ and $\beta_2^{(i)} = O(h_i^2)$. Therefore, in this case we have $\tilde{\omega}_0^{(i)} << \tilde{\omega}_2^{(i)}$ and $\tilde{\omega}_1^{(i)} << \tilde{\omega}_2^{(i)}$, which results in $\omega_0^{(i)} \approx 0$, $\omega_1^{(i)} \approx 0$ and $\omega_2^{(i)} \approx 1$. Thus, (5.2.25) gives the third order approximation for $u(x)$ at $x = x_{i+\frac{1}{2}}$ as it was expected to be.

- Suppose that $u(x)$ is smooth everywhere on the extended stencil S except one point of cell Ω_{i+1}, where $u(x)$ is discontinuous. Then, it is easy to verify that $\beta_0^{(i)} = O(h_i^2)$, $\beta_1^{(i)} = O(1)$ and $\beta_2^{(i)} = O(1)$. Therefore, in this case we have $\tilde{\omega}_0^{(i)} >> \tilde{\omega}_1^{(i)}$ and $\tilde{\omega}_0^{(i)} >> \tilde{\omega}_2^{(i)}$, which results in $\omega_0^{(i)} \approx 1$, $\omega_1^{(i)} \approx 0$ and $\omega_2^{(i)} \approx 0$. Thus, (5.2.25) gives the third order approximation for $u(x)$ at $x = x_{i+\frac{1}{2}}$ as it was expected to be.

- Assume that $u(x)$ is smooth everywhere on the extended stencil S except one point of cell Ω_{i+2}, where $u(x)$ or derivative of $u(x)$ is discontinuous. Then, it is easy to verify that $\beta_0^{(i)} = O(h_i^2)$, $\beta_1^{(i)} = O(h_i^2)$ and $\beta_2^{(i)} = O(1)$. Therefore, in this case we have $\tilde{\omega}_0^{(i)} >> \tilde{\omega}_2^{(i)}$ and $\tilde{\omega}_1^{(i)} >> \tilde{\omega}_2^{(i)}$, which results in $\omega_0^{(i)} + \omega_1^{(i)} \approx 0$ and $\omega_2^{(i)} \approx 0$. Thus, (5.2.25) gives the third order approximation for $u(x)$ at $x = x_{i+\frac{1}{2}}$ as it was expected to be.

CHAPTER 6

APPLICATION OF WENO METHODS TO ADVECTION DIFFUSION REACTION PROBLEMS WITH SINGULAR SOURCE TERMS

In this chapter, we will apply constructed WENO approximations for numerical solutions of Advection equations with singular source terms and Advection Diffusion equations with singular source terms.

6.1 ADVECTION PROBLEMS WITH SINGULAR SOURCE TERMS

In this section, we will construct the numerical scheme for approximate solution of the Advection equation

$$u_t + au_x = g(t)\delta(x-\xi), \quad 0 < x < l, \quad t > 0 \tag{6.1.1}$$

with dynamic singular point source term, where a is a positive constant and g is a smooth function.

6.1.1 Spatial discretization by using WENO methods

We define our grid, cells and cell centers as

$$0 = x_{\frac{1}{2}} < x_{\frac{3}{2}} < x_{\frac{5}{2}} < \ldots < x_{M-\frac{1}{2}} < x_{M+\frac{1}{2}} = l, \tag{6.1.2}$$

$$\Omega_i = \left[x_{i-\frac{1}{2}}, x_{i+\frac{1}{2}}\right], \quad i = 1, 2, \ldots, M, \tag{6.1.3}$$

$$x_i = \frac{x_{i-\frac{1}{2}} + x_{i+\frac{1}{2}}}{2}, \quad i = 1, 2, \ldots, M, \tag{6.1.4}$$

respectively (see Figure 5.1). We also define the mesh sizes as

$$h_i = x_{i+\frac{1}{2}} - x_{i-\frac{1}{2}}, \quad i = 1, 2, \ldots, M \tag{6.1.5}$$

Let the cell average value of function $u(x,t)$ be defined as

$$\bar{u}_i(t) = \frac{1}{h_i}\int\limits_{\Omega_i} u(x,t)dx, \quad i = 1, 2, \ldots, M. \tag{6.1.6}$$

The Finite Volume approach for (6.1.1) amounts for first integrating (6.1.1) over each cell Ω_i and dividing by the cell volume $|\Omega_i| = h_i$, which gives us:

$$\frac{1}{h_i}\int\limits_{\Omega_i} u_t dx + \frac{a}{h_i}\int\limits_{\Omega_i} u_x dx = \frac{1}{h_i}\int\limits_{\Omega_i} g(t)\delta(x-\xi)dx, \quad i = 1, \ldots, M. \tag{6.1.7}$$

Assuming that $\xi \in \Omega_j$, we obtain

$$\frac{\partial}{\partial t}\left(\frac{1}{h_i}\int\limits_{\Omega_i} u(x,t)dx\right) + \frac{a}{h_i}\int\limits_{\Omega_i}\frac{\partial}{\partial x}u(x,t)dx = g(t)\frac{\delta_{ij}}{h_i}, \quad i = 1, \ldots, M,$$

where δ_{ij} is the Kronecker delta symbol defined by (4.2.4). Then, applying the fundamental theorem of calculus, we have

$$\frac{d\bar{u}_i(t)}{dt} + \frac{a}{h_i}\left(u(x_{i+\frac{1}{2}},t) - u(x_{i-\frac{1}{2}},t)\right) = g(t)\frac{\delta_{ij}}{h_i}, \quad i = 1, 2, \ldots, M \tag{6.1.8}$$

Now, to finish the Finite Volume method for spatial discretization of equation (6.1.1), we have to express the terms $u(x_{i+\frac{1}{2}},t)$ and $u(x_{i-\frac{1}{2}},t)$ in (6.1.8) in terms of cell averages.

Firstly, we apply the WENO3 approximation (5.1.18), i.e.

$$\begin{aligned} u_{i+\frac{1}{2}} = \omega_0^{(i)}&\left(-\frac{h_i}{h_{i-1}+h_i}\bar{u}_{i-1} + \frac{h_{i-1}+2h_i}{h_{i-1}+h_i}\bar{u}_i\right) \\ &+ \omega_1^{(i)}\left(\frac{h_{i+1}}{h_i+h_{i+1}}\bar{u}_i + \frac{h_i}{h_i+h_{i+1}}\bar{u}_{i+1}\right), \end{aligned} \tag{6.1.9}$$

$$\begin{aligned} u_{i-\frac{1}{2}} = \omega_0^{(i-1)}&\left(-\frac{h_{i-1}}{h_{i-2}+h_{i-1}}\bar{u}_{i-2} + \frac{h_{i-2}+2h_{i-1}}{h_{i-2}+h_{i-1}}\bar{u}_{i-1}\right) \\ &+ \omega_1^{(i-1)}\left(\frac{h_i}{h_{i-1}+h_i}\bar{u}_{i-1} + \frac{h_{i-1}}{h_{i-1}+h_i}\bar{u}_i\right), \end{aligned} \tag{6.1.10}$$

where the weights $\omega_0^{(i)}$, $\omega_1^{(i)}$ are defined by (5.1.21)-(5.1.22) and the weights $\omega_0^{(i-1)}$, $\omega_1^{(i-1)}$ are obtained from (5.1.21)-(5.1.22) by shifting the index accordingly. Replacing $u(x_{i+\frac{1}{2}},t)$ and $u(x_{i-\frac{1}{2}},t)$ in (6.1.8) by (6.1.9) and (6.1.10), respectively, we obtain

$$\begin{aligned}\frac{d\bar{u}_i(t)}{dt} = \frac{a}{h_i}\Bigg[&\omega_0^{(i-1)}\left(-\frac{h_{i-1}}{h_{i-2}+h_{i-1}}\bar{u}_{i-2}+\frac{h_{i-2}+2h_{i-1}}{h_{i-2}+h_{i-1}}\bar{u}_{i-1}\right)\\ &+\omega_1^{(i-1)}\left(\frac{h_i}{h_{i-1}+h_i}\bar{u}_{i-1}+\frac{h_{i-1}}{h_{i-1}+h_i}\bar{u}_i\right)\\ &-\omega_0^{(i)}\left(-\frac{h_i}{h_{i-1}+h_i}\bar{u}_{i-1}+\frac{h_{i-1}+2h_i}{h_{i-1}+h_i}\bar{u}_i\right)\\ &-\omega_1^{(i)}\left(\frac{h_{i+1}}{h_i+h_{i+1}}\bar{u}_i+\frac{h_i}{h_i+h_{i+1}}\bar{u}_{i+1}\right)\Bigg]+g(t)\frac{\delta_{ij}}{h_i},\end{aligned} \tag{6.1.11}$$

which completes the Finite Volume WENO3 spatial discretization of equation (6.1.1).

Secondly, we apply the WENO5 approximation (5.2.25), i.e.

$$\begin{aligned}u_{i+\frac{1}{2}} = \omega_0^{(i)}\Bigg[&\frac{h_i(h_{i-1}+h_i)}{(h_{i-2}+h_{i-1})(h_{i-2}+h_{i-1}+h_i)}\bar{u}_{i-2}\\ -&\left(\frac{h_i(h_{i-1}+h_i)}{(h_{i-2}+h_{i-1})(h_{i-2}+h_{i-1}+h_i)}+\frac{h_i(h_{i-2}+2h_{i-1}+2h_i)}{(h_{i-1}+h_i)(h_{i-2}+h_{i-1}+h_i)}\right)\bar{u}_{i-1}\\ &+\left(1+\frac{h_i(h_{i-2}+2h_{i-1}+2h_i)}{(h_{i-1}+h_i)(h_{i-2}+h_{i-1}+h_i)}\right)\bar{u}_i\Bigg]\\ +\omega_1^{(i)}\Bigg[&-\frac{h_ih_{i+1}}{(h_{i-1}+h_i)(h_{i-1}+h_i+h_{i+1})}\bar{u}_{i-1}\\ +&\left(1+\frac{h_ih_{i+1}}{(h_{i-1}+h_i)(h_{i-1}+h_i+h_{i+1})}-\frac{h_i(h_{i-1}+h_i)}{(h_i+h_{i+1})(h_{i-1}+h_i+h_{i+1})}\right)\bar{u}_i\\ &+\frac{h_i(h_{i-1}+h_i)}{(h_i+h_{i+1})(h_{i-1}+h_i+h_{i+1})}\bar{u}_{i+1}\Bigg]\\ +\omega_2^{(i)}\Bigg[&\frac{h_{i+1}(h_{i+1}+h_{i+2})}{(h_i+h_{i+1})(h_i+h_{i+1}+h_{i+2})}\bar{u}_i\\ +&\left(1+\frac{h_ih_{i+1}}{(h_{i+1}+h_{i+2})(h_i+h_{i+1}+h_{i+2})}-\frac{h_{i+1}(h_{i+1}+h_{i+2})}{(h_i+h_{i+1})(h_i+h_{i+1}+h_{i+2})}\right)\bar{u}_{i+1}\\ &-\frac{h_ih_{i+1}}{(h_{i+1}+h_{i+2})(h_i+h_{i+1}+h_{i+2})}\bar{u}_{i+2}\Bigg],\end{aligned} \tag{6.1.12}$$

where the weights $\omega_0^{(i)}$, $\omega_1^{(i)}$, $\omega_2^{(i)}$ are defined by (5.2.28)-(5.2.29). By shifting the index in (6.1.12), we can obtain the WENO5 approximation $u_{i-\frac{1}{2}}$ in the similar way.

Now, replacing $u(x_{i+\frac{1}{2}}, t)$ and $u(x_{i-\frac{1}{2}}, t)$ in (6.1.8) by WENO5 approximations $u_{i+\frac{1}{2}}$ and $u_{i-\frac{1}{2}}$, respectively, we complete the Finite Volume WENO5 spatial discretization of equation (6.1.1).

Remark 6.1.1. Obviously, WENO3 approximations (6.1.9)-(6.1.10) and WENO5 approximations (6.1.12) have to be adjusted for cells at the left and at the right boundaries of the spatial domain where equation (6.1.1) is defined. One way is to fix the weights manually to 1 or 0, depending on whether the stencil is entirely inside of the interval $[0, l]$. In our numerical examples though we consider the problems with periodic solutions, so that WENO approximation formulas can be readily used without making any changes.

6.1.2 Temporal discretization

Spatial discretization by using Finite Volume WENO methods, introduced in Section 5, results in the system of ODEs

$$\frac{d\bar{U}(t)}{dt} = W\big(\bar{U}(t)\big)\bar{U}(t) + G(t). \tag{6.1.13}$$

Here, W is the matrix containing all nonlinear WENO weights and

$$\bar{U}(t) = \begin{pmatrix} \bar{u}_1(t) \\ \bar{u}_2(t) \\ \vdots \\ \bar{u}_M(t) \end{pmatrix}, \qquad G(t) = \begin{pmatrix} 0 \\ \vdots \\ \dfrac{g(t)}{h_j} \\ \vdots \\ 0 \end{pmatrix},$$

where vector G has zero entries except at entry j . Note that (6.1.13) is the system of nonlinear ODEs. For discretization of (6.1.13) we apply two different approaches, known in WENO literature, one being an explicit method and the other one being a semi-implicit method.

The most common way to discretize (6.1.13) is the strong-stability-preserving

(SSP) explicit third order Runge-Kutta method (Gottlieb et al., 2001).

$$\begin{aligned}
\bar{U}^{(1)} &= \bar{U}^n + \tau\Big(W\big(\bar{U}^n\big)\bar{U}^n + G(t)\Big),\\
\bar{U}^{(2)} &= \frac{3}{4}\bar{U}^n + \frac{1}{4}\bar{U}^{(1)} + \frac{\tau}{4}\Big(W\big(\bar{U}^{(1)}\big)\bar{U}^{(1)} + G(t_n+\tau)\Big),\\
\bar{U}^{n+1} &= \frac{1}{3}\bar{U}^n + \frac{2}{3}\bar{U}^{(2)} + \frac{2\tau}{3}\Big(W\big(\bar{U}^{(2)}\big)\bar{U}^{(2)} + G(t_n+\frac{\tau}{2})\Big),
\end{aligned} \tag{6.1.14}$$

where $\bar{U}^n$ is the numerical approximation of $\bar{U}(t)$ at $t = t_n = n\tau$ and $\tau > 0$ is the time step.

The other way to discretize (6.1.13) is the semi-implicit method introduced in (Gottlieb et al., 2006). On each time step, first the predictor $\tilde{U}^{n+1}$ is computed by using (6.1.14), i.e.

$$\begin{aligned}
\bar{U}^{(1)} &= \bar{U}^n + \tau\Big(W\big(\bar{U}^n\big)\bar{U}^n + G(t_n)\Big),\\
\bar{U}^{(2)} &= \frac{3}{4}\bar{U}^n + \frac{1}{4}\bar{U}^{(1)} + \frac{\tau}{4}\Big(W\big(\bar{U}^{(1)}\big)\bar{U}^{(1)} + G(t_n+\tau)\Big),\\
\tilde{U}^{n+1} &= \frac{1}{3}\bar{U}^n + \frac{2}{3}\bar{U}^{(2)} + \frac{2\tau}{3}\Big(W\big(\bar{U}^{(2)}\big)\bar{U}^{(2)} + G(t_n+\frac{\tau}{2})\Big).
\end{aligned} \tag{6.1.15}$$

Then, the Crank-Nicolson scheme is used to find the corrector:

$$\bar{U}^{n+1} = \bar{U}^n + \frac{\tau}{2}\Big(W\big(\bar{U}^n\big)\bar{U}^n + G(t_n) + W\big(\tilde{U}^{n+1}\big)U^{n+1} + G(t_{n+1})\Big). \tag{6.1.16}$$

Assume that the solution of the Advection equation (6.1.1) has to satisfy initial conditions $u(x, 0) = \phi(x)$, $0 \le x \le l$. Then, setting up $\bar{U}^0$ in (6.1.14) or in (6.1.15)-(6.1.16) completes the temporal discretization of (6.1.1).

6.1.3 Numerical Examples

In this section, we shall validate our findings by numerical illustrations for two simple test problems. Firstly, we consider the Advection problem without singular source terms. Obviously, such a problem has a smooth solution. We shall use this example to illustrate the correct orders of WENO methods. Secondly, we consider the Advection problem with singular source term, which has discontinuous solution.

Example 6.1.2. We consider the problem:

$$\begin{cases} u_t + u_x = 0, \quad 0 < t < 1, \quad 0 < x < 2, \\ u(x,0) = \sin(\pi x), \quad 0 \le x \le 1, \\ u(0,t) = 0, \quad 0 \le t \le 1. \end{cases} \tag{6.1.17}$$

The analytical solution of problem (6.1.17) is given by:

$$u(x,t) = sin(\pi(x-t)).$$

We set the non-uniform mesh in the following way. The mesh points are uniformly located in intervals $0 \le x \le 1$ and $1 \le x \le 2$. Spacing in the first interval is twice the spacing in the second interval, so that

$$h_i = \begin{cases} \dfrac{3}{M}, & \text{if } 1 \le i \le \dfrac{M}{3}, \\ \dfrac{3}{2M}, & \text{if } \dfrac{M}{3} < i \le M, \end{cases}$$

where M is the number of cells.

WENO3 and WENO5 methods are used for spatial discretization of problem (6.1.17) and semi-implicit scheme (6.1.15)-(6.1.16) is used for temporal discretization. To show the convergence rates of WENO methods and therefore to exclude the temporal errors, in all simulations we use $\tau = \dfrac{1}{N} = 5 \times 10^{-5}$ for time step. The errors are computed in two different norms. Firstly, accuracy is measured by means of the maximum norm:

$$\|Error\|_\infty = \max_{\substack{1 \le i \le M \\ 1 \le n \le N}} |\tilde{u}_i(t_n) - \bar{u}_i^n|, \tag{6.1.18}$$

where $\tilde{u}_i(t_n)$ is the exact cell average value in cell Ω_i at time point $t = t_n$ and $\bar{u}_i^n$ is the corresponding numerical solution. Secondly, accuracy is measured by means of the L^1 norm:

$$\begin{aligned} \|Error\|_{L^1} = \frac{1}{x_{M+\frac{1}{2}} - x_{\frac{1}{2}}} \Bigg[\sum_{i=1}^{M-1} \left| u(x_{i+\frac{1}{2}}, t_N) - u_{i+\frac{1}{2}}^N \right| \frac{h_i + h_{i+1}}{2} \\ + \left| u(x_{\frac{1}{2}}, t_N) - u_{\frac{1}{2}}^N \right| \frac{h_1}{2} + \left| u(x_{M+\frac{1}{2}}, t_N) - u_{M+\frac{1}{2}}^N \right| \frac{h_M}{2} \Bigg], \end{aligned} \tag{6.1.19}$$

where $u(x_{i+\frac{1}{2}}, t_N)$ is the exact solution at $x = x_{i+\frac{1}{2}}$ and $t = t_N$, $u_{i+\frac{1}{2}}^N$ is the corresponding numerical solution.

Table 6.1 shows the errors between the exact solution of problem (6.1.17) and the numerical solutions computed by semi-implicit WENO3 method for different values of M, as well as the convergence rates. We observe that the WENO3 scheme approaches the third order convergence for a high number of grid cells.

Table 6.1 The errors between the exact solution of the problem (6.1.17) and the numerical solutions computed by semi-implicit WENO3 method on non-uniform mesh for different values of M.

M	$\|Error\|_\infty$	$Order\ in\ \|\cdot\|_\infty$	$\|Error\|_{L^1}$	$Order\ in\ \|\cdot\|_{L^1}$
30	$1.03e-01$	–	$4.59e-02$	–
60	$4.22e-02$	1.2854	$1.32e-02$	1.8008
120	$1.60e-02$	1.4036	$3.18e-03$	2.0500
240	$5.03e-03$	1.6655	$6.22e-04$	2.3545
480	$9.21e-04$	2.4503	$6.92e-05$	3.1685

Table 6.2 shows the errors between the exact solution of problem (6.1.17) and the numerical solutions computed by semi-implicit WENO5 method for different values of M, as well as the convergence rates. We observe overall the fifth order convergence of the method, as it is expected. Obviously, the WENO5 method gives significant improvement in comparison with the WENO3 method (compare the results in Table 6.1 and Table 6.2).

Table 6.2 The errors between the exact solution of the problem (6.1.17) and the numerical solutions computed by semi-implicit WENO5 method on non-uniform mesh for different values of M.

M	$\|Error\|_\infty$	$Order\ in\ \|\cdot\|_\infty$	$\|Error\|_{L1}$	$Order\ in\ \|\cdot\|_{L1}$
$M=30$	$1.19e-03$	–	$3.90e-04$	–
$M=60$	$3.41e-05$	5.1255	$1.27e-05$	4.9377
$M=120$	$9.41e-07$	5.1795	$4.04e-07$	4.9766
$M=240$	$3.05e-08$	4.9465	$1.24e-08$	5.0308

Example 6.1.3. We consider the problem:

$$\begin{cases} u_t + u_x = sin(\pi t)\delta(x-\frac{1}{3}), & 0<x<1, \quad 0<t<0.5, \\ u(x,0)=0, & 0\le x\le 1, \\ u(0,t)=0, & 0\le t\le 0.5. \end{cases} \tag{6.1.20}$$

Let us first find the exact solution of problem (6.1.20). By taking the Laplace Transform with respect to t, from the first equality in (6.1.20) we obtain

$$sU(x,s) - u(x,0) + \frac{d}{dx}U(x,s) = \frac{\pi}{s^2+\pi^2}\delta(x-\frac{1}{3}),$$

where $U(x,s) = L\{u(x,t)\}$. Since $u(x,0)=0$, we have

$$\frac{d}{dx}U(x,s) + sU(x,s) = \frac{\pi}{s^2+\pi^2}\delta(x-\frac{1}{3})$$

or

$$\frac{d}{dx}\Big(e^{sx}U(x,s)\Big) = \frac{\pi}{s^2+\pi^2}e^{sx}\delta(x-\frac{1}{3}).$$

Integrating both sides of this equation from 0 to x, we get

$$e^{sx}U(x,s) = \frac{\pi}{s^2+\pi^2}\int_0^x e^{s\xi}\delta(\xi-\frac{1}{3})d\xi + C.$$

Since $u(0,t)=0$, we have $C = U(0,s) = L\{u(0,t)\} = 0$. Then,

$$U(x,s) = \frac{\pi}{s^2+\pi^2}e^{-sx}\int_0^x e^{s\xi}\delta(\xi-\frac{1}{3})d\xi.$$

Using (1.2.3), we get

$$U(x,s) = \begin{cases} 0, & x<\frac{1}{3} \\ \frac{\pi}{s^2+\pi^2}e^{-sx}e^{s/3}, & x\ge\frac{1}{3}. \end{cases}$$

Since

$$L^{-1}\left\{\frac{\pi}{s^2+\pi^2}e^{-(x-\frac{1}{3})s}\right\} = H(t-x+\frac{1}{3})\sin\Big(\pi(t-x+\frac{1}{3})\Big),$$

the analytical solution of problem (6.1.20) has the form

$$u(x,t) = \begin{cases} 0, & \text{if } x<\frac{1}{3}, \\ H(t-x+\frac{1}{3})\sin\Big(\pi(t-x+\frac{1}{3})\Big), & \text{if } x\ge\frac{1}{3} \end{cases}$$

or

$$u(x,t) = \begin{cases} 0, & \text{if } \ x < \dfrac{1}{3} \ \text{ or } \ x \geq \dfrac{1}{3} + t, \\ \sin\left(\pi(t - x + \dfrac{1}{3})\right), & \text{if } \ \dfrac{1}{3} \leq x < \dfrac{1}{3} + t. \end{cases} \tag{6.1.21}$$

Note that solution (6.1.21) has a jump discontinuity at $x = \dfrac{1}{3}$.

We first set the uniform mesh with mesh sizes $h = \dfrac{1}{M}$, where M is the number of cells. We apply the WENO3 and WENO5 methods on this uniform mesh for spatial discretization of problem (6.1.20) and semi-implicit scheme (6.1.15)-(6.1.16) for temporal discretization. In all simulations, we use $\tau = \dfrac{1}{N} = 5 \times 10^{-4}$ for time step.

Table 6.3 shows the errors in L^1 norm between the exact solution of problem (6.1.20) and the numerical solutions computed by semi-implicit WENO3 method on uniform mesh for different values of M, as well as the convergence rates. We observe that the WENO3 scheme has only the first order convergence. This order reduction from three to one obviously occurs here due to the discontinuity in the solution of problem (6.1.20).

Table 6.3 The errors between the exact solution of the problem (6.1.20) and the numerical solutions computed by semi-implicit WENO3 method on uniform mesh for different values of M.

M	$\|Error\|_{L^1}$	$Order\ in\ \|\cdot\|_{L^1}$
20	$3.74e-02$	$-$
80	$9.12e-03$	1.0185
320	$2.22e-03$	1.0186

Table 6.4 shows the errors in L^1 norm between the exact solution of problem (6.1.20) and the numerical solutions computed by semi-implicit WENO5 method on uniform mesh for different values of M, as well as the convergence rates. We observe that the WENO5 scheme has also the first order convergence. Moreover, there is no significant difference in the results compared to corresponding WENO3 results given in Table 6.3. This might look at first glance rather surprising. One would

expect better results from higher order of accuracy method. However, it is the case only for smooth functions. Recall that WENO5 method is based on approximations by using quadratic polynomials, while WENO3 method uses linear polynomials. For discontinuous functions higher order polynomials do not necessarily give better approximations.

Table 6.4 The errors between the exact solution of the problem (6.1.20) and the numerical solutions computed by semi-implicit WENO5 method on uniform mesh for different values of M.

M	$\|Error\|_{L^1}$	$Order\ in\ \|\cdot\|_{L^1}$
20	$3.54e-02$	$-$
80	$8.56e-03$	1.0237
320	$2.10e-03$	1.0124

Next, we set the non-uniform mesh in the following way. We first place 100 fine uniform cells in the interval $[0.3, 0.4]$ with cell size 0.001 each. Then, we place 15 coarse uniform cells in the interval $[0, 0.228]$ with cell size 0.0152 each and 35 coarse uniform cells in the interval $[0.472, 1]$ with cell size 0.0151 each. Two remaining intervals $[0.228, 0.3]$ and $[0.4, 0.472]$ are intermediate regions. In each intermediate region we place 15 cells such that cells sizes are increased by 20% from one cell to the next in the direction from the fine-mesh region to the coarse-mesh region. Thus, in total we have 180 cells and mesh sizes are defined as

$$h_i = \begin{cases} 0.0152, & \text{if} \;\; 1 \le i \le 15, \\ 0.001 \cdot (1.2)^{30-i}, & \text{if} \;\; 16 \le i \le 30, \\ 0.001, & \text{if} \;\; 31 \le i \le 130, \\ 0.001 \cdot (1.2)^{i-131}, & \text{if} \;\; 131 \le i \le 145, \\ 0.0151, & \text{if} \;\; 146 \le i \le 180. \end{cases}$$

Note that with this mesh choice, the discontinuity point $x = \dfrac{1}{3} \in \Omega_{64}$. We apply the WENO3 and WENO5 methods on this non-uniform mesh for spatial discretization of problem (6.1.20) and semi-implicit scheme (6.1.15)-(6.1.16) for temporal discretization. In both simulations, we use $\tau = \dfrac{1}{N} = 5 \times 10^{-4}$ for time step.

Figure 6.1 shows the exact solution (solid lines) of problem (6.1.20) at $t = 0.25$ along with the numerical solutions (crosses) computed by semi-implicit WENO3 (left) and WENO5 (right) methods on non-uniform mesh.

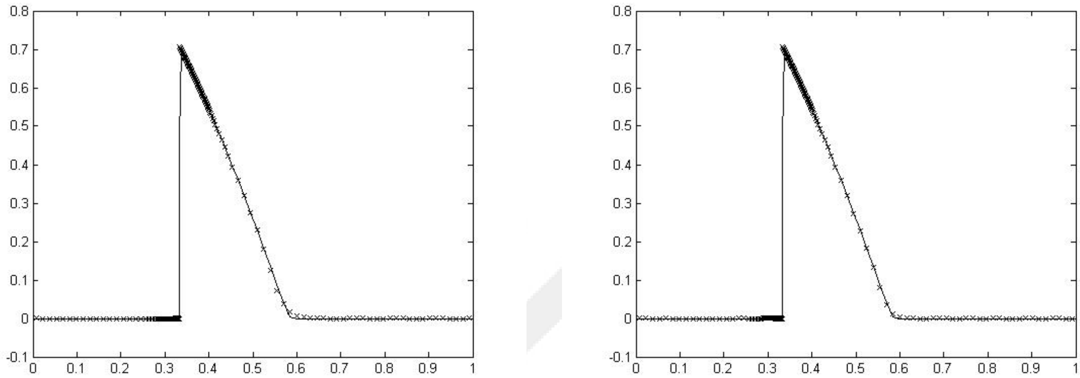

Figure 6.1 Exact solution (solid lines) of problem (6.1.20) at time $t = 0.25$ and corresponding numerical solutions (crosses) computed by semi-implicit WENO3 method (left) and semi-implicit WENO5 method (right) on non-uniform mesh.

Figure 6.2 shows the exact solution (solid lines) of problem (6.1.20) at $t = 0.5$ along with the numerical solutions (crosses) computed by semi-implicit WENO3 (left) and WENO5 (right) methods on non-uniform mesh.

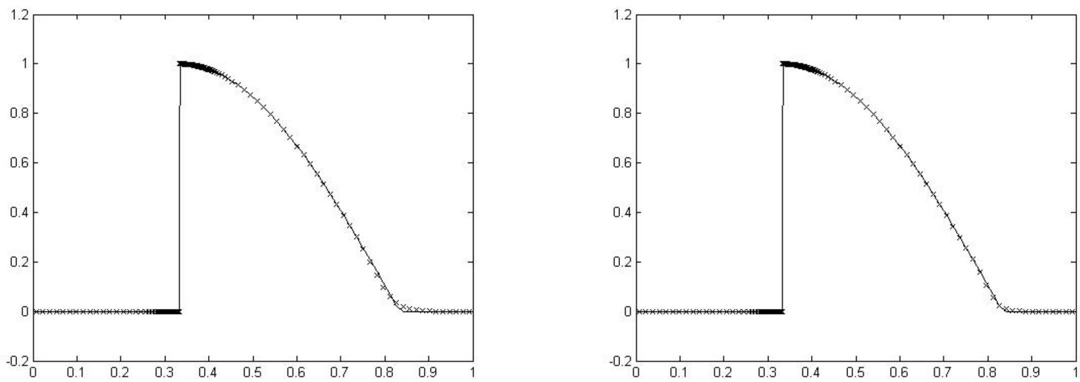

Figure 6.2 Exact solution (solid lines) of problem (6.1.20) at time $t = 0.5$ and corresponding numerical solutions (crosses) computed by semi-implicit WENO3 method (left) and semi-implicit WENO5 method (right) on non-uniform mesh.

The error in L^1 norm between the exact solution of the problem (6.1.20) and the numerical solution computed by semi-implicit WENO3 method on non-uniform mesh with 180 cells is

$$\|Error\|_{L^1} = 1.88e - 03.$$

Note that this numerical solution is more accurate than the one obtained on uniform mesh with 320 cells (see Table 6.3). This illustrates the advantage of using locally refined grids for numerical solution of problems with non-smooth solutions.

The error in L^1 norm between the exact solution of the problem (6.1.20) and the numerical solution computed by semi-implicit WENO5 method on non-uniform mesh with 180 cells is

$$\|Error\|_{L^1} = 9.91e - 04.$$

Although the accuracy of WENO5 method in this simulation is twice smaller than the accuracy of WENO3 method, the difference is not that drastic as it was in the case of problem with smooth solution (Example 6.1.2). Finally, note that this numerical solution is more accurate than the one obtained on uniform mesh with 320 cells (see Table 6.4).

6.2 ADVECTION DIFFUSION PROBLEMS WITH SINGULAR SOURCE TERMS

In this section, we will construct the numerical scheme for approximate solution of the Advection Diffusion equation

$$u_t + au_x = du_{xx} + g(t)\delta(x - \xi), \tag{6.2.1}$$

with dynamic singular point source term, where a and d are positive constants, g is a smooth function. We consider the problem (6.2.1) under the condition $d \ll a$, which means low diffusion.

6.2.1 Spatial discretization by using WENO methods

Let the grid, cells, cell centers and mesh sizes be defined by (6.1.2), (6.1.3), (6.1.4) and (6.1.5), respectively. Let the cell average values of function $u(x, t)$ be defined by (6.1.6).

The Finite Volume approach for (6.2.1) amounts for first integrating (6.2.1) over each cell Ω_i and dividing by the cell volume $|\Omega_i| = h_i$, which gives us:

$$\frac{1}{h_i}\int_{\Omega_i} u_t dx + \frac{a}{h_i}\int_{\Omega_i} u_x dx = \frac{d}{h_i}\int_{\Omega_i} u_{xx} dx + \frac{1}{h_i}\int_{\Omega_i} g(t)\delta(x-\xi)dx, \quad i = 1, \ldots, M.$$

Assuming that $\xi \in \Omega_j$, we obtain

$$\frac{\partial}{\partial t}\left(\frac{1}{h_i}\int_{\Omega_i} u(x,t)dx\right) + \frac{a}{h_i}\int_{\Omega_i}\frac{\partial}{\partial x}u(x,t)dx$$
$$= \frac{d}{h_i}\int_{\Omega_i}\frac{\partial^2}{\partial x^2}u(x,t)dx + g(t)\frac{\delta_{ij}}{h_i}, \quad i = 1, \ldots, M,$$

where δ_{ij} is the Kronecker delta symbol defined by (4.2.4). Then, applying the fundamental theorem of calculus, we have

$$\begin{aligned}\frac{d\bar{u}_i(t)}{dt} &+ \frac{a}{h_i}\left(u(x_{i+\frac{1}{2}},t) - u(x_{i-\frac{1}{2}},t)\right) \\ &= \frac{d}{h_i}\left(u_x(x_{i+\frac{1}{2}},t) - u_x(x_{i-\frac{1}{2}},t)\right) + g(t)\frac{\delta_{ij}}{h_i}, \quad i = 1, \ldots, M.\end{aligned} \tag{6.2.2}$$

Now, to finish the Finite Volume method for spatial discretization of equation (6.2.1), we have to express the terms $u(x_{i+\frac{1}{2}},t)$, $u(x_{i-\frac{1}{2}},t)$, $u_x(x_{i+\frac{1}{2}},t)$ and $u_x(x_{i-\frac{1}{2}},t)$ in (6.2.2) in terms of cell averages.

We denote

$$\varphi = u_x. \tag{6.2.3}$$

Then, (6.2.2) can be written as

$$\begin{aligned}\frac{d\bar{u}_i(t)}{dt} &= \frac{a}{h_i}(u(x_{i-\frac{1}{2}},t) - u(x_{i+\frac{1}{2}},t)) \\ &+ \frac{d}{h_i}\left(\varphi(x_{i+\frac{1}{2}},t) - \varphi(x_{i-\frac{1}{2}},t)\right) + g(t)\frac{\delta_{ij}}{h_i}, \quad i = 1, \ldots, M.\end{aligned} \tag{6.2.4}$$

Let us first describe the application of WENO3 method in (6.2.4). We can readily use the WENO3 approximations (6.1.9) and (6.1.10) for $u(x_{i+\frac{1}{2}},t)$ and $u(x_{i-\frac{1}{2}},t)$ in (6.2.4), respectively. Next, we will obtain the WENO3 approximation for $\varphi(x_{i+\frac{1}{2}},t)$ in (6.2.4). We use linear polynomials (5.1.1) and (5.1.6) to find two approximations on stencils $S_0 = \{\Omega_{i-1}, \Omega_i\}$ and $S_1 = \{\Omega_i, \Omega_{i+1}\}$, respectively (see Figure 5.1).

From (5.1.1) and (5.1.3) we have

$$\frac{d}{dx}p_0^{(i)}(x) = a_0^{(i)} = \frac{2}{h_{i-1}+h_i}\big(\bar{u}_i - \bar{u}_{i-1}\big).$$

Then, the approximation of $\varphi(x_{i+\frac{1}{2}}, t)$ on stencil $S_0 = \{\Omega_{i-1}, \Omega_i\}$ is given by

$$\varphi_{i+\frac{1}{2}}^{(0)} = \frac{2}{h_{i-1}+h_i}\big(\bar{u}_i - \bar{u}_{i-1}\big). \tag{6.2.5}$$

Similarly, from (5.1.6) and (5.1.8) we have

$$\frac{d}{dx}p_1^{(i)}(x) = a_1^{(i)} = \frac{2}{h_i+h_{i+1}}\big(\bar{u}_{i+1} - \bar{u}_i\big).$$

Then, the approximation of $\varphi(x_{i+\frac{1}{2}}, t)$ on stencil $S_1 = \{\Omega_i, \Omega_{i+1}\}$ is given by

$$\varphi_{i+\frac{1}{2}}^{(1)} = \frac{2}{h_i+h_{i+1}}\big(\bar{u}_{i+1} - \bar{u}_i\big). \tag{6.2.6}$$

Now, taking the convex combination of approximations $\varphi_{i+\frac{1}{2}}^{(0)}$ and $\varphi_{i+\frac{1}{2}}^{(1)}$ results in the WENO3 approximation for $\varphi(x_{i+\frac{1}{2}}, t)$. Namely,

$$\varphi_{i+\frac{1}{2}} = \omega_0^{(i)}\varphi_{i+\frac{1}{2}}^{(0)} + \omega_1^{(i)}\varphi_{i+\frac{1}{2}}^{(1)} = \frac{2\omega_0^{(i)}}{h_{i-1}+h_i}\big(\bar{u}_i - \bar{u}_{i-1}\big) + \frac{2\omega_1^{(i)}}{h_i+h_{i+1}}\big(\bar{u}_{i+1} - \bar{u}_i\big), \tag{6.2.7}$$

where the weights $\omega_0^{(i)}$ and $\omega_1^{(i)}$ are defined by (5.1.21)-(5.1.22). Note that in (6.2.7) we use the same weights as in WENO3 approximation (6.1.9) for $u(x_{i+\frac{1}{2}}, t)$. It is due to (6.2.3), i.e. if u is non-smooth in one of the stencils then so is φ.

Now, by shifting the index in (6.2.7), we obtain the WENO3 approximation for $\varphi(x_{i-\frac{1}{2}}, t)$. Namely,

$$\varphi_{i-\frac{1}{2}} = \frac{2\omega_0^{(i-1)}}{h_{i-2}+h_{i-1}}\big(\bar{u}_{i-1} - \bar{u}_{i-2}\big) + \frac{2\omega_1^{(i-1)}}{h_{i-1}+h_i}\big(\bar{u}_i - \bar{u}_{i-1}\big), \tag{6.2.8}$$

where the weights $\omega_0^{(i-1)}$ and $\omega_1^{(i-1)}$ are obtained from (5.1.21)-(5.1.22) by shifting the index accordingly.

Replacing $u(x_{i+\frac{1}{2}}, t)$, $u(x_{i-\frac{1}{2}}, t)$, $\varphi(x_{i+\frac{1}{2}}, t)$ and $\varphi(x_{i-\frac{1}{2}}, t)$ in (6.1.8) by (6.1.9), (6.1.10), (6.2.7) and (6.2.8), respectively, we obtain

$$\begin{aligned}\frac{d\bar{u}_i(t)}{dt} = \frac{a}{h_i}\Bigg[&\omega_0^{(i-1)}\left(-\frac{h_{i-1}}{h_{i-2}+h_{i-1}}\bar{u}_{i-2}+\frac{h_{i-2}+2h_{i-1}}{h_{i-2}+h_{i-1}}\bar{u}_{i-1}\right)\\ &+\omega_1^{(i-1)}\left(\frac{h_i}{h_{i-1}+h_i}\bar{u}_{i-1}+\frac{h_{i-1}}{h_{i-1}+h_i}\bar{u}_i\right)\\ &-\omega_0^{(i)}\left(-\frac{h_i}{h_{i-1}+h_i}\bar{u}_{i-1}+\frac{h_{i-1}+2h_i}{h_{i-1}+h_i}\bar{u}_i\right)\\ &-\omega_1^{(i)}\left(\frac{h_{i+1}}{h_i+h_{i+1}}\bar{u}_i+\frac{h_i}{h_i+h_{i+1}}\bar{u}_{i+1}\right)\Bigg]\\ +\frac{d}{h_i}\Bigg[&\frac{2\omega_0^{(i)}}{h_{i-1}+h_i}(\bar{u}_i-\bar{u}_{i-1})+\frac{2\omega_1^{(i)}}{h_i+h_{i+1}}(\bar{u}_{i+1}-\bar{u}_i)\\ &-\frac{2\omega_0^{(i-1)}}{h_{i-2}+h_{i-1}}(\bar{u}_{i-1}-\bar{u}_{i-2})-\frac{2\omega_1^{(i-1)}}{h_{i-1}+h_i}(\bar{u}_i-\bar{u}_{i-1})\Bigg]+g(t)\frac{\delta_{ij}}{h_i},\end{aligned} \tag{6.2.9}$$

which completes the Finite Volume WENO3 spatial discretization of equation (6.2.1).

Remark 6.2.1. Another way to approximate $\varphi(x_{i+\frac{1}{2}},t)$ and $\varphi(x_{i-\frac{1}{2}},t)$ in (6.2.4) is to use the WENO3 approximation formulas (6.1.9)-(6.1.9) to function φ. Namely,

$$\begin{aligned}\varphi_{i+\frac{1}{2}} = \omega_0^{(i)}&\left(-\frac{h_i}{h_{i-1}+h_i}\bar{\varphi}_{i-1}+\frac{h_{i-1}+2h_i}{h_{i-1}+h_i}\bar{\varphi}_i\right)\\ &+\omega_1^{(i)}\left(\frac{h_{i+1}}{h_i+h_{i+1}}\bar{\varphi}_i+\frac{h_i}{h_i+h_{i+1}}\bar{\varphi}_{i+1}\right),\end{aligned} \tag{6.2.10}$$

$$\begin{aligned}\varphi_{i-\frac{1}{2}} = \omega_0^{(i-1)}&\left(-\frac{h_{i-1}}{h_{i-2}+h_{i-1}}\bar{\varphi}_{i-2}+\frac{h_{i-2}+2h_{i-1}}{h_{i-2}+h_{i-1}}\bar{\varphi}_{i-1}\right)\\ &+\omega_1^{(i-1)}\left(\frac{h_i}{h_{i-1}+h_i}\bar{\varphi}_{i-1}+\frac{h_{i-1}}{h_{i-1}+h_i}\bar{\varphi}_i\right),\end{aligned} \tag{6.2.11}$$

where

$$\bar{\varphi}_i(t) = \frac{1}{h_i}\int\limits_{\Omega_i}\varphi(x,t)dx = \frac{1}{h_i}\int\limits_{\Omega_i}u_x(x,t)dx = \frac{u(x_{i+\frac{1}{2}},t)-u(x_{i-\frac{1}{2}},t)}{h_i},\ i=1,\ldots,M.$$

However, we did not use this approach in our numerical experiments.

Let us now describe the application of WENO5 method in (6.2.4). We can readily use the WENO5 approximation (6.1.12) for $u(x_{i+\frac{1}{2}},t)$ in (6.2.4). By shifting the index in (6.1.12), we can also obtain the WENO5 approximation for $u(x_{i-\frac{1}{2}}, t)$. Now, we will obtain the WENO5 approximation for $\varphi(x_{i+\frac{1}{2}}, t)$ in (6.2.4). We use quadratic polynomials (5.2.1), (5.2.8) and (5.2.13) to find three approximations on stencils $S_0 = \{\Omega_{i-2}, \Omega_{i-1}, \Omega_i\}$, $S_1 = \{\Omega_{i-1}, \Omega_i, \Omega_{i+1}\}$ and $S_2 = \{\Omega_i, \Omega_{i+1}, \Omega_{i+2}\}$, respectively (see Figure 5.1).

From (5.2.1) we have

$$\frac{d}{dx} p_0^{(i)}(x)\Big|_{x=x_{i+\frac{1}{2}}} = a_0^{(i)} h_i + b_0^{(i)},$$

where $a_0^{(i)}$ and $b_0^{(i)}$ are defined by (5.2.3) and (5.2.4), respectively. Then, using (5.2.3)-(5.2.4) we find the approximation of $\varphi(x_{i+\frac{1}{2}}, t)$ on stencil $S_0 = \{\Omega_{i-2}, \Omega_{i-1}, \Omega_i\}$ as following

$$\begin{aligned}
\varphi^{(0)}_{i+\frac{1}{2}} &= \frac{d}{dx} p_0^{(i)}(x)\Big|_{x=x_{i+\frac{1}{2}}} \\
&= \frac{2\,(h_{i-1} + 2h_i)}{(h_{i-2} + h_{i-1})(h_{i-2} + h_{i-1} + h_i)} \bar{u}_{i-2} \\
&\quad - \left(\frac{2\,(h_{i-1} + 2h_i)}{(h_{i-2} + h_{i-1})(h_{i-2} + h_{i-1} + h_i)} + \frac{2\,(h_{i-2} + 2h_{i-1} + 3h_i)}{(h_{i-1} + h_i)(h_{i-2} + h_{i-1} + h_i)} \right) \bar{u}_{i-1} \\
&\quad + \frac{2\,(h_{i-2} + 2h_{i-1} + 3h_i)}{(h_{i-1} + h_i)(h_{i-2} + h_{i-1} + h_i)} \bar{u}_i .
\end{aligned} \tag{6.2.12}$$

Similarly, from (5.2.8) we have

$$\frac{d}{dx} p_1^{(i)}(x)\Big|_{x=x_{i+\frac{1}{2}}} = a_1^{(i)} h_i + b_1^{(i)},$$

where $a_1^{(i)}$ and $b_1^{(i)}$ are defined by (5.2.10). Then, using (5.2.10) we find the approximation of $\varphi(x_{i+\frac{1}{2}}, t)$ on stencil $S_1 = \{\Omega_{i-1}, \Omega_i, \Omega_{i+1}\}$ as following

$$\begin{aligned}
\varphi^{(1)}_{i+\frac{1}{2}} &= \frac{2\,(h_i - h_{i+1})}{(h_{i-1} + h_i)(h_{i-1} + h_i + h_{i+1})} \bar{u}_{i-1} \\
&\quad - \left(\frac{2\,(h_i - h_{i+1})}{(h_{i-1} + h_i)(h_{i-1} + h_i + h_{i+1})} + \frac{2\,(h_{i-1} + 2h_i)}{(h_i + h_{i+1})(h_{i-1} + h_i + h_{i+1})} \right) \bar{u}_i \\
&\quad + \frac{2\,(h_{i-1} + 2h_i)}{(h_i + h_{i+1})(h_{i-1} + h_i + h_{i+1})} \bar{u}_{i+1} .
\end{aligned} \tag{6.2.13}$$

Finally, from (5.2.13) we have

$$\frac{d}{dx} p_2^{(i)}(x) \Big|_{x=x_{i+\frac{1}{2}}} = a_2^{(i)} h_i + b_2^{(i)},$$

where $a_2^{(i)}$ and $b_2^{(i)}$ are defined by (5.2.15). Then, using (5.2.15) we find the approximation of $\varphi(x_{i+\frac{1}{2}}, t)$ on stencil $S_2 = \{\Omega_i, \Omega_{i+1}, \Omega_{i+2}\}$ as following

$$\begin{aligned} \varphi_{i+\frac{1}{2}}^{(2)} = &-\frac{2\,(2h_{i+1} + h_{i+2})}{(h_i + h_{i+1})(h_i + h_{i+1} + h_{i+2})} \bar{u}_i \\ &+ \left(\frac{2\,(2h_{i+1} + h_{i+2})}{(h_i + h_{i+1})(h_i + h_{i+1} + h_{i+2})} + \frac{2\,(h_{i+1} - h_i)}{(h_{i+1} + h_{i+2})(h_i + h_{i+1} + h_{i+2})} \right) \bar{u}_{i+1} \\ &- \frac{2\,(h_{i+1} - h_i)}{(h_{i+1} + h_{i+2})(h_i + h_{i+1} + h_{i+2})} \bar{u}_{i+2}. \end{aligned} \tag{6.2.14}$$

Now, taking the convex combination of approximations $\varphi_{i+\frac{1}{2}}^{(0)}$, $\varphi_{i+\frac{1}{2}}^{(1)}$ and $\varphi_{i+\frac{1}{2}}^{(2)}$ results in the WENO5 approximation for $\varphi(x_{i+\frac{1}{2}}, t)$. Namely,

$$\varphi_{i+\frac{1}{2}} = \omega_0^{(i)} \varphi_{i+\frac{1}{2}}^{(0)} + \omega_1^{(i)} \varphi_{i+\frac{1}{2}}^{(1)} + \omega_2^{(i)} \varphi_{i+\frac{1}{2}}^{(2)}, \tag{6.2.15}$$

where the weights $\omega_0^{(i)}$, $\omega_1^{(i)}$ and $\omega_2^{(i)}$ are defined by (5.2.28)-(5.2.29). Note that in (6.2.15) we use the same weights as in WENO5 approximation (6.1.12) for $u(x_{i+\frac{1}{2}}, t)$. It is due to (6.2.3), i.e. if u is non-smooth in one of the stencils then so is φ.

By shifting the index in (6.2.15), we obtain the WENO5 approximation for $\varphi(x_{i-\frac{1}{2}}, t)$ as following

$$\varphi_{i-\frac{1}{2}} = \omega_0^{(i-1)} \varphi_{i-\frac{1}{2}}^{(0)} + \omega_1^{(i-1)} \varphi_{i-\frac{1}{2}}^{(1)} + \omega_2^{(i-1)} \varphi_{i-\frac{1}{2}}^{(2)}, \tag{6.2.16}$$

where the weights $\omega_0^{(i-1)}$, $\omega_1^{(i-1)}$, $\omega_2^{(i-1)}$ are obtained from (5.2.28)-(5.2.29) and approximations $\varphi_{i-\frac{1}{2}}^{(0)}$, $\varphi_{i-\frac{1}{2}}^{(1)}$, $\varphi_{i-\frac{1}{2}}^{(2)}$ are obtained from (6.2.12)-(6.2.14) by shifting the index accordingly.

Now, replacing $u(x_{i+\frac{1}{2}}, t)$, $u(x_{i-\frac{1}{2}}, t)$, $\varphi(x_{i+\frac{1}{2}}, t)$ and $\varphi(x_{i-\frac{1}{2}}, t)$ in (6.2.4) by WENO5 approximations $u_{i+\frac{1}{2}}$, $u_{i-\frac{1}{2}}$, $\varphi_{i+\frac{1}{2}}$ and $\varphi_{i-\frac{1}{2}}$ respectively, we complete the Finite Volume WENO5 spatial discretization of equation (6.2.1).

6.2.2 Numerical Examples

In this section, we shall validate our findings by numerical illustrations for two simple test problems. Firstly, we consider the Advection Diffusion problem without singular source terms. Obviously, such a problem has a smooth solution. We shall use this example to illustrate the correct orders of WENO methods. Secondly, we consider the Advection Diffusion problem with singular source terms, which has non-smooth solution.

Example 6.2.2. We consider the problem:

$$\begin{cases} u_t + u_x = 0.001u_{xx}, \quad 0 < t < 1, \quad 0 < x < 1, \\ u(x,0) = \sin(2\pi x), \quad 0 \le x \le 1, \\ u(0,t) = u(1,t) = 0, \quad 0 \le t \le 1. \end{cases} \tag{6.2.17}$$

The analytical solution of problem (6.2.17) is given by:

$$u(x,t) = \exp\left(-\frac{\pi^2 t}{250}\right) \sin\big(2\pi(x-t)\big) \tag{6.2.18}$$

We set the non-uniform mesh in the following way. The mesh points are uniformly located in intervals $0 \le x \le \frac{1}{2}$ and $\frac{1}{2} \le x \le 1$. Spacing in the first interval is twice the spacing in the second interval, so that

$$h_i = \begin{cases} \frac{3}{M}, & \text{if } 1 \le i \le \frac{M}{3}, \\ \frac{3}{2M}, & \text{if } \frac{M}{3} < i \le M, \end{cases}$$

where M is the number of cells.

WENO3 and WENO5 methods are used for spatial discretization of problem (6.2.17) and semi-implicit scheme (6.1.15)-(6.1.16) is used for temporal discretization. To show the convergence rates of WENO methods and therefore to exclude the temporal errors, in all simulations we use $\tau = \frac{1}{N} = 10^{-5}$ for time step. The errors are computed in two different norms, in maximum norm defined by (6.1.18) and L^1 norm defined by (6.1.19).

Table 6.5 shows the errors between the exact solution of problem (6.2.17) and the numerical solutions computed by semi-implicit WENO3 method for different values of M, as well as the convergence rates. We observe on average the second order convergence of the method in both norms.

Table 6.6 shows the errors between the exact solution of problem (6.2.17) and the numerical solutions computed by semi-implicit WENO5 method for different

Table 6.5 The errors between the exact solution of the problem (6.2.17) and the numerical solutions computed by semi-implicit WENO3 method on non-uniform mesh for different values of M.

M	$\|Error\|_\infty$	$Order\ in\ \|\cdot\|_\infty$	$\|Error\|_{L^1}$	$Order\ in\ \|\cdot\|_{L^1}$
15	$3.50e-01$	$-$	$1.81e-01$	$-$
30	$1.38e-01$	1.3424	$6.26e-02$	1.5326
60	$5.03e-02$	1.4579	$1.66e-02$	1.9171
120	$1.51e-02$	1.7314	$2.80e-03$	2.5689
240	$2.82e-03$	2.4245	$4.06e-04$	2.7819
480	$1.91e-04$	3.8856	$1.21e-04$	1.7519

values of M, as well as the convergence rates. We observe on average the fourth order convergence of the method. Obviously, the WENO5 method gives significant improvement in comparison with the WENO3 method (compare the results in Table 6.5 and Table 6.6). Finally, we note that for both methods one degree order reduction occurs although the solution (6.2.18) is the smooth function. Similar convergence results are obtained by both methods when uniform mesh is used (results are not given here).

Table 6.6 The errors between the exact solution of the problem (6.2.17) and the numerical solutions computed by semi-implicit WENO5 method on non-uniform mesh for different values of M.

M	$\|Error\|_\infty$	$Order\ in\ \|\cdot\|_\infty$	$\|Error\|_{L^1}$	$Order\ in\ \|\cdot\|_{L^1}$
15	$2.76e-02$	$-$	$1.29e-02$	$-$
30	$1.17e-03$	4.5543	$6.33e-04$	4.3497
60	$4.61e-05$	4.6724	$2.58e-05$	4.6144
120	$3.56e-06$	3.6937	$2.21e-06$	3.5496
240	$6.46e-07$	2.4635	$4.11e-07$	2.4254

Example 6.2.3. We consider the problem:

$$\begin{cases} u_t + u_x = 0.001 u_{xx} + 0.001 \left(\delta(x - \frac{1}{3}) - \delta(x - \frac{2}{3}) \right) \\ \qquad + \frac{1}{3} + H(x - \frac{2}{3}) - H(x - \frac{1}{3}), \quad 0 < t < 1, \quad 0 < x < 1, \\ u(x,0) = \sin(2\pi x) + z(x), \quad 0 \le x \le 1, \\ u(0,t) = u(1,t), \quad 0 \le t \le 1, \end{cases} \tag{6.2.19}$$

where

$$z(x) = \begin{cases} \frac{x}{3}, & 0 \le x \le \frac{1}{3}, \\ \frac{1-2x}{3}, & \frac{1}{3} < x \le \frac{2}{3}, \\ \frac{x-1}{3}, & \frac{2}{3} < x \le 1. \end{cases}$$

The analytical solution of problem (6.2.19) is given by:

$$u(x,t) = \exp\left(-\frac{\pi^2 t}{250} \right) \sin\big(2\pi(x-t)\big) + z(x). \tag{6.2.20}$$

Note that solution (6.2.20) is continuous function but is has discontinuous first derivative.

We first set the uniform mesh with mesh sizes $h = \frac{1}{M}$, where M is the number of cells. We apply the WENO3 and WENO5 methods on this uniform mesh for spatial discretization of problem (6.2.19) and semi-implicit scheme (6.1.15)-(6.1.16) for temporal discretization. In all simulations, we use $\tau = \frac{1}{N} = 10^{-5}$ for time step. The errors are computed in maximum norm defined by (6.1.18) and L^1 norm defined by (6.1.19).

Table 6.7 shows the errors between the exact solution of problem (6.2.19) and the numerical solutions computed by semi-implicit WENO3 method on uniform mesh for different values of M, as well as the convergence rates. We observe that the WENO3 scheme has on average the second order convergence in both norms.

Table 6.8 shows the errors between the exact solution of problem (6.2.19) and the numerical solutions computed by semi-implicit WENO5 method on uniform mesh for different values of M, as well as the convergence rates. We observe that the WENO5 scheme has only the first order convergence in the maximum norm and the second order convergence in L^1 norm. Although the WENO5 method gives

Table 6.7 The errors between the exact solution of the problem (6.2.19) and the numerical solutions computed by semi-implicit WENO3 method on uniform mesh for different values of M.

M	$\|Error\|_\infty$	$Order\ in\ \|\cdot\|_\infty$	$\|Error\|_{L^1}$	$Order\ in\ \|\cdot\|_{L^1}$
10	$4.97e-01$	–	$2.80e-01$	–
20	$1.87e-01$	1.4110	$8.12e-02$	1.7872
40	$6.84e-02$	1.4506	$2.71e-02$	1.5847
80	$2.00e-02$	1.7743	$4.65e-03$	2.5406
160	$3.58e-03$	2.4810	$6.47e-04$	2.8466
320	$7.36e-04$	2.2838	$1.67e-04$	1.9511

much more accurate results in L^1 norm than the WENO3 method does, there is no significant difference in results in maximum norm (compare the results in Table 6.7 and Table 6.8). Finally, we note that the order reduction for both WENO methods occurs here due to the non-smoothness of the solution of problem (6.2.19).

Table 6.8 The errors between the exact solution of the problem (6.2.19) and the numerical solutions computed by semi-implicit WENO5 method on uniform mesh for different values of M.

M	$\|Error\|_\infty$	$Order\ in\ \|\cdot\|_\infty$	$\|Error\|_{L^1}$	$Order\ in\ \|\cdot\|_{L^1}$
10	$5.00e-02$	–	$2.91e-02$	–
20	$7.14e-03$	2.8088	$1.54e-03$	4.2388
40	$5.86e-03$	0.2851	$5.46e-04$	1.4985
80	$3.04e-03$	0.9468	$1.44e-04$	1.9226
160	$1.39e-03$	1.1264	$3.54e-05$	2.0239
320	$6.88e-04$	1.0178	$8.73e-06$	2.0206

Next, we set the non-uniform mesh in the following way. We first place 100 fine uniform cells in the interval $[0.3, 0.4]$ and 100 fine uniform cells in the interval

$[0.6, 0.7]$ with cell size 0.001 each. Then, we place 15 coarse uniform cells in the interval $[0, 0.228]$ and 15 coarse uniform cells in the interval $[0.772, 1]$ with cell size 0.0152 each. Additionally, we place 4 coarse uniform cells in the interval $[0.472, 0.528]$ with cell size 0.014 each. Four remaining intervals $[0.228, 0.3]$, $[0.4, 0.472]$, $[0.528, 0.6]$ and $[0.7, 0.772]$ are intermediate regions. In each intermediate region we place 15 cells such that cells sizes are increased by 20% from one cell to the next in the direction from the fine-mesh region to the coarse-mesh region. Thus, in total we have 294 cells and mesh sizes are defined as:

$$h_i = \begin{cases} 0.0152, & \text{if } 1 \le i \le 15, \\ 0.001 \cdot (1.2)^{30-i}, & \text{if } 16 \le i \le 30, \\ 0.001, & \text{if } 31 \le i \le 130, \\ 0.001 \cdot (1.2)^{i-131}, & \text{if } 131 \le i \le 145, \\ 0.014, & \text{if } 146 \le i \le 149, \\ 0.001 \cdot (1.2)^{164-i}, & \text{if } 150 \le i \le 164, \\ 0.001, & \text{if } 165 \le i \le 264, \\ 0.001 \cdot (1.2)^{i-265}, & \text{if } 265 \le i \le 279, \\ 0.0152, & \text{if } 280 \le i \le 294. \end{cases}$$

With this mesh choice, we have $x = \dfrac{1}{3} \in \Omega_{64}$ and $x = \dfrac{2}{3} \in \Omega_{231}$. Note that this mesh is similar to the one used in Example 6.1.3.

We apply the WENO3 and WENO5 methods on this non-uniform mesh for spatial discretization of problem (6.2.19) and semi-implicit scheme (6.1.15)-(6.1.16) for temporal discretization. In both simulations, we use $\tau = \dfrac{1}{N} = 10^{-5}$ for time step. The errors are computed in maximum norm defined by (6.1.18) and L^1 norm defined by (6.1.19).

Table 6.9 shows the errors between the errors between the exact solution of the problem (6.2.19) and the numerical solutions computed by semi-implicit WENO3 and WENO5 methods on non-uniform mesh with 294 cells. We observe that with WENO3 method the numerical solution is as accurate as the one obtained on uniform mesh with 80 cells (see Table 6.7), which is rather poor. With WENO5 method the numerical solution is more accurate in L^1 norm than the one obtained on uniform mesh with 320 cells (see Table 6.8). However, the accuracy in maximum norm is still poor in comparison with the corresponding results on uniform mesh. So, we conclude that overall WENO methods on constructed non-uniform mesh with 294 cells do not yield better results than the ones on uniform mesh.

Table 6.9 The errors between the exact solution of the problem (6.2.19) and the numerical solutions computed by semi-implicit WENO3 and WENO5 methods on non-uniform mesh with 294 cells.

Method	$\|Error\|_\infty$	$\|Error\|_{L^1}$
WENO3	$2.17e-02$	$4.56e-03$
WENO5	$1.35e-03$	$7.96e-06$

Finally, we set different non-uniform mesh in the following way. We first place 10 fine uniform cells in the interval $[0.33, 0.34]$ and 10 fine uniform cells in the interval $[0.66, 0.67]$ with cell size 0.001 each. Then, we place 66 coarse uniform cells in the interval $[0, 0.33]$, 64 coarse uniform cells in the interval $[0.34, 0.66]$ and 66 coarse uniform cells in the interval $[0.67, 1]$ with cell size 0.005. Thus, in total we have 216 cells and the mesh sizes are defined as:

$$h_i = \begin{cases} 0.005, & \text{if} \quad 1 \leq i \leq 66, \\ 0.001, & \text{if} \quad 67 \leq i \leq 76, \\ 0.005, & \text{if} \quad 77 \leq i \leq 140, \\ 0.001, & \text{if} \quad 141 \leq i \leq 150, \\ 0.005, & \text{if} \quad 151 \leq i \leq 216. \end{cases}$$

With this mesh choice, we have $x = \dfrac{1}{3} \in \Omega_{70}$ and $x = \dfrac{2}{3} \in \Omega_{147}$.

We apply the WENO3 and WENO5 methods on this non-uniform mesh for spatial discretization of problem (6.2.19) and semi-implicit scheme (6.1.15)-(6.1.16) for temporal discretization. In both simulations, we use $\tau = \dfrac{1}{N} = 10^{-5}$ for time step. The errors are computed in maximum norm defined by (6.1.18) and L^1 norm defined by (6.1.19).

Table 6.10 shows the errors between the errors between the exact solution of the problem (6.2.19) and the numerical solutions computed by semi-implicit WENO3 and WENO5 methods on non-uniform mesh with 216 cells. First of all, we note that these numerical solutions are more accurate than the ones obtained on non-uniform mesh with 294 cells, especially for WENO3 method (compare the results in Table 6.9 and Table 6.10). Additionally, with both WENO methods on non-uniform mesh with 216 cells the numerical solutions in L^1 norm are as accurate as the ones obtained on uniform mesh with 320 cells, which illustrates again the advantage of using locally refined grids for numerical solution of problems with non-smooth solutions.

Table 6.10 The errors between the exact solution of the problem (6.2.19) and the numerical solutions computed by semi-implicit WENO3 and WENO5 methods on non-uniform mesh with 216 cells.

Method	$\|Error\|_\infty$	$\|Error\|_{L^1}$
WENO3	$1.90e-03$	$3.43e-04$
WENO5	$1.36e-03$	$5.56e-06$

Remark 6.2.4. We have presented here only the results of simulations for Advection Diffusion problems with low diffusion coefficient. Both WENO schemes give unsatisfactory results when larger values of diffusion coefficient are used (results are not presented here).

CHAPTER 7

NONLINEAR EQUATIONS

The Advection Diffusion problems, we have discussed so far, are all linear. In this chapter, we illustrate that presented material can be readily extended to nonlinear cases. As an example, we illustrate the construction of WENO3 method for non-homogeneous scalar hyperbolic conservation laws of the type:

$$u_t + f(u)_x = g(t)\delta(x-\xi), \tag{7.0.1}$$

where f and g are smooth functions.

Let the grid, cells, cell centers and mesh sizes be defined by (6.1.2), (6.1.3), (6.1.4) and (6.1.5), respectively. Let the cell average values of function $u(x,t)$ be defined by (6.1.6).

The Finite Volume approach for (7.0.1) amounts for first integrating (7.0.1) over each cell Ω_i and dividing by the cell volume $|\Omega_i| = h_i$, which gives us:

$$\frac{1}{h_i}\int\limits_{\Omega_i} u_t dx + \frac{1}{h_i}\int\limits_{\Omega_i} f(u)_x dx = \frac{1}{h_i}\int\limits_{\Omega_i} g(t)\delta(x-\xi)dx, \quad i = 1,\ldots,M.$$

Assuming that $\xi \in \Omega_j$, we obtain

$$\frac{\partial}{\partial t}\left(\frac{1}{h_i}\int\limits_{\Omega_i} u(x,t)dx\right) + \frac{1}{h_i}\int\limits_{\Omega_i} \frac{\partial}{\partial x} f\big(u(x,t)\big)dx = g(t)\frac{\delta_{ij}}{h_i}, \quad i = 1,\ldots,M,$$

where δ_{ij} is the Kronecker delta symbol defined by (4.2.4). Then, applying the fundamental theorem of calculus, we have

$$\frac{d\bar{u}_i(t)}{dt} + \frac{1}{h_i}\Big(f\big(u(x_{i+\frac{1}{2}},t)\big) - f\big(u(x_{i-\frac{1}{2}},t)\big)\Big) = g(t)\frac{\delta_{ij}}{h_i}, \quad i = 1,\ldots,M. \tag{7.0.2}$$

To have a stable numerical scheme, the physical fluxes $f\big(u(x_{i+\frac{1}{2}},t)\big)$ and $f\big(u(x_{i-\frac{1}{2}},t)\big)$ in (7.0.2) are usually replaced by monotone numerical fluxes $\hat{f}\big(u^-_{i+\frac{1}{2}}(t), u^+_{i+\frac{1}{2}}(t)\big)$ and $\hat{f}\big(u^-_{i-\frac{1}{2}}(t), u^+_{i-\frac{1}{2}}(t)\big)$, respectively.

There is a number of known monotone numerical fluxes used in the literature as listed below (Barth and Deconinck, 1999).

1. Godunov flux

$$\hat{f}(a,b) = \begin{cases} \min\limits_{a\le u\le b} f(u), & \text{if} \quad a \le b, \\ \max\limits_{b\le u\le a} f(u), & \text{if} \quad a > b. \end{cases} \tag{7.0.3}$$

2. Engquist-Osher flux

$$\hat{f}(a,b) = \int_0^a \max\big(f'(u),0\big)du + \int_0^b \min\big(f'(u),0\big)du + f(0). \tag{7.0.4}$$

3. Lax-Friedrichs flux

$$\hat{f}(a,b) = \frac{1}{2}\Big(f(a) + f(b) - \alpha(b-a)\Big), \tag{7.0.5}$$

where $\alpha = \max\limits_u |f'(u)|$.

Replacing the physical fluxes in (7.0.2) by monotone numerical fluxes, gives us

$$\frac{d\bar{u}_i(t)}{dt} + \frac{1}{h_i}\Big(\hat{f}(u^-_{i+\frac{1}{2}}, u^+_{i+\frac{1}{2}}) - \hat{f}(u^-_{i-\frac{1}{2}}, u^+_{i-\frac{1}{2}})\Big) = g(t)\frac{\delta_{ij}}{h_i}, \quad i = 1,\ldots,M. \tag{7.0.6}$$

The approximation $u^-_{i+\frac{1}{2}}$ in (7.0.6) is the WENO3 reconstruction which uses the three-cell stencil $\{\Omega_{i-1}, \Omega_i, \Omega_{i+1}\}$ (see Figure 5.1) and therefore it is the same as the approximation (6.1.9). Namely,

$$\begin{aligned} u^-_{i+\frac{1}{2}} = \omega_0^{(i)} &\left(-\frac{h_i}{h_{i-1}+h_i}\bar{u}_{i-1} + \frac{h_{i-1}+2h_i}{h_{i-1}+h_i}\bar{u}_i\right) \\ + \omega_1^{(i)} &\left(\frac{h_{i+1}}{h_i+h_{i+1}}\bar{u}_i + \frac{h_i}{h_i+h_{i+1}}\bar{u}_{i+1}\right), \end{aligned} \tag{7.0.7}$$

where the weights $\omega_0^{(i)}$ and $\omega_1^{(i)}$ are defined by (5.1.21)-(5.1.22). The WENO3 approximation $u^-_{i-\frac{1}{2}}$ in (7.0.6) can be obtained from (7.0.7) by shifting the index:

$$\begin{aligned} u^-_{i-\frac{1}{2}} = \omega_0^{(i-1)} &\left(-\frac{h_{i-1}}{h_{i-2}+h_{i-1}}\bar{u}_{i-2} + \frac{h_{i-2}+2h_{i-1}}{h_{i-2}+h_{i-1}}\bar{u}_{i-1}\right) \\ + \omega_1^{(i-1)} &\left(\frac{h_i}{h_{i-1}+h_i}\bar{u}_{i-1} + \frac{h_{i-1}}{h_{i-1}+h_i}\bar{u}_i\right), \end{aligned} \tag{7.0.8}$$

where the weights $\omega_0^{(i-1)}$ and $\omega_1^{(i-1)}$ are obtained from (5.1.21)-(5.1.22) by shifting the index accordingly.

The WENO3 approximation $u^+_{i+\frac{1}{2}}$ in (7.0.6) is constructed by using the three-cell stencil $\{\Omega_i, \Omega_{i+1}, \Omega_{i+2}\}$ (see Figure 5.1). We follow the same line as in Section 5.1.

Firstly, we consider the stencil $S_0 = \{\Omega_i, \Omega_{i+1}\}$ (see Figure 5.1). It is obvious that there is a unique linear polynomial whose cell average values on stencil S_0 agree with corresponding cell average values of function $u(x)$ on S_0. We search this polynomial in the following form:

$$\hat{p}_0^{(i)}(x) = \hat{a}_0^{(i)}(x - x_i) + \hat{b}_0^{(i)}. \tag{7.0.9}$$

Then,

$$\begin{cases} \dfrac{1}{h_i} \displaystyle\int\limits_{\Omega_i} \hat{p}_0^{(i)}(x)dx = \bar{u}_i, \\ \\ \dfrac{1}{h_{i+1}} \displaystyle\int\limits_{\Omega_{i+1}} \hat{p}_0^{(i)}(x)dx = \bar{u}_{i+1}. \end{cases} \tag{7.0.10}$$

Plugging (7.0.9) into (7.0.10) and evaluating integrals, we obtain:

$$\begin{cases} \hat{b}_0^{(i)} = \bar{u}_i, \\ \\ \dfrac{h_i + h_{i+1}}{2}\hat{a}_0^{(i)} + \hat{b}_0^{(i)} = \bar{u}_{i+1}, \end{cases}$$

Solving this system, we get

$$\hat{a}_0^{(i)} = \frac{2}{h_i + h_{i+1}}(\bar{u}_{i+1} - \bar{u}_i), \quad \hat{b}_0^{(i)} = \bar{u}_i. \tag{7.0.11}$$

Then, the approximation $\hat{u}^{(0)}_{i+\frac{1}{2}}$ for function $u(x)$ at $x = x_{i+\frac{1}{2}}$ using the polynomial (7.0.9) has the form:

$$\hat{u}^{(0)}_{i+\frac{1}{2}} = \hat{p}_0^{(i)}(x_{i+\frac{1}{2}}) = \frac{h_i}{2}\hat{a}_0^{(i)} + \hat{b}_0^{(i)}$$

or

$$\hat{u}^{(0)}_{i+\frac{1}{2}} = \frac{h_{i+1}}{h_i + h_{i+1}}\bar{u}_i + \frac{h_i}{h_i + h_{i+1}}\bar{u}_{i+1}. \tag{7.0.12}$$

Secondly, we consider the stencil $S_1 = \{\Omega_{i+1}, \Omega_i\}$ (see Figure 5.1). Obviously, there is a unique linear polynomial whose cell average values on stencil S_1 agree with corresponding cell average values of function $u(x)$ on S_1. We search this polynomial in the following form:

$$\hat{p}_1^{(i)}(x) = \hat{a}_1^{(i)}(x - x_i) + \hat{b}_1^{(i)}. \tag{7.0.13}$$

Then,

$$\begin{cases} \dfrac{1}{h_{i+1}} \displaystyle\int\limits_{\Omega_{i+1}} \hat{p}_1^{(i)}(x)dx = \bar{u}_{i+1}, \\ \dfrac{1}{h_{i+2}} \displaystyle\int\limits_{\Omega_{i+2}} \hat{p}_1^{(i)}(x)dx = \bar{u}_{i+2}. \end{cases} \tag{7.0.14}$$

Plugging (7.0.13) into (7.0.14) and evaluating integrals, we obtain:

$$\begin{cases} \dfrac{h_i + h_{i+1}}{2}\hat{a}_1^{(i)} + \hat{b}_1^{(i)} = \bar{u}_{i+1}, \\ \dfrac{h_i + 2h_{i+1} + h_{i+2}}{2}\hat{a}_1^{(i)} + \hat{b}_1^{(i)} = \bar{u}_{i+2}. \end{cases}$$

Solving this system, we get

$$\hat{a}_1^{(i)} = \frac{2}{h_{i+1} + h_{i+2}}(\bar{u}_{i+2} - \bar{u}_{i+1}), \quad \hat{b}_1^{(i)} = \bar{u}_{i+1} - \frac{h_i + h_{i+1}}{h_{i+1} + h_{i+2}}(\bar{u}_{i+2} - \bar{u}_{i+1}). \tag{7.0.15}$$

Then, the approximation $\hat{u}^{(1)}_{i+\frac{1}{2}}$ for function $u(x)$ at $x = x_{i+\frac{1}{2}}$ using the polynomial (7.0.13) has the form:

$$\hat{u}^{(1)}_{i+\frac{1}{2}} = \hat{p}_1^{(i)}(x_{i+\frac{1}{2}}) = \frac{h_i}{2}\hat{a}_1^{(i)} + \hat{b}_1^{(i)}$$

or

$$\hat{u}^{(1)}_{i+\frac{1}{2}} = \frac{2h_{i+1} + h_{i+2}}{h_{i+1} + h_{i+2}}\bar{u}_{i+1} - \frac{h_{i+1}}{h_{i+1} + h_{i+2}}\bar{u}_{i+2}. \tag{7.0.16}$$

Theorem 7.0.1.

- If $u(x)$ is sufficiently smooth on stencil $S_0 = \{\Omega_i, \Omega_{i+1}\}$ then (7.0.12) is the second order approximation for u(x) at $x = x_{i+\frac{1}{2}}$.
- If $u(x)$ is sufficiently smooth on stencil $S_1 = \{\Omega_{i+1}, \Omega_{i+2}\}$ then (7.0.16) is the second order approximation for u(x) at $x = x_{i+\frac{1}{2}}$.
- If $u(x)$ is sufficiently smooth on extended stencil $S = \{\Omega_i, \Omega_{i+1}, \Omega_{i+2}\}$ then there exist unique $\hat{\gamma}_0^{(i)}$ and $\hat{\gamma}_1^{(i)}$ values such that

  $$\hat{u}_{i+\frac{1}{2}} = \hat{\gamma}_0^{(i)}\hat{u}^{(0)}_{i+\frac{1}{2}} + \hat{\gamma}_1^{(i)}\hat{u}^{(1)}_{i+\frac{1}{2}} \tag{7.0.17}$$

  is the third order approximation for u(x) at $x = x_{i+\frac{1}{2}}$.

The proof of this theorem is similar to the proofs given in Section 5.1, so we skip it here. Note that (7.0.17) holds if and only if

$$\hat{\gamma}_0^{(i)} = \frac{h_{i+1} + h_{i+2}}{h_i + h_{i+1} + h_{i+2}}, \quad \hat{\gamma}_1^{(i)} = \frac{h_i}{h_i + h_{i+1} + h_{i+2}}. \tag{7.0.18}$$

Now, the WENO3 approximation $u^+_{i+\frac{1}{2}}$ is defined as a convex combination of approximations $\hat{u}^{(0)}_{i+\frac{1}{2}}$ and $\hat{u}^{(1)}_{i+\frac{1}{2}}$ defined by (7.0.12) and (7.0.16), respectively. In other words, (7.0.18) is replaced with:

$$u^+_{i+\frac{1}{2}} = \hat{\omega}_0^{(i)} \hat{u}^{(0)}_{i+\frac{1}{2}} + \hat{\omega}_1^{(i)} \hat{u}^{(1)}_{i+\frac{1}{2}}$$

or

$$\begin{aligned} u^+_{i+\frac{1}{2}} = \hat{\omega}_0^{(i)} &\left(\frac{h_{i+1}}{h_i + h_{i+1}} \bar{u}_i + \frac{h_i}{h_i + h_{i+1}} \bar{u}_{i+1} \right) \\ &+ \hat{\omega}_1^{(i)} \left(\frac{2h_{i+1} + h_{i+2}}{h_{i+1} + h_{i+2}} \bar{u}_{i+1} - \frac{h_{i+1}}{h_{i+1} + h_{i+2}} \bar{u}_{i+2} \right). \end{aligned} \tag{7.0.19}$$

Similar to (5.1.21)-(5.1.22), we define the nonlinear weights $\hat{\omega}_0^{(i)}$ and $\hat{\omega}_1^{(i)}$ in (7.0.19) in following way:

$$\hat{\omega}_0^{(i)} = \frac{\tilde{\omega}_0^{(i)}}{\tilde{\omega}_0^{(i)} + \tilde{\omega}_1^{(i)}}, \qquad \hat{\omega}_1^{(i)} = \frac{\tilde{\omega}_1^{(i)}}{\tilde{\omega}_0^{(i)} + \tilde{\omega}_1^{(i)}}, \tag{7.0.20}$$

where

$$\tilde{\omega}_0^{(i)} = \frac{\hat{\gamma}_0^{(i)}}{\left(\epsilon + \hat{\beta}_0^{(i)}\right)^2}, \qquad \tilde{\omega}_1^{(i)} = \frac{\hat{\gamma}_1^{(i)}}{\left(\epsilon + \hat{\beta}_1^{(i)}\right)^2}. \tag{7.0.21}$$

Here, $\epsilon = 10^{-6}$ is taken to prevent the denominators becoming zero and smoothness indicators $\hat{\beta}_0^{(i)}$ and $\hat{\beta}_1^{(i)}$ are defined as following:

$$\hat{\beta}_0^{(i)} = h_i \int_{\Omega_i} \left(\frac{d}{dx} \hat{p}_0^{(i)}(x) \right)^2 dx = h_i \int_{\Omega_i} \left(\hat{a}_0^{(i)} \right)^2 dx = \left(h_i \hat{a}_0^{(i)} \right)^2 = \frac{4h_i^2 (\bar{u}_{i+1} - \bar{u}_i)^2}{(h_i + h_{i+1})^2},$$

$$\hat{\beta}_1^{(i)} = h_i \int_{\Omega_i} \left(\frac{d}{dx} \hat{p}_1^{(i)}(x) \right)^2 dx = h_i \int_{\Omega_i} \left(\hat{a}_1^{(i)} \right)^2 dx = \left(h_i \hat{a}_1^{(i)} \right)^2 = \frac{4h_i^2 (\bar{u}_{i+2} - \bar{u}_{i+1})^2}{(h_{i+1} + h_{i+2})^2}.$$

Finally, the WENO3 approximation $u^+_{i-\frac{1}{2}}$ in (7.0.6) can be obtained from (7.0.19) by shifting the index:

$$\begin{aligned} u^+_{i-\frac{1}{2}} = \hat{\omega}_0^{(i-1)} &\left(\frac{h_i}{h_{i-1} + h_i} \bar{u}_{i-1} + \frac{h_{i-1}}{h_{i-1} + h_i} \bar{u}_i \right) \\ &+ \hat{\omega}_1^{(i-1)} \left(\frac{2h_i + h_{i+1}}{h_i + h_{i+1}} \bar{u}_i - \frac{h_i}{h_i + h_{i+1}} \bar{u}_{i+1} \right), \end{aligned} \tag{7.0.22}$$

where the weights $\hat{\omega}_0^{(i-1)}$ and $\hat{\omega}_1^{(i-1)}$ are obtained from (7.0.20)-(7.0.21) by shifting the index accordingly.

By putting (7.0.7), (7.0.8), (7.0.19) and (7.0.22) in (7.0.6), we complete the Finite Volume WENO3 spatial discretization of equation (7.0.1).

Remark 7.0.2. In the similar way, the Finite Volume WENO5 spatial discretization of equation (7.0.1) can be constructed as well.

CHAPTER 8

CONCLUSION

The research described in this thesis is devoted to the numerical methods for Advection Diffusion problems with singular source terms. Singular in the sense that within the spatial domain the source is defined by a Dirac delta function. Solutions of such problems have discontinuities or discontinuous derivatives which forms an obstacle for standard numerical methods.

We have shown that for simple mathematical model from gaz hydrodynamics, a coupled system of Diffusion and Advection equations with singular source terms, the analytical solution can be obtained by using known theoretical methods.

We have applied the Finite Difference and Finite Volume methods for one-dimensional Advection Diffusion problem with source term. The difference between the methods is discussed when the source term is singular. On the base of simple Diffusion problem with singular source term, we illustrated how and why the Finite Volume approach has advantage over the Finite Difference methods.

We have constructed and analyzed the third order of accuracy and the fifth order of accuracy Finite Volume Weighted essentially non-oscillatory (WENO) schemes on non-uniform meshes. The order of accuracy of each method in case of smooth functions has been established.

We have applied constructed Finite Volume WENO schemes for Advection equation with singular source term and Advection Diffusion equation with singular source terms. We have validated our theoretical findings by numerical illustrations for two types of test problems. Firstly, we considered the Advection problem and the Advection Diffusion problem without singular source terms. We observed the correct orders of WENO methods for these problems having smooth solutions. Secondly, we considered the Advection problem and the Advection Diffusion problem with singular source terms. For Advection problem with singular source term, which has a discontinuous solution, we observed the first order convergence of both WENO schemes. Moreover, we illustrated a drastic improvement in the accuracy, as well as efficiency, when appropriate non-uniform mesh is used instead of uniform mesh. For Advection Diffusion problem with singular source terms, which has non-smooth solution, we observed the second order convergence of both WENO schemes. We have shown that more accurate numerical solutions in more efficient way can be obtained on specially designed non-uniform meshes.

Finally, we have discussed the possible extension of the WENO approximations which can be used for non-linear problems.

REFERENCES

Ashyraliyev, M., Blom, J., and Verwer, J., "On the numerical solution of diffusion-reaction equations with singular source terms", *Journal of Computational and Applied Mathematics*, Vol. 216, No. 1, pp. 20–38, 2008.

Barth, T. and Deconinck, H., *High-Order Methods for Computational Physics, Lecture Notes in Computational Science and Engineering*, Vol. 9, Springer, 1999.

Basniev, K.S., Vlasov, A.M., Kochina, I.N., and Maksimov, V.M., *Underground Hydrodynamics*, Nedra, Moscow, 1986.

Bedrikovetskii, P.G., Manevich, P.G., and Esedulaev, R., "Two-phase displacement of compressible fluids from stratified reservoirs", *Fluid Dynamics*, Vol. 28, No. 2, pp. 214–222, 1993.

Cadiou, A. and Tenaud, C., "Implicit WENO shock capturing scheme for unsteady flows. Application to one-dimensional Euler equations", *International Journal for Numerical Methods in Fluids*, Vol. 45, pp. 197–229, 2004.

Crnjaric-Zic, N. and Crnkovic, B., "High order accurate semi-implicit WENO schemes for hyperbolic balance laws", *Applied Mathematics and Computation*, Vol. 217, pp. 8611–8629, 2011.

Elias, J. and Clairambault, J., "Reaction-diffusion systems for spatio-temporal intracellular protein networks: A beginner's guide with two examples", *Computational and Structural Biotechnology Journal*, Vol. 10, No. 16, pp. 12–22, 2014.

Ge, J., Kim, K.I., Lin, Z., and Zhu, H., "A {SIS} reactiondiffusionadvection model in a low-risk and high-risk domain", *Journal of Differential Equations*, Vol. 259, No. 10, pp. 5486 – 5509, 2015.

Gonzalez-Pinto, S., Hernandez-Abreu, D., and Perez-Rodriguez, S., "AMF-RungeKutta formulas and error estimates for the time integration of advection diffusion reaction {PDEs}", *Journal of Computational and Applied Mathematics*, Vol. 289, pp. 3 – 21, 2015.

Gottlieb, S., Mullen, J.S., and Ruuth, S.J., "A Fifth Order Flux Implicit WENO Method", *Journal of Scientific Computing*, Vol. 27, pp. 271–287, 2006.

Gottlieb, S., Shu, C.W., and Tadmor, E., "Strong Stability-Preserving High-Order Time Discretization Methods", *SIAM Reviewer*, Vol. 43, pp. 89–112, 2001.

Harten, A., Engquist, B., Osher, S., and Chakravarthy, S.R., "Uniformly High Order Essentially Non-oscillatory Schemes III", *Journal of Computational Physics*, Vol. 71, No. 2, pp. 231–303, 1987.

Harten, A. and Osher, S., "Uniformly high-order accurate nonoscillatory schemes", *SIAM Journal of Numerical Analysis*, Vol. 4, pp. 279–309, 1987.

Huang, C.S., Arbogast, T., and Hung, C.H., "A re-averaged WENO reconstruction and a third order CWENO scheme for hyperbolic conservation laws", *Journal of Computational Physics*, Vol. 262, pp. 291–312, 2014.

Hundsdorfer, W. and Verwer, J.G., *Numerical Solution of Time-Dependent Advection-Diffusion-Reaction Equations, Springer Series in Computational Mathematics*, Vol. 33, Springer, Berlin, 2003.

Jiang, G.S. and Shu, C.W., "Efficient Implementation of Weighted ENO Schemes", *Journal of Computational Physics*, Vol. 126, pp. 202–228, 1996.

Jung, J.H. and Don, W.S., "Collocation Methods for Hyperbolic Partial Differential Equations with Singular Sources", *Advances in Applied Mathematics and Mechanics*, Vol. 1, No. 6, pp. 769–780, 2009.

Kunkel, P. and Mehrmann, V., *Differential-Algebraic Equations: Analysis and Numerical Solution*, European Mathematical Society, 2006.

LeVeque, R.V., *Finite Volume Methods for Hyperbolic Problems*, Cambridge University Press, 2002.

LeVeque, R.V., *Finite Difference Methods for Ordinary and Partial Differential Equations*, SIAM, 2007.

Levy, D., Puppo, G., and Russo, G., "Central WENO Schemes for Hyperbolic Systems of Conservation Laws", *MATH. MODEL. NUMER. ANAL*, Vol. 33, pp. 547–571, 1999.

Liu, X.D. and Osher, S., "Convex ENO High Order Multi-dimensional Schemes without Field by Field Decomposition or Staggered Grids", *Journal of Computational Physics*, Vol. 142, pp. 304–330, 2008.

Liu, X.D., Osher, S., and Chan, T., "Weighted Essentially Non-oscillatory Schemes", *Journal of Computational Physics*, Vol. 115, pp. 200–212, 1994.

Olver, P.J., *Introduction to Partial Differential Equations (Undergraduate Texts in Mathematics)*, Springer, 2013.

Owolabi, K.M. and Patidar, K.C., "Higher-order time-stepping methods for time-dependent reactiondiffusion equations arising in biology", *Applied Mathematics and Computation*, Vol. 240, pp. 30–50, 2014.

Pudykiewicz, J.A., "Numerical solution of the reaction-advection-diffusion equation on the sphere", *Journal of Computational Physics*, Vol. 213, pp. 358–390, 2006.

Ross, S.L., *Introduction to Ordinary Differential Equations*, Wiley, 1989.

Rubio, Zalts, A., and El Hasi, C., "Numerical solution of the advection-reaction-diffusion equation at different scales", *Environmental Modelling & Software*, Vol. 23, No. 1, pp. 90–95, 2008.

Salso, S., *Partial Differential Equations in action, from Modeling to Theory*, Springer, 2008.

Santos, J. and de Oliveira, P., "A converging finite volume scheme for hyperbolic conservation laws with source terms", *Journal of Computational and Applied Mathematics*, Vol. 111, No. 1/2, pp. 239–251, 1999.

Shen, C., Qiu, J.M., and Christlieb, A., "Adaptive mesh refinement based on high order finite difference WENO scheme for multi-scale simulations", *Journal of Computational Physics*, Vol. 230, pp. 3780–3802, 2011.

Shen, Y., Wang, B., and Zha, G., "Implicit WENO scheme and high order viscous formulas for compressible flows", in *AIAA Applied Aerodynamics Conference*, number AIAA 2007-4431, American Institute of Aeronautics and Astronautics, Miami,FL, 2007.

Shu, C.W., "High Order Weighted Essentially Nonoscillatory Schemes for Convection Dominated Problems", *SIAM REVIEW*, Vol. 51, pp. 82–126, 2009.

Shu, C.W., "WENO methods"2011, http://www.scholarpedia.org/article/WENO_methods.

Smit, J., Annaland, M.v.S., and Kuipers, J., "Grid adaptation with WENO schemes for non-uniform grids to solve convection-dominated partial differential equations", *Chemical Engineering Science*, Vol. 60, pp. 2609–2619, 2005.

Smith, H., *An Introduction to Delay Differential Equations with Applications to the Life Sciences*, Springer, 2011.

Titarev, V.A. and Toro, E.F., "Central WENO Schemes for Hyperbolic Systems of Conservation Laws", *Journal of Computational Physics*, Vol. 201, pp. 238–260, 2004.

Tornberg, A.K. and Engquist, B., "Regularization Techniques for Numerical Approximation of PDEs with Singularities", *Journal of Scientific Computing*, Vol. 19, pp. 527–552, 2003.

Tornberg, A.K. and Engquist, B., "Numerical approximations of singular source terms in differential equations", *Journal of Computational Physics*, Vol. 200, pp. 462–488, 2004.

Wang, C., Dong, X., and Shu, C.W., "Parallel adaptive mesh refinement method based on {WENO} finite difference scheme for the simulation of multi-dimensional detonation", *Journal of Computational Physics*, Vol. 298, pp. 161 – 175, 2015a.

Wang, F.B., Hsu, S.B., and Zhao, X.Q., "A reactiondiffusionadvection model of harmful algae growth with toxin degradation", *Journal of Differential Equations*, Vol. 259, No. 7, pp. 3178 – 3201, 2015b.

Wang, R., Feng, H., and Spiteri, R.J., "Observations on the fifth-order WENO method with non-uniform meshes", *Applied Mathematics and Computation*, Vol. 196, pp. 433–447, 2008.

Zakirov, S.N. and Vasilyev, V.I., *Forecasting and development of gas reservoirs (in Russian)*, Nedra, Moscow, 1984.

Zhang, T., "Advection-diffusion constrained metabolic reaction in bioreactor analysis for hydrogen production", *Biomass and Bioenergy*, Vol. 47, pp. 324–333, 2012.

APPENDIX A

DECLARATION STATEMENT FOR THE ORIGINALITY OF THE THESIS, FURTHER STUDIES AND PUBLICATIONS FROM THESIS WORK

A.1 DECLARATION STATEMENT FOR THE ORIGINALITY OF THE THESIS

I hereby declare that this thesis comprises my original work. No material in this thesis has been previously published and written by another person, except where due reference is made in the text of the thesis. I further declare that this thesis contains no material which has been submitted for a degree or diploma or other qualifications at any other university.

Signature:

Date: 6.27.2016

A.2 PUBLICATIONS FROM THESIS WORK

1. Irfan Turk, Maksat Ashyraliyev, "On the numerical solution of diffusion problem with singular source terms", AIP Conference Proceedings, Vol. 1470, Aug. 2012, pp.176-178

2. Irfan Turk, Maksat Ashyraliyev, "On the numerical solution of hyperbolic equations with singular source terms", AIP Conference Proceedings, Vol. 1611, Aug. 2014, pp.374-379

APPENDIX B

MATLAB CODES

B.1 CONSTRUCTION OF WENO5 METHOD

In this part, we give the code which is used to obtain the formulas for construction of WENO5 method by using the symbolic toolbox of MATLAB.

```
syms h1 h2 h3 h4 h5
syms u1 u2 u3 u4 u5
syms a b c d e x xi

pol2 = a*(x-xi)^2 + b*(x-xi) + c;
I1 = int(pol2,'x','(xi-h1-h2-h3/2)','(xi-h2-h3/2)');
I2 = int(pol2,'x','(xi-h2-h3/2)','(xi-h3/2)');
I3 = int(pol2,'x','(xi-h3/2)','(xi+h3/2)');
I4 = int(pol2,'x','(xi+h3/2)','(xi+h3/2+h4)');
I5 = int(pol2,'x','(xi+h3/2+h4)','(xi+h3/2+h4+h5)');

% Constructing p0
a11=(1/h1)*diff(I1,'a');
a12=(1/h1)*diff(I1,'b');
a13=(1/h1)*diff(I1,'c');
a21=(1/h2)*diff(I2,'a');
a22=(1/h2)*diff(I2,'b');
a23=(1/h2)*diff(I2,'c');
a31=(1/h3)*diff(I3,'a');
a32=(1/h3)*diff(I3,'b');
a33=(1/h3)*diff(I3,'c');
```

```
p0AA = [a11 a12 a13; a21 a22 a23; a31 a32 a33];
p0BB    = [u1;u2;u3];
p0Cevap = inv(p0AA)*p0BB;
p0Ce    = simplify(p0Cevap);
p0A=p0Ce(1); p0B=p0Ce(2); p0C=p0Ce(3);
p0_A_u_im2 = diff(p0A,'u1'); p0_A_u_im2 = simplify(p0_A_u_im2)
p0_A_u_im1 = diff(p0A,'u2'); p0_A_u_im1 = simplify(p0_A_u_im1)
p0_A_u_i   = diff(p0A,'u3'); p0_A_u_i   = simplify(p0_A_u_i)
p0_B_u_im2 = diff(p0B,'u1'); p0_B_u_im2 = simplify(p0_B_u_im2)
p0_B_u_im1 = diff(p0B,'u2'); p0_B_u_im1 = simplify(p0_B_u_im1)
p0_B_u_i   = diff(p0B,'u3'); p0_B_u_i   = simplify(p0_B_u_i)
p0_C_u_im2 = diff(p0C,'u1'); p0_C_u_im2 = simplify(p0_C_u_im2)
p0_C_u_im1 = diff(p0C,'u2'); p0_C_u_im1 = simplify(p0_C_u_im1)
p0_C_u_i   = diff(p0C,'u3'); p0_C_u_i   = simplify(p0_C_u_i)
p0         = p0A*((h3^2)/4)+p0B*(h3/2)+p0C;
SadeHali0 = simplify(p0);
p0         = collect(SadeHali0);
p0_Uim2 = diff(p0,'u1'); p0_Uim2 = simplify(p0_Uim2)
p0_Uim1 = diff(p0,'u2'); p0_Uim1 = simplify(p0_Uim1)
p0_Ui   = diff(p0,'u3'); p0_Ui   = simplify(p0_Ui)

% Constructing p1
a11=(1/h2)*diff(I2,'a');
a12=(1/h2)*diff(I2,'b');
a13=(1/h2)*diff(I2,'c');
a21=(1/h3)*diff(I3,'a');
a22=(1/h3)*diff(I3,'b');
a23=(1/h3)*diff(I3,'c');
a31=(1/h4)*diff(I4,'a');
a32=(1/h4)*diff(I4,'b');
a33=(1/h4)*diff(I4,'c');
p1AA=[a11 a12 a13; a21 a22 a23; a31 a32 a33];
p1BB    = [u2;u3;u4];
p1Cevap = inv(p1AA)*p1BB;
```

```
p1Ce    = simplify(p1Cevap);
p1A=p1Ce(1); p1B=p1Ce(2); p1C=p1Ce(3);
p1_A_u_im1 = diff(p1A,'u2'); p1_A_u_im1 = simplify(p1_A_u_im1);
p1_A_u_i   = diff(p1A,'u3'); p1_A_u_i   = simplify(p1_A_u_i);
p1_A_u_ip1 = diff(p1A,'u4'); p1_A_u_ip1 = simplify(p1_A_u_ip1);
p1_B_u_im1 = diff(p1B,'u2'); p1_B_u_im1 = simplify(p1_B_u_im1);
p1_B_u_i   = diff(p1B,'u3'); p1_B_u_i   = simplify(p1_B_u_i);
p1_B_u_ip1 = diff(p1B,'u4'); p1_B_u_ip1 = simplify(p1_B_u_ip1);
p1_C_u_im1 = diff(p1C,'u2'); p1_C_u_im1 = simplify(p1_C_u_im1);
p1_C_u_i   = diff(p1C,'u3'); p1_C_u_i   = simplify(p1_C_u_i);
p1_C_u_ip1 = diff(p1C,'u4'); p1_C_u_ip1 = simplify(p1_C_u_ip1);
p1        = p1A*((h3^2)/4)+p1B*(h3/2)+p1C;
SadeHali1 = simplify(p1);
p1        = collect(SadeHali1);
p1_Uim1 = diff(p1,'u2'); p1_Uim1 = simplify(p1_Uim1)
p1_Ui   = diff(p1,'u3'); p1_Ui   = simplify(p1_Ui)
p1_Uip1 = diff(p1,'u4'); p1_Uip1 = simplify(p1_Uip1)

% Constructing p2
a11=(1/h3)*diff(I3,'a');
a12=(1/h3)*diff(I3,'b');
a13=(1/h3)*diff(I3,'c');
a21=(1/h4)*diff(I4,'a');
a22=(1/h4)*diff(I4,'b');
a23=(1/h4)*diff(I4,'c');
a31=(1/h5)*diff(I5,'a');
a32=(1/h5)*diff(I5,'b');
a33=(1/h5)*diff(I5,'c');
p2AA=[a11 a12 a13; a21 a22 a23; a31 a32 a33];
p2BB    = [u3;u4;u5];
p2Cevap = inv(p2AA)*p2BB;
p2Ce    = simplify(p2Cevap);
p2A=p2Ce(1); p2B=p2Ce(2); p2C=p2Ce(3);
p2_A_u_i   = diff(p2A,'u3'); p2_A_u_i   = simplify(p2_A_u_i)
```

```
p2_A_u_ip1 = diff(p2A,'u4'); p2_A_u_ip1  = simplify(p2_A_u_ip1)
p2_A_u_ip2 = diff(p2A,'u5'); p2_A_u_ip2 = simplify(p2_A_u_ip2)
p2_B_u_i   = diff(p2B,'u3'); p2_B_u_i   = simplify(p2_B_u_i)
p2_B_u_ip1 = diff(p2B,'u4'); p2_B_u_ip1 = simplify(p2_B_u_ip1)
p2_B_u_ip2 = diff(p2B,'u5'); p2_B_u_ip2 = simplify(p2_B_u_ip2)
p2_C_u_i   = diff(p2C,'u3'); p2_C_u_i   = simplify(p2_C_u_i)
p2_C_u_ip1 = diff(p2C,'u4'); p2_C_u_ip1 = simplify(p2_C_u_ip1)
p2_C_u_ip2 = diff(p2C,'u5'); p2_C_u_ip2 = simplify(p2_C_u_ip2)
p2        = p2A*((h3^2)/4)+p2B*(h3/2)+p2C;
SadeHali2 = simplify(p2);
p2        = collect(SadeHali2);
p2_Ui    = diff(p2,'u3'); p2_Ui    = simplify(p2_Ui)
p2_Uip1  = diff(p2,'u4'); p2_Uip1  = simplify(p2_Uip1)
p2_Uip2  = diff(p2,'u5'); p2_Uip2  = simplify(p2_Uip2)

% Construction of big polynomial
pol4 = a*(x-xi)^4 + b*(x-xi)^3 + c*(x-xi)^2 + d*(x-xi) + e;
I1=int(pol4,'x','(xi-h1-h2-h3/2)','(xi-h2-h3/2)');
I2=int(pol4,'x','(xi-h2-h3/2)','(xi-h3/2)');
I3=int(pol4,'x','(xi-h3/2)','(xi+h3/2)');
I4=int(pol4,'x','(xi+h3/2)','(xi+h3/2+h4)');
I5=int(pol4,'x','(xi+h3/2+h4)','(xi+h3/2+h4+h5)');
a11=(1/h1)*diff(I1,'a');
a12=(1/h1)*diff(I1,'b');
a13=(1/h1)*diff(I1,'c');
a14=(1/h1)*diff(I1,'d');
a15=(1/h1)*diff(I1,'e');
a21=(1/h2)*diff(I2,'a');
a22=(1/h2)*diff(I2,'b');
a23=(1/h2)*diff(I2,'c');
a24=(1/h2)*diff(I2,'d');
a25=(1/h2)*diff(I2,'e');
a31=(1/h3)*diff(I3,'a');
a32=(1/h3)*diff(I3,'b');
```

```
a33=(1/h3)*diff(I3,'c');
a34=(1/h3)*diff(I3,'d');
a35=(1/h3)*diff(I3,'e');
a41=(1/h4)*diff(I4,'a');
a42=(1/h4)*diff(I4,'b');
a43=(1/h4)*diff(I4,'c');
a44=(1/h4)*diff(I4,'d');
a45=(1/h4)*diff(I4,'e');
a51=(1/h5)*diff(I5,'a');
a52=(1/h5)*diff(I5,'b');
a53=(1/h5)*diff(I5,'c');
a54=(1/h5)*diff(I5,'d');
a55=(1/h5)*diff(I5,'e');
p4AA=[a11 a12 a13 a14 a15; a21 a22 a23 a24 a25; a31 a32 a33 a34 a35; ...
      a41 a42 a43 a44 a45; a51 a52 a53 a54 a55];
p4BB=[u1;u2;u3;u4;u5];
p4Ce=inv(p4AA)*p4BB;
p4A=p4Ce(1); p4B=p4Ce(2); p4C=p4Ce(3); p4D=p4Ce(4); p4E=p4Ce(5);
p4_A_u_im2 = diff(p4A,'u1'); p4_A_u_im2 = simplify(p4_A_u_im2)
p4_A_u_im1 = diff(p4A,'u2'); p4_A_u_im1 = simplify(p4_A_u_im1)
p4_A_u_i   = diff(p4A,'u3'); p4_A_u_i   = simplify(p4_A_u_i)
p4_A_u_ip1 = diff(p4A,'u4'); p4_A_u_ip1 = simplify(p4_A_u_ip1)
p4_A_u_ip2 = diff(p4A,'u5'); p4_A_u_ip2 = simplify(p4_A_u_ip2)
p4_B_u_im2 = diff(p4B,'u1'); p4_B_u_im2 = simplify(p4_B_u_im2)
p4_B_u_im1 = diff(p4B,'u2'); p4_B_u_im1 = simplify(p4_B_u_im1)
p4_B_u_i   = diff(p4B,'u3'); p4_B_u_i   = simplify(p4_B_u_i)
p4_B_u_ip1 = diff(p4B,'u4'); p4_B_u_ip1 = simplify(p4_B_u_ip1)
p4_B_u_ip2 = diff(p4B,'u5'); p4_B_u_ip2 = simplify(p4_B_u_ip2)
p4_C_u_im2 = diff(p4C,'u1'); p4_C_u_im2 = simplify(p4_C_u_im2)
p4_C_u_im1 = diff(p4C,'u2'); p4_C_u_im1 = simplify(p4_C_u_im1)
p4_C_u_i   = diff(p4C,'u3'); p4_C_u_i   = simplify(p4_C_u_i)
p4_C_u_ip1 = diff(p4C,'u4'); p4_C_u_ip1 = simplify(p4_C_u_ip1)
p4_C_u_ip2 = diff(p4C,'u5'); p4_C_u_ip2 = simplify(p4_C_u_ip2)
p4_D_u_im2 = diff(p4D,'u1'); p4_D_u_im2 = simplify(p4_D_u_im2)
```

```
p4_D_u_im1 = diff(p4D,'u2'); p4_D_u_im1 = simplify(p4_D_u_im1)
p4_D_u_i   = diff(p4D,'u3'); p4_D_u_i   = simplify(p4_D_u_i)
p4_D_u_ip1 = diff(p4D,'u4'); p4_D_u_ip1 = simplify(p4_D_u_ip1)
p4_D_u_ip2 = diff(p4D,'u5'); p4_D_u_ip2 = simplify(p4_D_u_ip2)
p4_E_u_im2 = diff(p4E,'u1'); p4_E_u_im2 = simplify(p4_E_u_im2)
p4_E_u_im1 = diff(p4E,'u2'); p4_E_u_im1 = simplify(p4_E_u_im1)
p4_E_u_i   = diff(p4E,'u3'); p4_E_u_i   = simplify(p4_E_u_i)
p4_E_u_ip1 = diff(p4E,'u4'); p4_E_u_ip1 = simplify(p4_E_u_ip1)
p4_E_u_ip2 = diff(p4E,'u5'); p4_E_u_ip2 = simplify(p4_E_u_ip2)
p4        = p4A*((h3^4)/16)+p4B*(h3^3/8)+p4C*(h3^2/4)+p4D*(h3/2)+p4E;
SadeHali4 = simplify(p4);
p4        = collect(SadeHali4);
p4_Uim2  = diff(p4,'u1'); p4_Uim2  = simplify(p4_Uim2)
p4_Uim1  = diff(p4,'u2'); p4_Uim1  = simplify(p4_Uim1)
p4_Ui    = diff(p4,'u3'); p4_Ui    = simplify(p4_Ui)
p4_Uip1  = diff(p4,'u4'); p4_Uip1  = simplify(p4_Uip1)
p4_Uip2  = diff(p4,'u5'); p4_Uip2  = simplify(p4_Uip2)

Gama0 = p4_Uim2 / p0_Uim2; Gama0 = simplify(Gama0)
Gama2 = p4_Uip2 / p2_Uip2; Gama2 = simplify(Gama2)
Gama1 = (p4_Uim1 - p0_Uim1*Gama0)/p1_Uim1; Gama1 = simplify(Gama1)
Beta_0 = (13/3)*(h3^4)*(p0A^2)+(h3*p0B)^2
Beta_1 = (13/3)*(h3^4)*(p1A^2)+(h3*p1B)^2
Beta_2 = (13/3)*(h3^4)*(p2A^2)+(h3*p2B)^2
```

B.2 MATLAB CODES FOR ADVECTION PROBLEMS

In this part, we give the Matlab codes which are used to obtain the numerical solutions of problems (6.1.17) and (6.1.20) by using the semi-implicit WENO3 and WENO5 methods, respectively.

B.2.1 WENO3 code for problem (6.1.17)

```
function weno3_ex_6_1_2
clear all; close all;
format long
global epsiln h n k1 k2 k3 k4 gama0 gama1

T0=0.0; Tfinal=1.0;
N=20001; M=321; n=3*(M-1)/2;

tau=(Tfinal-T0)/(N-1); % time step
tvalues = linspace(T0,Tfinal,N);
rk21=3.0/4.0; rk22=1.0/4.0;
rk31=1.0/3.0; rk32=2.0/3.0;

% Non-uniform mesh
hh=2.0/(M-1); hr=0.5*hh;
h(1:(M-1)/2)=hh;
h((M+1)/2:n)=hr;
for m=1:((M+1)/2)
   xb(m)=(m-1)*hh;
end
for m=1:M-1
   xb((M+1)/2+m)=1.0+m*hr;
end

for m=1:n
    xvalues(m)=0.5*(xb(m)+xb(m+1));
    u(m)=(cos(pi*xb(m))-cos(pi*xb(m+1)))/(pi*h(m));
end

epsiln=0.000001; time=0.0; error_max=0.0;
exactsol_u=zeros(1,n); Iden=eye(n);

% Calculating Gammas and k coefficients
for i=1:n
```

```
    hi=h(i);
    if i==1
        him1=h(n); hip1=h(i+1);
    elseif i==n
        him1=h(i-1); hip1=h(1);
    else
        him1=h(i-1); hip1=h(i+1);
    end

   gama0(i)=hip1/(him1+hi+hip1);
   gama1(i)=(him1+hi)/(him1+hi+hip1);
   k1(i) = -hi/(him1+hi);
   k2(i) = (him1+2.0*hi)/(him1+hi);
   k3(i) = hip1/(hi+hip1);
   k4(i) = hi/(hi+hip1);
end

for jj=1:N-1
      % First Runge-Kutta for predictor
        % First step
      [L_u_main,Vhalf]=My_func(u);
      L_u = L_u_main*u';
      L_u_copy=L_u_main;
      u_1 = u' + tau*L_u;
        % Second step
      [L_u_main,Vhalf]=My_func(u_1);
      L_u_1 = L_u_main*u_1;
      u_2 = rk21*u' + rk22*(u_1+tau*L_u_1);
        % Third step
      [L_u_main,Vhalf]=My_func(u_2);
      L_u_2 = L_u_main*u_2;
      u_3 = rk31*u' + rk32*(u_2+tau*L_u_2);
      % Second Crank-Nicolson for corrector
      [L_u_main,Vhalf]=My_func(u_3);
```

```
        AA=(Iden - (tau/2.0)*L_u_main);
        BB=(Iden + (tau/2.0)*L_u_copy)*u';
        u_np1=AA\BB;
        u=u_np1';

        for i=1:n
            exactsol_u(i)=(cos(pi*(xb(i)-tvalues(jj+1)))- ...
                          cos(pi*(xb(i+1)-tvalues(jj+1))))/(pi*h(i));
        end

        temp=norm(abs(u-exactsol_u),inf);
        if temp>error_max
            error_max=temp;
        end

        time=jj*tau;
end
disp(error_max)

error_L1=0.0;
time=tvalues(N);
[L_u_main,Vhalf]=My_func(u);
exactsol_u(n)=sin(pi*(xb(n+1)-time));
error_L1=abs(Vhalf(n)-exactsol_u(n))*(h(1)+h(n))*0.5;
for i=1:n-1
  exactsol_u(i)=sin(pi*(xb(i+1)-time));
  error_L1=error_L1+(abs(Vhalf(i)-exactsol_u(i))*(h(i)+h(i+1))*0.5);
end
error_L1=error_L1/2;
disp(error_L1)
end

function [L_u_main,Vhalf]=My_func(u)
global epsiln h n k1 k2 k3 k4 gama0 gama1
```

```
for i=1:n
    hi=h(i); ui=u(i);
    if i==1
        him1=h(n); hip1=h(i+1); uim1=u(n); uip1=u(i+1);
    elseif i==n
        him1=h(i-1); hip1=h(1); uim1=u(i-1); uip1=u(1);
    else
        him1=h(i-1); hip1=h(i+1); uim1=u(i-1); uip1=u(i+1);
    end

    a0=2.0*(ui-uim1)/(him1+hi);
    a1=2.0*(uip1-ui)/(hi+hip1);
    beta0=(hi*a0)^2;
    beta1=(hi*a1)^2;

    omega0_bar = gama0(i)/((epsiln + beta0)^2);
    omega1_bar = gama1(i)/((epsiln + beta1)^2);
    sum_omega_bar=omega0_bar + omega1_bar;
    omega0(i) = omega0_bar/sum_omega_bar;
    omega1(i) = omega1_bar/sum_omega_bar;

    Vhalf(i) = omega0(i)*(k1(i)*uim1+k2(i)*ui) + ...
               omega1(i)*(k3(i)*ui+k4(i)*uip1);
end

% Constructing L matrix
% First row
L_u_main(1,n-1)=k1(n)*omega0(n)/h(1);
L_u_main(1,n)=(k2(n)*omega0(n)+k3(n)*omega1(n)-k1(1)*omega0(1))/h(1);
L_u_main(1,1)=(k4(n)*omega1(n)-k2(1)*omega0(1)-k3(1)*omega1(1))/h(1);
L_u_main(1,2)=-k4(1)*omega1(1)/h(1);
% Second row
L_u_main(2,n)=k1(1)*omega0(1)/h(2);
```

```
L_u_main(2,1)=(k2(1)*omega0(1)+k3(1)*omega1(1)-k1(2)*omega0(2))/h(2);
L_u_main(2,2)=(k4(1)*omega1(1)-k2(2)*omega0(2)-k3(2)*omega1(2))/h(2);
L_u_main(2,3)=-k4(2)*omega1(2)/h(2);
% n-th row
L_u_main(n,n-2)=k1(n-1)*omega0(n-1)/h(n);
L_u_main(n,n-1)=(k2(n-1)*omega0(n-1)+k3(n-1)*omega1(n-1)- ...
                 k1(n)*omega0(n))/h(n);
L_u_main(n,n)=(k4(n-1)*omega1(n-1)-k2(n)*omega0(n)-k3(n)*omega1(n))/h(n);
L_u_main(n,1)=-k4(n)*omega1(n)/h(n);
% 3,4,...,n-1 th rows
for i=3:(n-1)
   L_u_main(i,i-2)=k1(i-1)*omega0(i-1)/h(i);
   L_u_main(i,i-1)=(k2(i-1)*omega0(i-1)+k3(i-1)*omega1(i-1)- ...
                    k1(i)*omega0(i))/h(i);
   L_u_main(i,i)=(k4(i-1)*omega1(i-1)-k2(i)*omega0(i)-k3(i)*omega1(i))/h(i);
   L_u_main(i,i+1)=-k4(i)*omega1(i)/h(i);
end
end
```

B.2.2 WENO5 code for problem (6.1.20)

```
function weno5_ex_6_1_3
format long
global epsiln c1 h n gama0 gama1 gama2
global k1 k2 k3 k4 k5 k6 k7 k8 k9

T0=0.0; Tfinal=0.5;
N=1001; M=181; n=M-1;
xi=1.0/3.0;

tau=(Tfinal-T0)/(N-1); % time step
tvalues = linspace(T0,Tfinal,N);
rk21=3.0/4.0; rk22=1.0/4.0;
rk31=1.0/3.0; rk32=2.0/3.0; c1=13.0/3.0;
```

```
% Non-uniform mesh
h(31:130)=0.001;
for i=16:30
    h(i)=0.001*(1.2)^(30-i);
end
for i=131:145
    h(i)=0.001*(1.2)^(i-131);
end
sizeinterm=sum(h(16:30));
h(1:15)=(0.3-sizeinterm)/15;
h(146:n)=(0.6-sizeinterm)/35;

xb(1)=0.0;
for m=1:n
    xb(m+1)=xb(m)+h(m);
end

indeks1=64;

for m=1:n
    xvalues(m)=0.5*(xb(m)+xb(m+1));
end

u0 = zeros(1,n); u=u0; % initial condition

epsiln=0.000001; time=0.0; maxerror_u=0.0;
exactsol_u=zeros(1,n); Iden=eye(n);

% Calculating Gammas and k coefficients

for i=1:n
    hi=h(i);
    if i==1
```

```
        him1=h(n); him2=h(n-1); hip1=h(i+1); hip2=h(i+2);
    elseif i==2
        him1=h(i-1); him2=h(n); hip1=h(i+1); hip2=h(i+2);
    elseif i==n
        him1=h(i-1); him2=h(i-2); hip1=h(1); hip2=h(2);
    elseif i==(n-1)
        him1=h(i-1); him2=h(i-2); hip1=h(i+1); hip2=h(1);
    else
        him1=h(i-1); him2=h(i-2); hip1=h(i+1); hip2=h(i+2);
    end

   sum_h12=him2+him1; sum_h23=him1+hi; sum_h34=hi+hip1; sum_h45=hip1+hip2;
   sum_h123=sum_h12+hi; sum_h234=sum_h23+hip1; sum_h345=sum_h34+hip2;
   sum_h1234=sum_h123+hip1; sum_h2345=sum_h23+sum_h45;
   sum_h12345=sum_h1234+hip2;

   gama0(i)=(hip1*sum_h45)/(sum_h1234*sum_h12345);
   gama1(i)=(sum_h123*sum_h45*(sum_h12345+sum_h234))/ ...
              (sum_h2345*sum_h1234*sum_h12345);
   gama2(i)=(sum_h23*sum_h123)/(sum_h2345*sum_h12345);

   temp = (hi*(sum_h123+sum_h23))/(sum_h23*sum_h123);
   k1(i) = (hi*sum_h23)/(sum_h12*sum_h123);
   k2(i) = -(k1(i) + temp);
   k3(i) = 1.0 + temp;

   k4(i) = -(hi*hip1)/(sum_h23*sum_h234);
   k6(i) = (hi*sum_h23)/(sum_h34*sum_h234);
   k5(i) = 1.0 - (k4(i) + k6(i));

   k7(i) = (hip1*sum_h45)/(sum_h34*sum_h345);
   k9(i) = -(hi*hip1)/(sum_h45*sum_h345);
   k8(i) = 1.0 - (k7(i) + k9(i));
end
```

```
for jj=1:N-1
      % First Runge-Kutta for predictor
        % First step
      [L_u_main,Vhalf]=My_func(u);
      L_u = L_u_main*u';
      L_u_copy=L_u_main; %% this is for implicit step
      L_u(indeks1)=L_u(indeks1)+(1.0/h(indeks1))*sin(pi*time);
      u_1 = u' + tau*L_u;
        % Second step
      [L_u_main,Vhalf]=My_func(u_1);
      L_u_1 = L_u_main*u_1;
      L_u_1(indeks1)=L_u_1(indeks1)+(1.0/h(indeks1))*sin(pi*(time+tau));
      u_2 = rk21*u' + rk22*(u_1+tau*L_u_1);
        % Third step
      [L_u_main,Vhalf]=My_func(u_2);
      L_u_2 = L_u_main*u_2;
      L_u_2(indeks1)=L_u_2(indeks1)+(1.0/h(indeks1))*sin(pi*(time+0.5*tau));
      u_3 = rk31*u' + rk32*(u_2+tau*L_u_2);
      % Second Crank-Nicolson for corrector
      [L_u_main,Vhalf]=My_func(u_3);
      AA=(Iden - (tau/2.0)*L_u_main);
      BB=(Iden + (tau/2.0)*L_u_copy)*u';
      BB(indeks1)=BB(indeks1)+(tau/(2.0*h(indeks1)))* ...
                   (sin(pi*time)+sin(pi*(time+tau)));
      u_np1=AA\BB;
      u=u_np1';

     for i=1:n
         if((xb(i)>xi)&&(xb(i+1)<(xi+tvalues(jj+1))))
             exactsol_u(i)=(cos(pi*(xi+tvalues(jj+1)-xb(i+1)))- ...
                           cos(pi*(xi+tvalues(jj+1)-xb(i))))/(pi*h(i));
         elseif((xb(i)<xi)&&((xb(i+1))>xi))
             exactsol_u(i)=(cos(pi*(xi+tvalues(jj+1)-xb(i+1)))-...
```

```
                        cos(pi*tvalues(jj+1)))/(pi*h(i));
        elseif((xb(i)<(xi+tvalues(jj+1)))&&(xb(i+1)>(xi+tvalues(jj+1))))
            exactsol_u(i)=(1.0-cos(pi*(xi+tvalues(jj+1)-xb(i))))/(pi*h(i));
        else
            exactsol_u(i)=0.0;
        end
    end
     temp=norm(abs(u-exactsol_u),inf);
     if temp>maxerror_u
         maxerror_u=temp;
     end

     time=jj*tau;
end
disp(maxerror_u)

l1_error=0.0;
time=tvalues(N);
[L_u_main,Vhalf]=My_func(u);
exactsol_u(n)=0;
l1_error=abs(Vhalf(n)-exactsol_u(n))*(h(1)+h(n))*0.5;
for i=1:n-1
  if((xb(i+1)<xi)||(xb(i+1)>=xi+time))
      exactsol_u(i)=0.0;
  else
      exactsol_u(i)=sin(pi*(xi+time-xb(i+1)));
  end
  l1_error=l1_error+(abs(Vhalf(i)-exactsol_u(i))*(h(i)+h(i+1))*0.5);
end
disp(l1_error)
end

function [L_u_main,Vhalf]=My_func(u)
global epsiln c1 h n gama0 gama1 gama2
```

```
global k1 k2 k3 k4 k5 k6 k7 k8 k9

for i=1:n
    if i==1
        him1=h(n); him2=h(n-1); hip1=h(i+1); hip2=h(i+2);
        uim1=u(n); uim2=u(n-1); uip1=u(i+1); uip2=u(i+2);
    elseif i==2
        him1=h(i-1); him2=h(n); hip1=h(i+1); hip2=h(i+2);
        uim1=u(i-1); uim2=u(n); uip1=u(i+1); uip2=u(i+2);
    elseif i==n
        him1=h(i-1); him2=h(i-2); hip1=h(1); hip2=h(2);
        uim1=u(i-1); uim2=u(i-2); uip1=u(1); uip2=u(2);
    elseif i==(n-1)
        him1=h(i-1); him2=h(i-2); hip1=h(i+1); hip2=h(1);
        uim1=u(i-1); uim2=u(i-2); uip1=u(i+1); uip2=u(1);
    else
        him1=h(i-1); him2=h(i-2); hip1=h(i+1); hip2=h(i+2);
        uim1=u(i-1); uim2=u(i-2); uip1=u(i+1); uip2=u(i+2);
    end
    hi=h(i); ui=u(i);
    hi2=hi^2;

    sum_h12=him2+him1; sum_h23=him1+hi; sum_h34=hi+hip1; sum_h45=hip1+hip2;
    sum_h123=sum_h12+hi; sum_h234=sum_h23+hip1; sum_h345=sum_h34+hip2;

    a0=3.0*(uim2/sum_h12-((sum_h123+him1)/(sum_h12*sum_h23))*uim1 + ...
               ui/sum_h23)/sum_h123;
    a1=3.0*(uim1/sum_h23 - ((sum_h234+hi)/(sum_h23*sum_h34))*ui + ...
               uip1/sum_h34)/sum_h234;
    a2=3.0*(ui/sum_h34 - ((sum_h345+hip1)/(sum_h34*sum_h45))*uip1 + ...
               uip2/sum_h45)/sum_h345;

    b0=(((sum_h23+him1)/sum_h12)*uim2 - ...
        ((3.0*him2*hi+6.0*him1*(him2+hi) + ...
```

```
          2.0*(him2)^2+6.0*(him1)^2+hi2)/(sum_h12*sum_h23))*uim1 +...
        ((2.0*(sum_h123+him1)+hi)/sum_h23)*ui)/sum_h123;
    b1=(-((sum_h34+hip1)/sum_h23)*uim1 +...
        ((hip1-him1)*(2.0*sum_h234+hi)/(sum_h23*sum_h34))*ui +...
        ((sum_h23+him1)/sum_h34)*uip1)/sum_h234;
    b2=(-((2.0*(sum_h345+hip1)+hi)/sum_h34)*ui +...
        ((3.0*hip2*hi+6.0*hip1*(hip2+hi)+ ...
          2.0*(hip2)^2+6.0*(hip1)^2+hi2)/(sum_h34*sum_h45))*uip1-...
        ((sum_h34+hip1)/sum_h45)*uip2)/sum_h345;

    beta0=hi2*(c1*hi2*(a0)^2+(b0)^2);
    beta1=hi2*(c1*hi2*(a1)^2+(b1)^2);
    beta2=hi2*(c1*hi2*(a2)^2+(b2)^2);

    omega0_bar = gama0(i)/((epsiln + beta0)^2);
    omega1_bar = gama1(i)/((epsiln + beta1)^2);
    omega2_bar = gama2(i)/((epsiln + beta2)^2);
    sum_omega_bar=omega0_bar + omega1_bar + omega2_bar;
    omega0(i) = omega0_bar/sum_omega_bar;
    omega1(i) = omega1_bar/sum_omega_bar;
    omega2(i) = omega2_bar/sum_omega_bar;

    Vhalf(i) = omega0(i)*(k1(i)*uim2+k2(i)*uim1+k3(i)*ui) + ...
               omega1(i)*(k4(i)*uim1+k5(i)*ui+k6(i)*uip1) + ...
               omega2(i)*(k7(i)*ui+k8(i)*uip1+k9(i)*uip2);
end

% Construction of L matrix
   % First row
L_u_main(1,1) = (k6(n)*omega1(n)+k8(n)*omega2(n)-k3(1)*omega0(1)- ...
                k5(1)*omega1(1)-k7(1)*omega2(1))/h(1);
L_u_main(1,2) = (k9(n)*omega2(n)-k6(1)*omega1(1)-k8(1)*omega2(1))/h(1);
L_u_main(1,3) = -k9(1)*omega2(1)/h(1);
L_u_main(1,n-2) = k1(n)*omega0(n)/h(1);
```

```
L_u_main(1,n-1) = (k2(n)*omega0(n)+k4(n)*omega1(n)-k1(1)*omega0(1))/h(1);
L_u_main(1,n) = (k3(n)*omega0(n)+k5(n)*omega1(n)+k7(n)*omega2(n)-...
                 k2(1)*omega0(1)-k4(1)*omega1(1))/h(1);
   % Second row
L_u_main(2,1) = (k3(1)*omega0(1)+k5(1)*omega1(1)+k7(1)*omega2(1)-...
                 k2(2)*omega0(2)-k4(2)*omega1(2))/h(2);
L_u_main(2,2) = (k6(1)*omega1(1)+k8(1)*omega2(1)-k3(2)*omega0(2)-...
                 k5(2)*omega1(2)-k7(2)*omega2(2))/h(2);
L_u_main(2,3) = (k9(1)*omega2(1)-k6(2)*omega1(2)-k8(2)*omega2(2))/h(2);
L_u_main(2,4) = -k9(2)*omega2(2)/h(2);
L_u_main(2,n-1) = k1(1)*omega0(1)/h(2);
L_u_main(2,n) = (k2(1)*omega0(1)+k4(1)*omega1(1)-k1(2)*omega0(2))/h(2);
   % Third row
L_u_main(3,1) = (k2(2)*omega0(2)+k4(2)*omega1(2)-k1(3)*omega0(3))/h(3);
L_u_main(3,2) = (k3(2)*omega0(2)+k5(2)*omega1(2)+k7(2)*omega2(2)-...
                 k2(3)*omega0(3)-k4(3)*omega1(3))/h(3);
L_u_main(3,3) = (k6(2)*omega1(2)+k8(2)*omega2(2)-k3(3)*omega0(3)-...
                 k5(3)*omega1(3)-k7(3)*omega2(3))/h(3);
L_u_main(3,4) = (k9(2)*omega2(2)-k6(3)*omega1(3)-k8(3)*omega2(3))/h(3);
L_u_main(3,5) = -k9(3)*omega2(3)/h(3);
L_u_main(3,n) = k1(2)*omega0(2)/h(3);
% 'n-1'-th row
L_u_main(n-1,n-4) = k1(n-2)*omega0(n-2)/h(n-1);
L_u_main(n-1,n-3) = (k2(n-2)*omega0(n-2)+k4(n-2)*omega1(n-2)-...
                     k1(n-1)*omega0(n-1))/h(n-1);
L_u_main(n-1,n-2) = (k3(n-2)*omega0(n-2)+k5(n-2)*omega1(n-2)+...
                     k7(n-2)*omega2(n-2)-k2(n-1)*omega0(n-1)-...
                     k4(n-1)*omega1(n-1))/h(n-1);
L_u_main(n-1,n-1) = (k6(n-2)*omega1(n-2)+k8(n-2)*omega2(n-2)-...
                     k3(n-1)*omega0(n-1)-k5(n-1)*omega1(n-1)-...
                     k7(n-1)*omega2(n-1))/h(n-1);
L_u_main(n-1,n) = (k9(n-2)*omega2(n-2)-k6(n-1)*omega1(n-1)-...
                     k8(n-1)*omega2(n-1))/h(n-1);
L_u_main(n-1,1) = -k9(n-1)*omega2(n-1)/h(n-1);
```

```
   % n-th row
L_u_main(n,n-3) = k1(n-1)*omega0(n-1)/h(n);
L_u_main(n,n-2) = (k2(n-1)*omega0(n-1)+k4(n-1)*omega1(n-1)-...
                     k1(n)*omega0(n))/h(n);
L_u_main(n,n-1) = (k3(n-1)*omega0(n-1)+k5(n-1)*omega1(n-1)+...
                     k7(n-1)*omega2(n-1)-k2(n)*omega0(n)-...
                     k4(n)*omega1(n))/h(n);
L_u_main(n,n) = (k6(n-1)*omega1(n-1)+k8(n-1)*omega2(n-1)-...
                     k3(n)*omega0(n)-k5(n)*omega1(n)-k7(n)*omega2(n))/h(n);
L_u_main(n,1) = (k9(n-1)*omega2(n-1)-k6(n)*omega1(n)-k8(n)*omega2(n))/h(n);
L_u_main(n,2) = -k9(n)*omega2(n)/h(n);
   % 4,5,...,n-2 th rows
for i=4:(n-2)
    L_u_main(i,i-3) = k1(i-1)*omega0(i-1)/h(i);
    L_u_main(i,i-2) = (k2(i-1)*omega0(i-1)+k4(i-1)*omega1(i-1)-...
                       k1(i)*omega0(i))/h(i);
    L_u_main(i,i-1) = (k3(i-1)*omega0(i-1)+k5(i-1)*omega1(i-1)+...
                       k7(i-1)*omega2(i-1)-k2(i)*omega0(i)-...
                       k4(i)*omega1(i))/h(i);
    L_u_main(i,i) = (k6(i-1)*omega1(i-1)+k8(i-1)*omega2(i-1)-...
                    k3(i)*omega0(i)-k5(i)*omega1(i)-k7(i)*omega2(i))/h(i);
    L_u_main(i,i+1) = (k9(i-1)*omega2(i-1)-k6(i)*omega1(i)-...
                      k8(i)*omega2(i))/h(i);
    L_u_main(i,i+2) = -k9(i)*omega2(i)/h(i);
end
end
```

CURRICULUM VITAE

CONTACT INFORMATION

İrfan TÜRK
Address: Fevzi Cakmak Mah. Guven Sok.,No:27, Apt No: 14, B. Evler, İstanbul, Turkey
Telephone: +902125523677
Email: irfanturk@gmail.com
Personal URL: http://www.teachmatlab.com/

EDUCATION

İstanbul University, Institute of Graduate Studies in Sciences and Engineering, İstanbul, Turkey
Doctor of Philosophy in Mathematics
June 2016
Thesis Title: On Numerical Solution of Advection-Diffusion-Reaction Equations with Singular Source Terms
Supervisors: Maksat Ashyraliyev, Okan Gerek

The University Texas at Arlington, Graduate School, Arlington, TX, U.S.A.
Master of Science in Mathematics
August 2011
Thesis Title: A Mathematical Model for Swine Flu 2009 with Vaccination
Supervisor: Hristo Kojouharov

Fatih University, Istanbul, Turkey
Bachelor of Science in Mathematics
August 2002

PROFESSIONAL EXPERIENCE

- Lecturer, Fatih University, Civil Eng. Dept., September 2013 - January 2014

- Lecturer, Bursa Orhangazi University, Civil Eng. Dept.,, September 2014 - July 2016

PUBLICATIONS

Books/Book Chapters

1. A Mathematical Model for Swine Flu 2009 with Vaccination, by Irfan Turk, ProQuest, UMI Dissertation Publishing. July 17, 2012

Conference Proceedings

1. Irfan Turk, Maksat Ashyraliyev, "On the numerical solution of diffusion problem with singular source terms", AIP Conference Proceedings, Vol. 1470, Aug. 2012, pp.176-178
2. Irfan Turk, Maksat Ashyraliyev, "On the numerical solution of hyperbolic equations with singular source terms", AIP Conference Proceedings, Vol. 1611, Aug. 2014, pp.374-379

SEMINARS

Seminars/Presentations

1. On the numerical solution of Advection-Diffusion-Reaction Equations with Singular Source Terms, by Irfan Turk, Analysis and Applied Mathematics Seminar Series, Istanbul, Turkey, 06/06/2016
2. On the numerical solution of hyperbolic equations with singular source terms, by Irfan Turk and Maksat Ashyraliyev, ICAAM 2014, Shymkent, Kazakhstan 9/11/2014 – 9/13/2014
3. A Mathematical Model of Swine Flu 2009 with Vaccination, by Irfan Turk and Hristo Kojouharov, ATIM 2013, Istanbul, Turkey 9/12/2013 – 9/14/2013
4. On the numerical solution of Advection-Diffusion-Reaction Equations with Singular Source Terms, by Irfan Turk and Maksat Ashyraliyev, ICAAMM 2013, Istanbul, Turkey, 6/03/2013
5. On the numerical solution of diffusion problem with singular source terms, by Irfan Turk and Maksat Ashyraliyev, ICAAM 2012, Gumushane, Turkey 10/18/2012 – 10/21/2012

6. The SIR Model for Swine Flu, by Irfan Turk and Krishna Acharya, Project Presentation, Arlington, Texas, December 12, 2010
7. ode23s as MATLAB ODE Solver, by Irfan Turk and Krishna Acharya, Project Presentation, Arlington, Texas, November 1, 2010
8. Comparison of Dijstra?s and Floyd-Warshall Algorithms for Shortest Path, by Irfan Turk, Project Presentation, Arlington, Texas, May 7, 2010

AFFILIATIONS

- American Mathematical Society
- Society for Industrial and Applied Mathematics
- International Association of Engineers

SKILLS/INTERESTS

Numerical Solution of Ordinary and Partial Differential Equations, Scientific Computing, Numerical Analysis, Mathematical Modeling, Mathematical Biology, Programming in MATLAB and Python, Cryptography